ENGINEERING PROKARYOTIC PHOSHOLIPASE A_2

BIDHAN CHANDRA NAYAK

M.Sc., Biochemistry

A THESIS SUBMITTED FOR THE DEGREE OF DOCTOR OF PHILOSOPHY

DEPARTMENT OF BIOLOGICAL SCIENCES

FACULTY OF SCIENCE

NATIONAL UNIVERSITY OF SINGAPORE

2015

Declaration

I hereby declare that the thesis is my original work and it has been written by me in its entirety.

I have duly acknowledged all the sources of information which have been used in the thesis.

This thesis has also not been submitted for any degree in any university previously.

Bidhan Chandra Nayak

23rd January 2015

Acknowledgements

This thesis would not be possible without the support and encouragement of numerous people including my well-wishers, friends and colleagues. It is my pleasure to express my thanks to all those who contributed, in many ways, to the success of this study and made it an unforgettable experience for me.

At this moment of accomplishment, first of all I extend my deep sense of gratitude to National University of Singapore for awarding me the research scholarship. I am thankful to the Department of Biological Sciences for giving me an opportunity to conduct research.

I pay homage to my supervisor, Prof. R. Manjunatha Kini. This work would not have been possible without his guidance, support and encouragement. He has inspired me to become an independent researcher and helped me realize the power of critical reasoning. Under his guidance I successfully overcame many hurdles and overall it has been a huge learning experience.

I am most grateful to the members of my thesis advisory committee for constructive feedbacks towards improving my Ph.D work. I gratefully acknowledge Prof. Sivaraman, Prof. Maxey for constant encouragement and personal attention, which have provided positive energy through difficult times and keep progress in track.

My sincere thanks must also go to the administrative staffs, lab officers Ms. Tay Bee Ling and Ms. Xu Liyuan for the great help. Thanks to Ms. Reena and

Ms. Priscilla, Mrs Chan for all official work, queries and kind care.

I would like to extend my thanks to the past members of our lab, Dr. Guna, Dr. Aktar, Dr. Sheena, Aldo, Angie, Nazir, Hoi Yee, Vui Yin, Cheng Mun and Si Yun. My special regards to my seniors Dr. Amrita, Dr. Girish and Dr. Bhaskar for helping me learn the lab basics during the initial days and being such great and supportive colleagues all the times.

My warm appreciation to all current lab mates who kept the lab lively all the time. Thanks to Dr. Ryan, Dr. Saran, Dr. Guillaume, Ritu, Varuna, Summer, Janaki, Norrapat, Feng Jian, Ben and Chen Wan.

My special thanks to Dr. Sindhuja for all her great help in experimental troubleshooting, practical suggestions and moral support. Words are short to express my deep sense of gratitude towards her.

In the journey of PhD, friends serve as buffers in failures and frustations. I cannot forget friends who stood by me in the hard times and cheered me on. Thanks to Pradeep, Pavithra and Pramila with whom I have shared my moments of success, failure, joy and sorrow. I also thank my flat-mates Pradeep, Hemant, Manish and Gurpeet for their cooperation.

It’s my fortune to gratefully acknowledge the support of two special individuals Digant and Sarath from structure biology lab 5. They have been my buddies and have supported me in my hard times.

I would also like to acknowledge other members of surrounding labs for

helping me with experiments, equipment or reagents. Manjeet, Tangavelu, Abhilash, Jobi, Apoorv, Anirudh, Priyanka, Lakshmi, YC and Sunil from SBL 5, Shani, Anindita and Jiao from SBL 4, Garvita from SBL 3, Rusha from SBL 2, Sang, Karthik and Ahmed from SBL 1, Vivek, Vijay, Prathibha, Pavithra, Amrit and Bhusan from plant morphogenesis lab. I would also like to thank Chye Fong for granting me access to the equipment in the teaching lab.

Last but not least, I would like to pay high regards to my parents, siblings and in-laws for their constant support, love and sincere encouragement. At the end I would like to express appreciation to my beloved wife Shruthi who was always my support and inspiration throughout my research work. Your prayer for me was what sustained me thus far.

Besides this, I would like to thank several people who have helped me knowingly and unknowingly in the successful completion of this project.

Bidhan Chandra Nayak

January, 2015

Table of contents

Summary

Prokaryotic PLA_2 from *Streptomyces violaceoruber*, shows an unusual property to be secreted into the culture medium, instead of its retention in the bacterial periplasmic space when overexpressed in *E. coli* using the pelB periplasmic signal. Moreover, this molecule is structurally the least complex and one of the smallest among PLA_2 enzymes. Hence, in my doctoral study I have attempted to engineer PLA_2 to (a) develop an extracellular expression system; and (b) design a mini PLA_2 scaffold.

The secretory nature of prokaryotic PLA_2 was exploited by using it as a tag to express other disulphide rich proteins in the extracellular medium, as it would provide an oxidative environment for folding. Using this system, we successfully expressed fusion protein PLA_2-Krait natriuretic peptide (one disulphide) and PLA_2-Denmotoxin (a three-finger toxin with five disulphides) in the culture medium. After cleavage, correctly folded, functionally-active Krait natriuretic peptide was obtained. Although PLA_2-Denmotoxin was expressed as soluble fusion with all the cysteines oxidized, it resisted protease cleavage, probably due to stearic hindrance, which could be overcome by providing optimal linker size for protease access (current ongoing work). Thus, we demonstrated the utility of prokaryotic PLA_2 in the expression of complex proteins.

The prokaryotic PLA_2 has a unique three dimensional structure. Although it possess the conserved three-helix catalytic core seen in other secretory PLA_2s

it has a two-helix domain located away from its catalytic core, which seems to have no direct role in catalysis. With just two disulphide bonds and this structural uniqueness, this enzyme provided us a model to attempt the design of minimal PLA_2 scaffolds and study its structure and activity. To achieve this, two generations of mutants were created. The first generation of mutants (ΔHelix-1, ΔHelix-1, 2) evaluated the requirement of the first two helices in the PLA_2 activity. Both mutants did not show any enzymatic activity although they were folded with wild-type like disulphide linkages. The second generation of mutant was designed to stabilize the interactions on the exposed hydrophobic surface (F66Q and Y71Q) of ΔHelix-1, 2. Despite the replacement with polar residues, the minimal scaffold lacked PLA_2 activity suggesting the necessity to study the three dimensional structure of the minimized mutants and re-design existing mutants to stabilize the molecule further. Hence from this study we were able to use the PLA_2 as an expression tag and probe the structural requirements for enzymatic activity.

List of tables

List of figures

Abbreviations

Single and three letter abbreviations of amino acids were followed as per the recommendations of the IUPAC-IUBMB Joint Commission on Biochemical Nomenclature.

Chemicals and reagents

HEPES	4-(2-Hydroxyethyl)piperazine-1-ethanesulfonic acid
APS	Ammonium persulfate
BSA	Bovine serum albumin
$CaCl_2$	Calcium chloride
DMEM	Dulbecco's Modified Eagle's Medium
dNTP	Deoxyribonucleotide triphosphate
DTT	Dithiothreitol
EDTA	Ethylenediamine tetraacetic acid
FA	Formic acid
HCl	Hydrochloric acid
IPTG	Isopropyl β-D-thiogalactoside
KCl	Potassium chloride
KH_2PO_4	Potassium di-hydrogen phosphate
LB	Luria bertani
$MgCl_2$	Magnesium chloride
$MgSO_4$	Magnesium sulphate
NaCl	Sodium Chloride

$NaHCO_3$	Sodium bicarbonate
NaOH	Sodium hydroxide
PBS	Phosphate-buffered saline
SDS	Sodium dodecyl sulfate
TEMED	N,N,N′,N′-Tetramethylethylenediamine
TFA	Trifluoroacetic acid
Tris	Tris(hydroxymethyl)-aminomethane

Units

Å	Angstrom
cm	Centi meter
CPS	Counts per secon
Da	Daltons
°C	Degree Celsius
U	Enzyme unit
g	Gram
h	Hour
kDa	Kilo Daltons
kg	Kilo gram
l	Litre
µg	Micro gram
µl	Micro litre
µM	Micro molar
µmol	Micro mole
µm	Micron
mAU	Milli absorbance unit
mg	Milli gram
ml	Milli liter
mm	Milli meter

mm Hg	Milli meter mercury
mM	Milli molar
min	Minute
M	Molar
ng	Nano gram
nm	Nano meter
nmol	Nano mole
nM	Nano molar
rpm	Revolutions per minute
s	Second
V	Volt

Others

ANP	Atrial natriuretic peptide
ATP	Adenosine triphosphate
Ca^{2+}	Calcium
cDNA	Complementary DNA
cGMP	cyclic guanosine monophophate
CIEX	Cation exchange chromatography
C-terminus	Carboxy terminus
ESI-MS	Electrospray ionization-mass spectrometry
KNP	Krait natriuretic peptide
LC-MS	Liquid chromatography- mass spectrometry
m/z	Mass to charge ratio
NP	Natriuretic peptide
NPR	Natriuretic peptide receptor
N-terminus	Amino terminus
OD_{600}	Optical density at 600 nm
PCR	Polymerase chain reaction

pI	Isoelectric point
RP-HPLC	Reverse phase-high performance liquid chromatography
SDS-PAGE	Sodium dodecyl sulfate polyacrylamide gel electrophoresis
TEV	Tobacco-etch-virus
Trx	Thioredoxin
α	Alpha
β	Beta
Δ	Delta

CHAPTER ONE

Introduction

1 CHAPTER ONE: Introduction

1.1 Protein engineering

Protein engineering is an area of protein science, first described by scientist Kevin M. Ulmer in 1983 with the paper titled 'Protein Engineering' (Ulmer, 1983). At that time, protein engineering was performed with basic techniques like mutagenesis mostly to enhance the properties of commercially useful products like enzymes. Since then, till the time of compiling this thesis, a lot of advancements have taken place in the field of protein design and engineering. It is a broad area comprising of a several tools and techniques to design proteins with improved or new function. Although it is an interesting area, it is equally challenging, partly due to our lack of complete understanding of protein folding and the complex nature of proteins (Dill and MacCallum, 2012). The field of protein design and engineering has two broad approaches, rational design and de-novo design.

1.1.1 Rational protein design

In the rational approach, proteins are designed and engineered from a known starting molecule whose structure and properties are well studied. Although the final aim is to gain or enhance a desired function, the alterations in the molecule are based on the known information of its structure, fold and

mechanism (Berry and Lu, 2011). This strategy includes redesign of existing proteins with or without combinatorial approaches.

1.1.2 De-novo protein design

In the de-novo approach, entirely new proteins are designed from the scratch only with the idea of the final desired function. This approach relies heavily on computer algorithms to obtain the final predicted design. This strategy is gradually improving with time with the availability of numerous three dimensional structures of proteins in the databases and advancements in programming and computational power (Huang et al., 2011; Khatib et al., 2011).

Proteins are engineered either for our understanding of its structure-function relationship or dissection of action mechanism. Proteins are also engineered for improving its function for commercial benefits (Tsigos et al., 2001; Van den Burg et al., 1998). The proteins which are engineered are mostly antibodies or enzymes. While antibodies are engineered to enhance its affinity towards antigens (Holliger and Hudson, 2005; Presta, 2005; Reiter et al., 1996), enzymes are mostly engineered to improve its catalytic properties (Lutz, 2010; Narayan and Sherman, 2013).

1.2 Enzyme engineering

Enzymes are very efficient biological catalyst. For a long time enzymes were the prime targets for protein engineering primarily for its industrial and commercial importance (Arnold et al., 2015). Nevertheless enzymes are engineered for understanding its catalytic mechanism. Recent development in de-novo enzyme design has led to a few successes in development of enzymes with completely new catalytic function (Nanda and Koder, 2010; Rothlisberger et al., 2008; Siegel et al., 2010). Further some of these enzymes were later improved by additional remodeling and combinatorial techniques (Eiben et al., 2012). Therefore today enzyme engineering is accomplished by rational approach, combinatorial techniques or de-novo design.

1.3 Phospholipases

Phospholipases are a widespread group of enzymes possessing the ability to cleave various bonds in phospholipids (Figure 1.1). They play diverse roles from defence in snake to signal transduction, production of lipid mediators and digestion in humans (Aloulou et al., 2012). Based on the specific bond they cleave in phospholipids, they are named as phospholipase A_1, A_2, C and D.

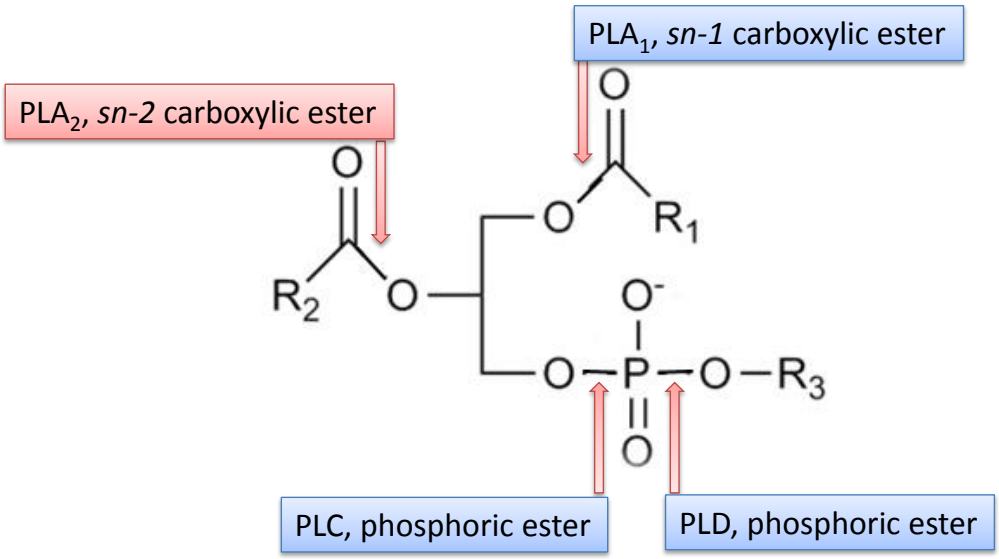

Figure 1.1 Different phospholipases and the bond they cleave

Four different phospholipases, named after the specific bonds on the lipid molecule it cleaves.

1.4 Phospholipase A_2

Phospholipase A_2 (EC 3.1.1.4) stereospecifically hydrolyze the sn-2 carboxylic ester bond of phospholipids (Figure 1.1). This group of enzyme is very interesting because of its unusual property to perform catalysis in the interface between protein and organized lipids (Scott and Sigler, 1994). Moreover the synthesis of arachidonic acid as a result of phospholipid catalysis plays a key role in the prostaglandin production including other inflammatory mediators (Ricciotti and FitzGerald, 2011). An exclusive kinetic property of secretory phospholipase A_2 ($sPLA_2$) is their preference for organized substrates such as monolayers, membranes, vesicles or micelles (Scott and Sigler, 1994). This is evident form the fact that $sPLA_2$s show

enhanced activity (up to three orders of magnitude greater) on lipid aggregates than dispersed substrates. $sPLA_2$s are calcium dependent enzymes. Although calcium is weakly bound (K_d greater than 10^{-4} M), it is necessary for catalysis (Scott and Sigler, 1994). This group of enzymes has been thoroughly investigated due to its availability in milligram quantities from sources such as pancreas and reptile venoms, before the advent of heterologous protein expression systems.

1.4.1 Classification

The superfamily of PLA_2 enzymes can be classified into 15 groups (including subgroups), which includes five types of distinct enzymes, namely secretory phospholipase A_2 ($sPLA_2$), cytosolic phospholipase A_2 ($cPLA_2$), calcium independent phospholipase A_2 ($iPLA_2$), platelet-activating factor acetyl hydrolases (PAF-AH) and lysosomal PLA_2s (Schaloske and Dennis, 2006). This classification is based on the group numbering system updated in the year 2006, although a number of new PLA_2 have been discovered till date as a result of substantial investigations in this field. Group 1 and 2 comprises of secretory enzymes from old world and new world snake venoms respectively. The group 3 comprises of bee venom PLA_2 and the group 14 comprises the prokaryotic PLA_2 investigated in this thesis.

1.4.2 Catalysis

PLA_2s are unique in the fact that they are highly water soluble enzymes capable of hydrolyzing water insoluble substrates, i.e, phospholipids (Kini, 2003). They possess the ability to hydrolyze lipids in monomeric, micellar or bilayer forms, with an increase in catalytic activity up to 10,000 folds at the critical micellar concentration (CMC) of the phospholipids (Verger and De Haas, 1973). This is due to interfacial activation, a phenomenon common among PLA_2s. This unusual property is aided by an interfacial recognition site, which is independent of the catalytic site. PLA_2s also exhibit distinct phospholipid head group preferences. Bilayer vesicles are hydrolyzed in two distinct modes. In hopping mode of catalysis, binding to the bilayer and desorption occurs during each catalytic turnover cycles. In scooting mode of catalysis, the enzyme remains bound to the interface between the catalytic turnover cycles (Kini, 2003). These distinct modes of catalysis have been characterized by different experimental conditions (Jain and Berg, 1989).

1.4.3 Pharmacological effects

Reptilian venom PLA_2s exhibits a variety of pharmacological effects such as neurotoxicity, myotoxicity, cardiotoxicity, anticoagulant effects, hemolytic effects and edema inducing activity to mention a few (Kini, 2003). The pharmacological effects exhibited by the snake PLA_2s are mostly independent of other components with a few exceptions. For a few PLA_2s the full potential

of pharmacological activity is seen only when in complex with other proteins. In case of β-bungarotoxin the components are held together by covalent bonds whereas in case of crotoxin, the components are associated with each other by non-covalent interactions.

1.5 Structural homology in PLA_2s

Secretory PLA_2s are highly homologous containing between 119 to 143 amino acid residues. This homology is based on mostly their tertiary structure displaying a large proportion of invariant residues. Conserved residues directly participate in catalysis or occupy structurally sensitive positions in the enzyme structure (Scott and Sigler, 1994). The number of cysteine residues range from 4 to 14 and are involved in disuphide bonds, stabilizing the tertiary structure.

The following are the conserved substructures seen in secretory PLA_2s

1.5.1 Three-helix catalytic core

All secretory PLA_2s possesses the conserved three helix catalytic core. This core contains the active site residues which are conserved in secretory PLA_2s. Although the tertiary structure might contain loops and β-strands holding the three-helix core in place, the three helix bundle is conserved in all secretory PLA_2s (Figure 1.2 a).

1.5.2 Active site geometry

The catalytic triad in the active site of secretory PLA_2s is made of histidine, aspartic acid and a water molecule. Because it is a calcium dependent enzyme, the position of calcium in the tertiary structure is crucial for the catalysis. In the active site of all secretory PLA_2s the geometry of active site histidine, aspartic acid and calcium is conserved. The distance between histidine and aspartic acid is around 2.9 Å whereas the distance between histidine and calcium is around 6.3 Å (Figure 1.2 b).

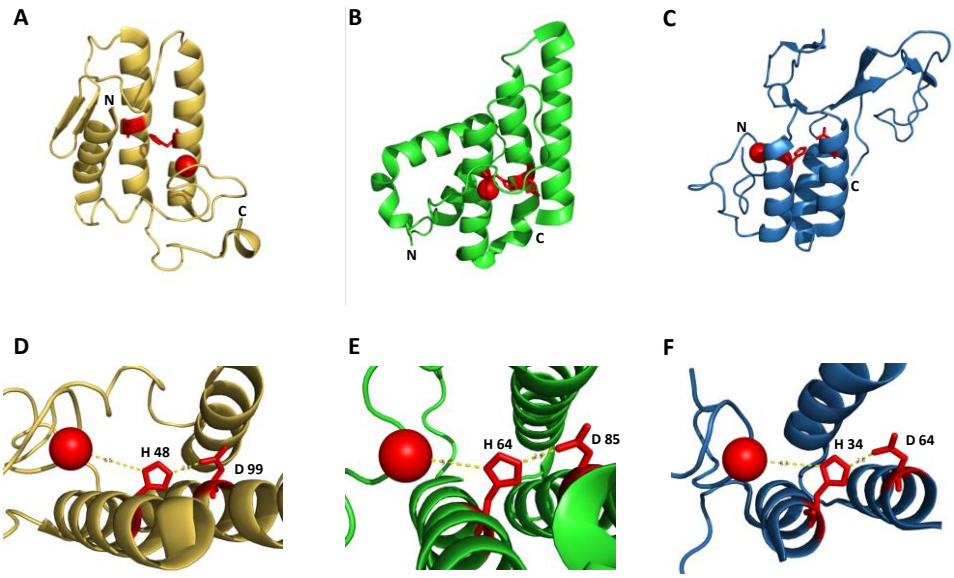

Figure 1.2 Structural similarity in phospholipase A_2

A. Cobra venom PLA_2 B. Prokaryotic PLA_2 C. Bee venom PLA_2. Active site histidine, aspartic acid and calcium are shown in red.
D, E and F. Same PLA_2 structures as above, with active site zoomed in. Although the three well studied molecules belong to three different class of phospholipases, they share the same three dimensional topology containing the three helix catalytic core.
The distances between the active site histidine, aspartic acid and calcium is very similar in all the three molecules.

1.5.3 Calcium binding loop

All secretory PLA_2s have a loop which contains the residues that co-ordinate the calcium ion. Oxygen atoms form the backbone carbonyls, carboxylate of aspartate and solvent water co-ordinate the calcium with a co-ordination number of 7 forming a pentagonal bipyramidal co-ordination cage. This calcium binding loop also forms the superior wall of the substrate-binding pocket (Scott and Sigler, 1994).

1.5.4 Antiparallel helices

Secretory PLA_2s show another common substructure, the antiparallel helices. Two helices among the three in the catalytic core are linked together by disulphide bridges to form a stable structure holding several important residues involved in catalysis. Side chains arising from these helices aid in coordination of calcium ion. It also forms the deeper regions of the hydrophobic channel (Scott and Sigler, 1994).

1.6 Prokaryotic phospholipase A_2

The prokaryotic phospholipase A_2 is the first secretory PLA_2 identified from a soil bacterium, *Streptomyces violaceoruber* (Sugiyama et al., 2002). This enzyme has been characterized both functionally and structurally. Structural investigations of this new class of secretory PLA_2 have yielded both the NMR

solution and x-ray crystal structures in calcium free and bound form (Matoba et al., 2002; Sugiyama et al., 2002). From the NMR and x-ray data, interesting insights regarding this new class of molecule was elucidated. It was the first secretory PLA_2 with relatively simple structure containing only two disulphide linkages. Unlike other well studied secretory PLA_2s which contains both α-helices and β-strands, this enzyme contains only α-helices in its tertiary structure. It was one of the the smallest secretory PLA_2 described with only 122 amino acid residues and a molecular weight of 13.5 kDa (Figure 1.3 a, b).

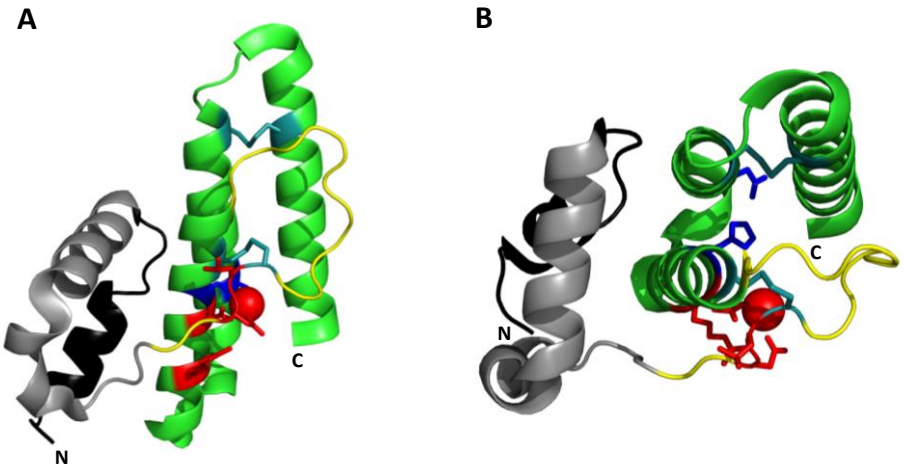

Figure 1.3 Crystal structure of prokaryotic PLA_2 (1FAZ)

A. Side view B. Top view. Three green helices form the core of the enzyme. Relevant structures are coloured.

Dark blue, catalytic residues; red, residues involved in calcium co-ordination; light blue, disulfide bonds. Helices 1 (black) and 2 (grey) appear to be away from active site and hence predicted to play no role in catalysis.

1.7 Unique properties of prokaryotic PLA_2

The prokaryotic PLA_2 is the first secretory PLA_2 identified from soil bacteria. This enzyme possesses a few unique and interesting characteristics which are exploited in the studies described in this thesis.

1.7.1 Unique structural features of prokaryotic PLA_2

The structure elucidated from the NMR and crystal data, shows the presence of only two disulphide bonds compared to the other well studied secretory PLA_2s which have 10-14 disulphides. Therefore this bacterial PLA_2 is the only one with the simplest structure among all known secretory PLA_2s. Figure 1.4 shows the disulphides in red circles. Moreover it has only five α-helices, compared to other well studied secretory PLA_2s, which are composed of both α-helices and β-strands in their tertiary structure. More interestingly, the molecule seems to be comprised of two domains with N-terminal 2-helix bundle and C-terminal 3-helix bundle. The C-terminal 3-helix core is the catalytic core of the molecule containing the conserved residues needed for catalysis. The N-terminal 2-helix bundle seems be located away from the C-terminal catalytic domain, hence predicted to not to take part in catalysis Figure 1.4, red square box). This secretory PLA_2 is one of the smallest in size with 122 amino acid residues and has a molecular weight of 13.5 kDa.

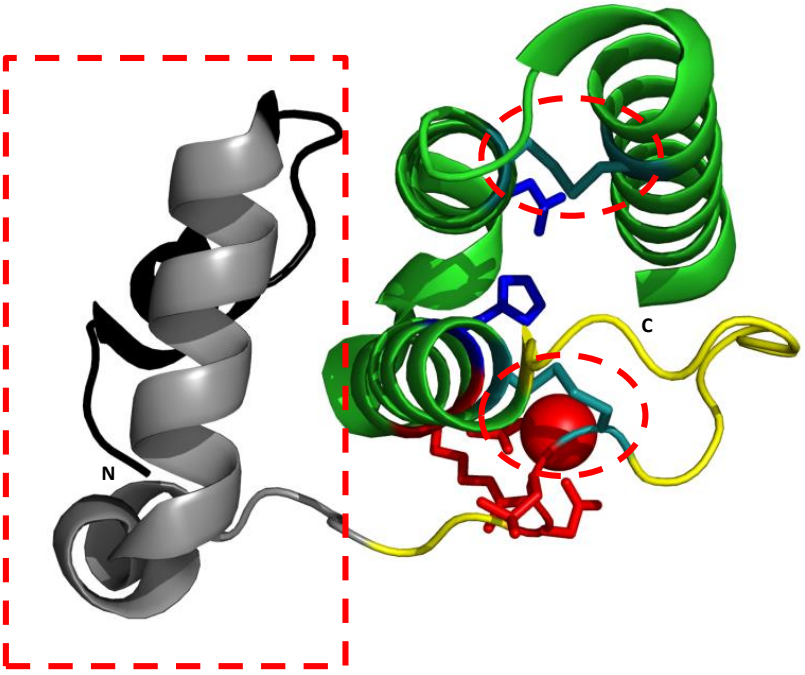

Figure 1.4 Unique structural features of prokaryotic PLA_2

The two disulphide bonds shown in red circles.
The N-terminal 2-helix bundle is shown in red rectangle.

These structural features make this molecule one of the smallest and simplest secretory PLA_2. This provided us with a model to minimize the size of the enzyme to develop a small PLA_2 scaffold, by retaining the catalytic domain and its enzymatic activity. This forms one part of my thesis to design smaller PLA_2 scaffolds, evaluate its structure and test its function.

1.7.2 Unique expression properties of prokaryotic PLA_2

The prokaryotic PLA_2 when expressed with pelB signal sequence using the pET 22b vector system was shown to be expressed in the extracellular medium instead of its retention in the periplasmic space (Takemori et al., 2012). Although the plasmid construct was designed for periplasmic expression of PLA_2, most of the activity was seen in the culture medium when compared to the cytosol (Takemori et al., 2012). The comparison between this unusual extracellular expression of PLA_2 using the pelB signal and the usual periplasmic expression of protein X is shown in Figure 1.5 a and b.

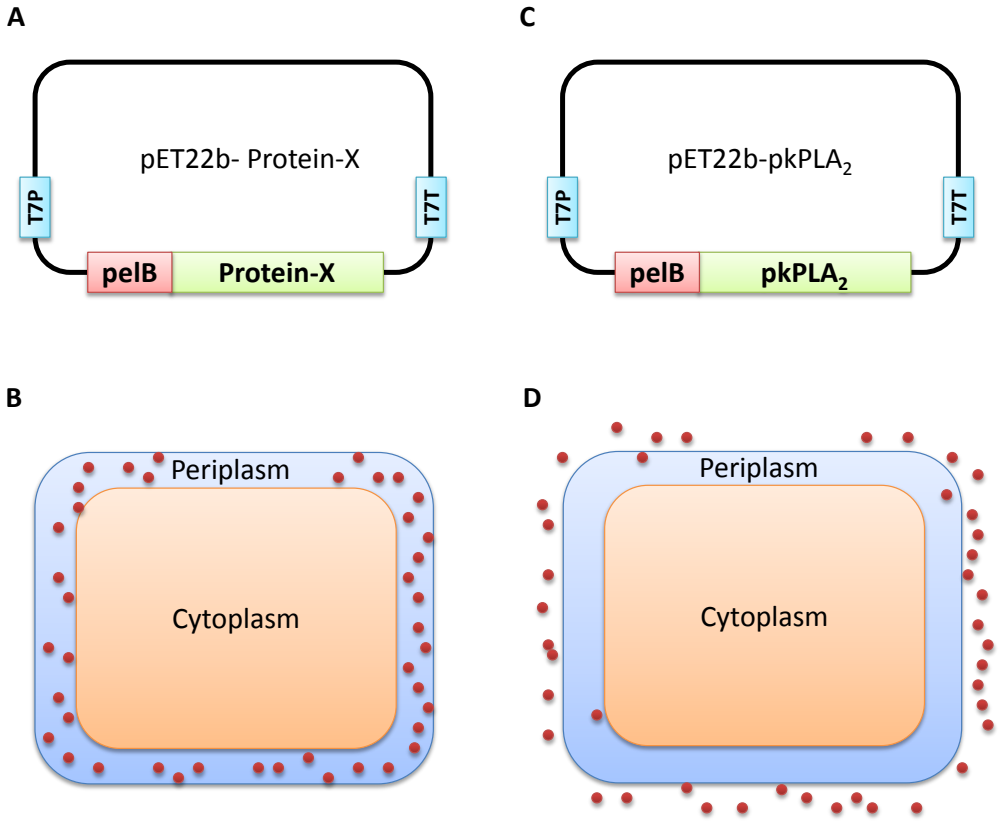

Figure 1.5 Periplasmic expression compared to extracellular expression

A and B. The common periplasmic expression, where the protein is signaled to the bacterial periplasm where it is retained.
Top: pET22b plasmid showing pelB signal and protein-X.
Bottom: Schematic representation of a *E. coli* cell showing retention of proteins in the bacterial periplasm.
B. Extracellular expression seen in case of pelB-PLA_2, where the expressed protein is secreted into the culture medium.
Top: pET22b plasmid showing pelB signal and $pkPLA_2$.
Bottom: Schematic representation of a *E. coli* cell showing secretion of $pkPLA_2$ from the bacterial periplasm to extracellular medium.

The yield of purified prokaryotic PLA_2 obtained from this system of extracellular expression was reported to by 20 mg/l culture supernatant (Takemori et al., 2012). Although the mechanism of this extracellular export of the prokaryotic PLA_2 from the periplasm to the extracellular medium is

unclear, this phenomenon is independent of the catalytic activity of PLA_2 (Takemori et al., 2012).

The prokaryotic PLA_2, although containing two disulphides was able to express in considerably large quantities, fold and function like the authentic enzyme, led us to hypothesize that the prokaryotic PLA_2 could be used as a carrier to express other disulphide rich proteins of interest in the extracellular medium. This forms the first part of my thesis, to test this system of extracellular expression using the prokaryotic PLA_2 as an expression tag.

1.8 Structural minimization of Proteins

Mini proteins or protein domains are considered to be the smallest functional unit of a protein. Protein minimization, a type of protein engineering endeavor, helps us understand the first principles of protein folding, structure-function relationship and design of stable scaffolds.

1.8.1 Importance of mini proteins

Although proteins are complex molecules with distinct folds and functions, the determinants leading to their signature folds and thus functions are not very clear. Even though a lot of investigations are done in this direction, our ability to design any molecule with a defined function, just from its primary sequence is limited by our understanding of protein folding. Functional proteins with

minimal structure provide us excellent models for studying protein folding. Smaller motifs also offer simple and traceable models for understanding determinants of protein stability, structure and function (Braisted and Wells, 1996). Moreover smaller proteins are more amenable to synthetic chemistry, making it easier for further design and engineering.

Mini proteins serve as stable scaffolds which can be used as a starting template for the design of other useful molecules. Desired function can be imparted into small scaffolds by grafting of active sites (Stricher et al., 2006). Small stable scaffolds with a desired biological activity can be used for the design of other modular biologics or biotechnological tools.

1.8.2 Strategies for minimization

The minimization strategy usually start from rational design of minimal domains, followed by combinatorial and evolution methods to gain or enhance its function followed by further minimization and so on, until the desired structure and function is attained. Grafting of active sites into a structurally defined stable scaffold is also a strategy for minimization (Stricher et al., 2006).

1.8.3 Mini protein design endeavors

Protein engineering is a challenging area which navigates between chance and reason (Baker, 2011; Corey and Corey, 1996). Not a lot of protein/enzyme minimization efforts have been successful. Protein A domain was minimized from 59 residues to 33 residues (Braisted and Wells, 1996), ANP was minimized from 28 residues to 15 residues (Li et al., 1995). Scorpion toxin scaffold, with 37 amino acid residues was used as a natural scaffold to impart zinc binding activity (Vita et al., 1995).

1.9 Importance of recombinant protein expression

Recombinant protein expression has been one of the key technologies in the advancement of our understanding of numerous biological processes. As the increasing research and commercial applications require large quantities of high quality proteins, the strategies for efficient production of recombinant proteins are gaining importance (Terpe, 2006).

1.9.1 Recombinant protein expression systems

Till date, there are several well standardized systems for overexpressing proteins (Assenberg et al., 2013). Although there are various limitations in each of these systems, the expression systems for use in each target protein

needs to be chosen based on properties of the target protein. The following are some of the most common systems for recombinant protein expression:

1.9.2 Bacterial systems

Prokaryotic systems including Gram negative and Gram positive bacteria are utilized for production of recombinant proteins (de Vos et al., 1997; Vrancken et al., 2010). Although both Gram positive and Gram negative bacteria have been able to express recombinant proteins, the Gram negative bacteria E. coli is the system of choice for various reasons.

E. coli was the first Gram negative bacterium utilized for recombinant pharmaceutical protein production (Assenberg et al., 2013). Till date large amount of information have been gained about its manipulation and usage (Baneyx, 1999; Prazeres et al., 1999). It can be grown to very high cell densities with simple defined media requirements (Ozturk, 1996). A very high level of expression is possible using commercially available pET vector systems. Despite all these advantages, there are several other drawbacks such as inability to correctly fold complex and disulphide rich proteins due to reducing environment of the cytoplasm. Formation of posttranslational modifications including glycosylation and acylation is not possible, which might be desirable in some proteins of interest.

On the other hand, Gram positive bacteria have been used for recombinant protein expression with the advantage of production of large amounts of

folded proteins and low amounts pyrogens (Harwood, 1992). The production of protease subtilisin by B. subtilis, is an example of its usage. Although Gram positive bacteria are capable of producing recombinant proteins, the yields are lower compared to the Gram negative counterparts. Moreover, the recombinant plasmids are not stable hence chromosomal integration of the gene of interest is the only route to obtain stable recombinant cells.

1.9.3 Yeast systems

The yeast expression system includes the species *S. cerevisiae* and *P. pastoris*, which are commonly used. The first manipulated yeast species for recombinant expression was *S. cerevisiae* (Kjeldsen, 2000). Although recombinantly expressed proteins using *S. cerevisiae* sytem can secrete folded proteins to the extracellular media, the effects of extracellular proteases and post translational modification limits its use.

Methylotrophic yeasts, such as *P. pastoris* are hosts with high potential (Gellissen, 2000). It was a host proposed for recombinant protein expression as early as in the 1980s (Cereghino and Cregg, 2000). *P. pastoris* has been reported to grow up to very high cell densities (100 g/l dry biomass) with protein yield up to 1 g/l (Cereghino and Cregg, 2000). Although it has advantages, handling yeast is more troublesome than bacteria. The growth rate being slow (culturing requires 4 to 6 days), makes this a comparatively less efficient expression method. Moreover transformation and selection of stable

integrants of gene in yeast system is more laborious compared to transformation of plasmid in bacterial system.

1.9.4 Mammalian system

The mammalian system for recombinant protein production is the most sophisticated system available. The ability of mammalian cells to fold and perform complex posttranslational modifications in the expressed protein is unmatched by any other system. Moreover this system has been optimized for culture up to 10,000 l scale. But there are several hurdles in expression of proteins using this system. Factors like expression yield, time required for gene manipulation, time required for protein production, prone to contamination and expenses in bioreactor and culture conditions, make this system less reliable for most protein production endeavors.

1.9.5 Tags for bacterial expression systems

Although there are sophisticated systems to express recombinant proteins, the bacterial system is the most robust due to its ease of handling, fast growth, easy genetic manipulation and high levels of expression. Therefore many strategies have been developed to get the most out of bacterial expression system, despite its limitations. For aiding the production of soluble proteins and purification, tags have been developed for the purpose of either increasing the solubility or aiding purification or both.

1.9.5.1 Histidine tag (6x His)

This is the simplest tag consisting of six tandem repeats of histidine, devised for purification of protein expressed in the bacterial cytoplasm. It was designed for affinity purification of tagged proteins by immobilized metal affinity chromatography (IMAC) (Choe et al., 2002). It has the most versatile use in bacterial expression system. But this tag has only chelation property and do not contribute to the enhancement of solubility of the target proteins. It can be used with both soluble and denatured inclusion body proteins.

1.9.5.2 Thioredoxin (Trx) tag

Thioredoxin is a moderate size (~12 kDa) expression tag which is usually used for enhancing solubility of the target protein. The thioredoxin molecule used is from bacterial source. The high solubility of Trx is evident from the fact that, when it is expressed from plasmid vectors in E. coli, it accumulates up to 40% of the total cellular proteins, while remaining completely soluble (Lunn et al., 1984). The fold of thioredoxin is very compact with 90% of primary sequence involved in prominent elements of secondary structure. In the tertiary structure, Trx is exposed to the surface both at the N and C-terminus of the molecule, allowing it to be linked at any terminus (Katti et al., 1990). Thiredoxin is proposed to serve as covalently linked chaperone protein, by holding the folding intermediates of the heterologous protein in soluble form

long enough, until it attains its final confirmation (LaVallie et al., 1993). Moreover Trx tag when fused to 6x His tag, can be used for both enhancing solubility and assisting in affinity purification.

1.9.5.3 Glutathione S-transferase (GST) tag

Glutathione S-transferase (GST) is a 26 kDa naturally occurring protein form eukaryotic cells. This protein was identified from the parasitic helminth *Schistosoma japonicum*, which was later used in the design of expression tag in the pGEX vector system (Harper and Speicher, 2011; Smith and Johnson, 1988). GST is used as a fusion partner in expression systems because it exhibits chaperone like properties, aiding in folding proteins (Harper and Speicher, 2011). It serves both as a solubilization and an affinity tag. The fusion can be affinity purified by the use of immobilized glutathione resin and eluted by use of reduced glutathione.

1.9.5.4 Maltose binding protein (MBP) tag

Maltose binding protein (MBP) is a ~40 kDa expression tag which serves dual purpose of solubilization and affinity purification of heterologous proteins expressed in E. coli. This protein was originally developed as a tag by NEB in the late 1980s (http://www.neb.sg/applications/protein-expression-and-purification/coupled-protein-expression-and-purification/maltose-binding-

protein-expression). The fusion can be bound by amylose resin and eluted with maltose.

1.9.5.5 Expression with pelB signal (export tag)

pelB leader sequence is a sequence of 22 amino acid residues, which when attached to any protein, exports it to the bacterial periplasm. pelB specifically refers to pectate lyase B of *Erwinia carotovora*. The gene sequence of this signal must be attached to the gene of interest to transport the translated sequence to the periplasm, where the signal is processed leading to the accumulation of the target protein. The transport from cytoplasm to periplasm is mediated mostly by the Sec-pathway or the Tat pathway. In Sec dependent pathway, SecB (cytosolic chaperone) or the ribonucleoprotein SRP (signal recognition particle) binds to the unfolded preprotein harboring the N-terminal signal and transports then to inner membrane bound SecA (Yoon et al., 2010). Proteins entering the bacterial periplasmic space are exposed to a relatively oxidizing environment, hence aids in the formation of disulphide bonds in structurally complex proteins.

1.9.6 pET vector system for bacterial expression

The most powerful system developed till date for the cloning and expression of recombinant proteins in *E. coli* is the pET system. pET vector system is derived from the pBR322 plasmid and modified to take the advantage of the

T7 bacteriophage gene 10. This promotes high-level transcription and translation by the encoded RNA pol that is highly specific for the T7 promoter sequences, rarely found in genomes other than T7 phage. Target genes are silent in the uninduced state, preventing expression (important if genes expressed are toxic for the cell) and upon induction, the target gene will only be transcribed by highly active polymerase. The T7 RNA pol is so active and selective that, when fully induced, most of the cell's resources are diverted to target gene expression, such that the target product could constitute more than 50% of cell's proteins in a few hours of induction (Novagen pET manual, 10th edition).

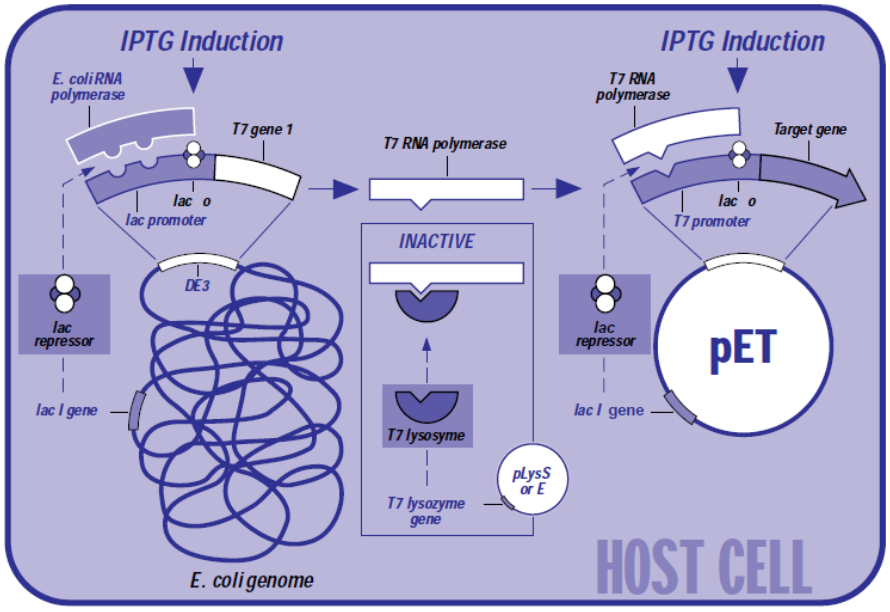

Figure 1.6 Control elements of the pET system

Components of the pET expression vector system (Source: Novagen pET manual, 10th edition)

1.10 Aim and scope of the study

Prokaryotic PLA_2 from *Streptomyces violaceoruber*, shows an unusual property to be secreted into the culture medium, instead of its retention in the bacterial periplasmic space when overexpressed in *E. coli* using the pelB periplasmic signal. The PLA_2 secreted to the medium was shown to be completely active and a total yield of 20 mg/l culture supernatant. The PLA_2 having two disulphides was efficiently folded with a considerably good yield, gave us an idea to use its potential to export other complex disulphide rich proteins of interest to the extracellular medium. Moreover, this molecule is structurally the least complex with two disulphide bonds and one of the smallest among PLA_2 enzymes. Having a unique structure with its catalytic core separated from the N-terminal 2-helix bundle, provided us a model to design a mini PLA_2 scaffold.

In this thesis we wanted to exploit the two interesting and unique features of the prokaryotic phospholipase A_2 to

1. **Design an extracellular expression system**

- Using the full length prokaryotic PLA_2 as a tag for expression of disulphide rich proteins in the extracellular medium
- Study of minimal region of prokaryotic PLA_2 for necessary for export
- Study of properties of the tag: point mutations and culture conditions

2. Design a mini PLA_2 scaffold

- Design, expression and refolding of 1st generation mutants (Δ Helix 1 and Δ Helix 1 & 2)
- Structural and functional assessment of the 1st generation mutants
- Design, expression and refolding of 2nd generation mutants (Δ Helix 1 & 2- F66Q-Y71Q)
- Structural and functional assessment of the 2st generation mutants

CHAPTER TWO

Prokaryotic PLA_2 as a tag for extracellular expression

2 CHAPTER TWO: Prokaryotic PLA_2 as a tag for extracellular expression

2.1 Introduction

Recombinant protein expression has been one of the key technologies in the advancement of our understanding of numerous biological processes. As the increasing research and commercial applications require large quantities of high quality proteins, the strategies for efficient production of recombinant proteins are gaining importance (Terpe, 2006).

Until date, although there are several well standardized systems for overexpressing proteins there are various limitations in each of these systems pertaining to soluble protein production and correct folding of disulphide rich proteins.

The prokaryotic PLA_2 exhibits a unique property of being secreted into the culture medium when expressed with pelB periplasmic signal (Takemori et al., 2012). Therefore we wanted to exploit this unusual property of the prokaryotic PLA_2 to design an extracellular expression system.

Structurally complex proteins containing multiple disulphides are difficult to express in correctly folded, soluble form using bacterial expression systems. The reducing environment of bacterial cytoplasm does not provide the optimal condition for disulphide bond formation, hence leads to protein misfolding and inclusion body formation. Although refolding proteins from the inclusion body

is the only way to produce structurally complex disulphide rich proteins in reasonable quantities, the method and the steps involved are often painstaking (Cabrita and Bottomley, 2004). Moreover, the refolding conditions need to be developed strategically and often empirically to get a considerable yield of the final refolded protein.

The prokaryotic PLA_2 which is secreted into the extracellular medium, first enters the periplasmic space (with relatively more oxidizing environment compared to cytoplasm) where the signal is processed, following which it exits the periplasm into the culture medium. This type of expression pathway not only provides the disulphide rich proteins a suitable environment to fold correctly, but also eases the downstream purification strategies. Additionally, being an enzyme, the extent of extracellular expression could be readily evaluated from the total activity in the culture medium using any simple assay technique.

With the ease of handling and robustness of bacterial system combined with advantages of folding disulphide rich proteins (usually seen in expression system involving higher organisms), this system could provide us a valuable tool to express other complex proteins.

In this chapter we look into a few aspects of the prokaryotic PLA_2 to design an extracellular expression system. Primarily we have used the molecule as an expression tag to express other target proteins in the culture medium.

Furthermore, we have also tried to study the minimal region for export and effect of mutations and culture conditions on the overall expression.

2.2 Materials and Methods

2.2.1 Materials:

Materials used in the experiments were obtained from the following sources:

Codon optimized synthetic DNA of prokaryotic PLA_2 was cloned in pUC-57 from Genscript corporation (Piscataway, NJ, USA). $sPLA_2$ assay kits were purchased from Cayman Chemical (Ann Arbor, MI, USA). Luria Burtani - broth and agar (Q.BIOgene, Irvine, CA, USA), QIAquick gel extraction kit (Qiagen, Hilden, Germany), HiFi polymerase (KAPA Biosystem, Cape Town, South Africa), Fast Digest Nde1 and Xho1 restriction enzymes, T4 DNA Fast Ligase, (Fermentas, Ontario, Canada), DNA Gene ruler (Fermentas, Ontario, Canada), pET-22b vector (Novagen, Merck biosciences), DNA oligos for amplification from 1st Base Asia (Singapore), plasmid extraction kit (GeneAll plasmid miniprep kit, Korea), Big Dye (Life Technologies, Carlsbad, USA), Precision Plus Protein™ Dual-Colour Standards (Biorad, Hercules, CA, USA), acetonitrile and trifluoroacetic acid, formic acid (Merck KGaA,Darmstadt, Germany), Tris-HCl, Urea, NaCl from 1st Base Asia (Singapore, Singapore), methanol (Merck chemicals, NY, USA), RP- Jupiter C18 columns (300 Å, 5 μm, 250 mm X 21.2 mm and 250 mm X 10 mm) from Phenomenex (Torrance, CA, USA), Hi-Prep 16/60 gel filtration column and Hi-Trap-Sulfopropyl (SP)-Sepharose column (GE healthcare, Little chatfont, UK)..

CHO-K1 cell line (American Type Culture Collection, Manassas, VA, USA), tissue culture plates (Corning, NY, USA), trypsin and trypsin neutralizer (GIBCO, Invitrogen, CA, USA), L-NAME, indomethacin, Dulbecco's Modified Eagle's Medium (DMEM), IBMX, saline, heparin (5000 IU/ml), penicillin-streptomycin, ODQ (Cayman Chemical, Ann Arbor, MI, USA), BSA (Sigma-Aldrich, St. Louis, MO, USA), sodium pentobarbital (NUS, Pharmacy, Comparative medicine).

2.2.2 Cloning of prokaryotic PLA_2 and mutants

The DNA sequence encoding prokaryotic PLA_2 in *Escherichia coli* was optimized for expression. The obtained synthetic gene was cloned using pUC57 vector. This gene fragment was amplified by both forward and reverse primers containing restriction sites Nco1 and Xho1, using the sequence from gene of interest. Synthetic DNA (0.1 μg) containing plasmid was amplified with 1 μl of 10 μM primer stock, 1 μl of 10 mM dNTPs, 1 unit of KAPA HiFi polymerase and 10 μl of 5X PCR buffer containing $MgCl_2$ in a 50 μl reaction. The amplification cycling parameters were programmed to one cycle of 98 ºC for 2 min, 35 cycles of 98 ºC for 10 s, 60 ºC for 30 s and 72 ºC for 45 s, and a final extension at 72 ºC for 7 min. The product amplified was fractionated using 1% (w/v) agarose gel electrophoresis. The obtained product was extracted from the gel using the Qiagen gel extraction kit using the manufacturer's protocol.

Both DNA fragments and pET-22b (vector into which the DNA fragment is to be cloned) were double digested with Nco1 and Xho1 enzymes (1 unit enzyme

per μg DNA) for 30 min at 37 °C. Digested pET-22b was fractionated on 1 % (w/v) agarose gel and band corresponding to the linear plasmid was extracted from the gel. The double digested DNA fragment of PLA_2 produced was subjected to PCR purification. Concentrations of the purified digested DNA fragments and the vector were estimated using NanoDrop ND-1000 Spectrophotometer (NanoDrop Technologies) with software ND-1000 V3.3.0. The DNA fragments (insert) and vector were ligated at 3:1 molar ratio. To ligate the DNA fragments with vector, 1 unit of T4 DNA ligase along with 2 μl of 5X ligase buffer were added to the mixture of a total volume of 10 μl and was incubated at 4 °C for overnight.

The point mutations in the protein sequence were inserted by site directed mutagenesis. For the mutagenesis experiments, the desired mutations were incorporated into the forward and reverse primers designed specifically for this purpose. A PCR reaction was performed using the mutagenic primers following the protocol as described earlier. 20 μl of the reaction mixture was digested with Dpn1 enzyme at 37 °C for 1 h. 5 μl of this digested solution was used for transforming competent cells, as described below. Plasmid isolation and DNA sequencing was performed to confirm the presence of mutation, as described below.

2.2.3 Preparation of competent cells and transformation

The competent cells for *E. coli* JM109 (copy number increase strain) and BL21 DE3 (expression strain) were prepared and used for experiments in this study. The cell stocks were thawed and streaked on antibiotic free LB agar plates and were grown at 37 °C for 16 h. The following day, a single colony from plate was inoculated in 2 ml of antibiotic free LB broth and was cultured at 37 °C, 200 rpm, 16 h. 1 ml of the overnight culture was used to inoculate 100 ml of antibiotic free LB broth and was grown until the optical density (OD) at 600 nm reached a value between 0.6-1 OD at 37 °C, 200 rpm. The bacterial culture was poured into an ice-cold falcon tube and centrifuged at 2000 g, 4 °C for 10 min. The supernatant was discarded as waste and the cells were resuspended in 1 ml of 100 mM $CaCl_2$ that was further diluted to 50 ml with the same solution. This mixture was kept on ice for 40 min, following which it centrifuged at 2000 g, 4 °C for 10 min. The cell pellet was resuspended gently in 8-10 ml of 100 mM $CaCl_2$ containing 10% glycerol (sterilized) and was split into 50 µl aliquots in pre-chilled 1.5 ml Eppendorf tubes.

These prepared competent cells were transformed using the plasmid DNA. Vial containing cells was thawed on ice and the ligation mix was added and allowed to incubate on ice for 30 min. After incubation, the cells were subjected to heat shock at 42 °C for 90 sec and were immediately transferred on ice for 5 min. This was followed by the addition of 200 µl of LB broth to revive cells by incubating at 37 °C, 200 rpm for 30 min. This transformed

mixture was spread on ampicillin (100 μg/ml) containing LB agar plate. The plates were incubated at 37 °C for 16- 18 h.

2.2.4 Plasmid isolation and DNA sequencing

Isolated transformants from the plates were inoculated in 2 ml ampicillin (100 μg/ml) containing LB broth and cultured for 16 h at 37 °C, 200 rpm. Plasmids were isolated from the cultured cells using GeneAll™ plasmid extraction kit, using the manufacturer's protocol. Concentration of the DNA was estimated as described previously.

The plasmid DNA was sequenced using ABI PRISM® Big Dye™ Terminator Cycle Sequencing Ready Reaction Kit (version 3.0) (PE-Applied Biosystems, CA, USA). Each 5 μl reaction constituted, 100 ng of plasmid DNA that was mixed with 2 μl of BigDye™ and 1 μM T7 promoter or terminator primers.. The reactions were amplified using the following conditions: 25 cycles of denaturation at 96 ºC for 10 s, annealing at 50 ºC for 5 s and extension at 60 ºC for 4 min. The PCR product was purified using Cleanseq magnetic beads and the purified DNA was dissolved in 40 μl of autoclaved water. The obtained DNA mixture was loaded on to automated ABI PRISM® 3130XL Genetic Analyzer (Applied Biosystems, Foster City, CA, USA). The sequences were analyzed using FinchTV and Generunner softwares.

2.2.5 Expression of prokaryotic PLA_2

After validating the sequence, clones encoding the fusion protein were transformed into *E. coli* expression strain BL21 DE3 as described previously.

A single colony was inoculated in 100 ml of ampicillin (100 µg/ml) containing LB Broth and grown for 16 h at 37 °C at 200 rpm. This culture was used for inoculating 500 ml LB broth containing 100 µg/ml ampicillin in 1: 100 (culture: broth) ratio and was grown at 37 °C, 200 rpm until the cell density reached ~ 0.6 OD at 600 nm. Protein expression was induced using 0.02 mM IPTG (isopropyl *β*-D-thiogalactoside) and the culture was grown further at 27 °C, 150 rpm for 16-18 h. The cells were then harvested by spinning at 5,000 g for 15 min at 4 °C. Both cell pellet and the culture supernatant were checked for the expressed protein. The expression of recombinant protein was fractionated using SDS-PAGE on a 15% polyacrylamide gel.

Bio-Rad Mini-PROTEAN™ gel system was used for running SDS-PAGE. Sample preparation was carried out by mixing 20 µl of sample and 5 µl of 5X loading dye and incubated the mixture at 100 °C for 10 min. The samples were centrifuged at 10, 000 g and 10 µl of this mixture was used for loading on to the gel. On the first lane molecular weight ladder, Precision Plus Protein™ Dual-Colour Standards (5 µl) was added. Electrophoresis separation was carried out at 120 V until the dye front reached the base of the gel. The gel was stained with Coomassie Brilliant Blue-R250 for the visibility of the protein bands.

2.2.6 Purification of prokaryotic PLA_2

The expressed protein was purified in several steps. First the culture supernatant was fractionated by ammonium sulphate precipitation. The protein

was salted out at 50% ammonium sulphate saturation. Salt precipitation was performed at 4 °C by gradual addition of salt with continuous stirring. After completion of salt addition, the culture supernatant was stirred for additional 4 h to ensure complete salt dissolution and precipitation. The saturated solution was next centrifuged at 8000 rpm (rotor radius =80 mm) for 30 min and the precipitate was dissolved in 10 ml deionised water. This salted out sample was further purified by gel filtration chromatography using Superdex 75 column (GE Healthcare Life Sciences, Little Chatfont, UK) in 50 mM Tris-HCl pH 8. The peaks from the purification profile were run on SDS-PAGE to confirm the presence of the expected protein.

2.2.7 Cloning, expression and purification of PLA_2-ΔHelix KNP and PLA_2-Denmotoxin

For cloning the PLA_2 fusion protein sequences, the two fragment genes were joined by extension overhang PCR technique with the incorporation of restriction sites, linker and protease cleavage sites. Briefly, the individual segments were amplified with specific primers designed such that the forward primer of the first segment contained the restriction site and reverse primer contained the linker and protease site sequences. For the second segment the forward primer contained the sequences complimentary to the linker and protease site and the reverse primer contained the restriction site. Following the first step of PCR amplification as described above, equal volumes of the two PCR products and the forward primer for the first segment and reverse

primer for the second segment were used in a second step PCR amplification as described earlier. The fusion gene was cloned by double digestion and ligation technique as described above. Strategies of expression involved were same as described above. The fusion proteins were purified by size exclusion chromatography as described above. The peak containing the fusion protein was identified by SDS-PAGE analysis and the mass of the fusion protein was analysed using Electrospray-ionization (ESI) - Mass Spectrometer (MS) (LCQ Fleet Ion trap, Thermoscientific, Massachusettes, USA). The fusion protein was next subjected to protease cleavage using recombinantly expressed and purified TEV protease in the ratio 50:1 (fusion protein:TEV protease) in 50 mM Tris-HCl containing 0.5 mM EDTA pH 8, overnight at 4 °C. The cleavage product was purified by cation exchange chromatography, performed with 50 mM Tris-HCl pH 8 as buffer A and 50 mM Tris-HCl, 1 M NaCl pH 8 as buffer B, on a Hi-Trap SP Sepharose column (34 μm, 16 X 25 mm). Next the cleaved protein peak of ion exchange chromatography was purified to homogeneity using RP-HPLC with Jupiter C18 column (5 μm, 300 Å, 250 mm X 10 mm) with buffer A- 0.01 % TFA and buffer B- 0.01% TFA with 100% Acetonitrile on a linear gradient of 20-40% B. Purified protein peak was analysed on ESI-MS for its purity and freeze dried. The protein was later reconstituted in phosphate buffer saline (PBS) and quantified by absorbance at 280 nm before performing the assay.

2.2.8 Cell culture

CHO-K1 cells was preserved in high-glucose Dulbeco's modified eagle's medium (DMEM) supplemented with 10% foetal bovine serum (FBS), 100 µg/ml streptomycin and 100 U/ml penicillin and 2 mM glutamine in a humidified incubator at 37 °C with 5% CO_2. The cells were sub-cultured by trypsinization once every three days. The density of cells was obtained from Bio-Rad TC20™ automated cell counter.

2.2.9 NPR-A plasmid preparation

Plasmids encoding NPR-A and NPR-B were generously gifted by Prof. Micheala Kuhn (University of Wurzburg) and Dr. Ruey-Bing Yang (Academia Sinica). The plasmids were transformed into JM109 as reported previously. A single colony of the transformant was inoculated in 100 µg/ml ampicillin containing 100 ml of LB broth and was grown at 37 °C, 200 rpm for 22-24 h. The cells were harvested by centrifuging at 5,000 g for 20 min and the plasmids were extracted as per the manufacturer's protocol using Pureyield™ plasmid maxiprep kit (Promega). The DNA concentration was estimated using nanodrop as described previously.

2.2.10 Transfection of CHO-K1 cells

1×10^5 cells were seeded per well in a 24- well plate. The cells were grown for ~20-22 h before transfection. The used media was aspirated from the wells and

refilled with 400 µl of DMEM containing 10% FBS without any antibiotics. Each well was maintained with 0.8 µg plasmid diluted in 50 µl of serum free DMEM media. Then 2 µl of lipofectamine™ 2000 was diluted in 50 µl of serum free DMEM media was added. Diluted DNA and transfection reagents were thoroughly mixed and allowed to stand at room temperature for 10-15 min. The DNA- lipofectamine mixture (100 µl/ well) was directly transferred to the cells within 30 min. The cells were incubated with the DNA-lipid complex for 6 h at 37 °C with 5% CO_2. After 6 h the media containing DNA and lipofectamine was aspirated and replaced with DMEM containing 10% FBS and antibiotics. These cells were incubated at 37 °C with 5% CO_2 for 16-20 h before it was treated with the peptides.

2.2.11 Whole cell cGMP elevation assay

CHO-K1 cells transfected either with NPR-A/ NPR-B/ empty-vector pCMV4.0 were used for the experiments. Post transfection, aspirated media and cells were washed with 500 µl of PBS. The cells were incubated for 30 min after adding 150 µl of 0.5 mM IBMX containing vascular growth media. Meanwhile, peptides were reconstituted in 4X concentrations. After incubation for 30 min, 50 µl of peptide solution was added to the cells, followed by further incubation for 30 min at 37 °C with 5% CO_2. Subsequently, peptide containing basal media was removed and changed to 150 µl of 0.1 M HCl.This mixture was incubated at room temperature for 30 min with shaking at 50 rpm. The cell lysates were collected and the cGMP levels were estimated using

Enzo life sciences cGMP ELISA kit, as described in the manufacturer's protocol. The total protein of the cell lysates from a few wells was estimated by BCA (bichinchonic acid) assay and the results were used to normalize across different 24 well plates used. Three independent experiments were carried out for each peptide and the statistical comparison between ANP and ΔHelix KNP related peptides was conducted using one-tail ANOVA with t-test and curves with a P-value <0.05 was considered as significant difference.

2.3 Results

2.3.1 Expression and purification of wild type prokaryotic PLA_2

The wild type PLA_2 was expressed and purified as a control. The enzyme was expressed by the optimized protocol described above (materials and methods). The culture was done in 2.8 l flask with 500 ml LB broth to provide sufficient head space for adequate aeration during the incubation. Following 18 h incubation at 27°C post induction, the culture was centrifuged and the supernatant was analyzed on SDS PAGE to confirm the extracellular expression of the wild type PLA_2 (Figure 2.1 a). After confirmation of expression, the culture supernatant was salted out to 50% saturation by ammonium sulphate. The precipitate was purified by size exclusion chromatography by loading onto GE Superdex 75 prep column The protein peak indicated by an arrow (Figure 2.1 b) was analyzed by ESI LCMS to confirm the fully oxidized mass (Figure 2.1 c). After confirmation of the mass, the peak was pooled and lyophilized.

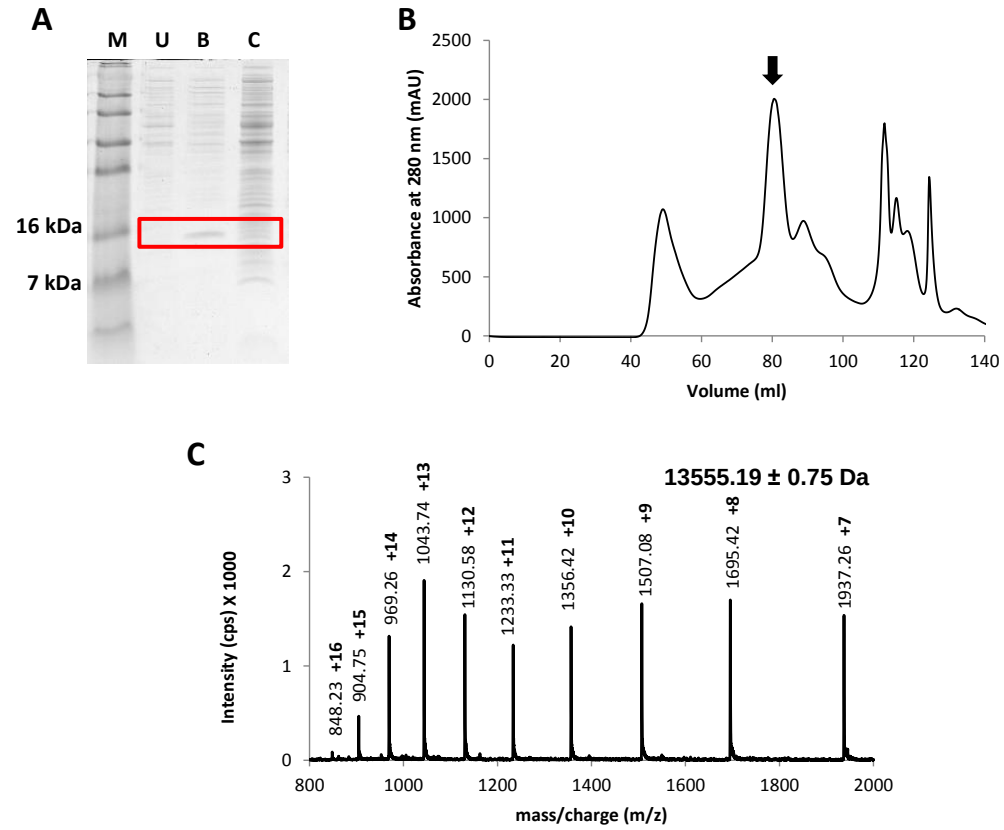

Figure 2.1 Expression and purification of wild type PLA_2

A. SDS PAGE analysis showing extracellular expression of wild type PLA_2. M- Marker, U- Uninduced whole cell lysate, B- Culture broth, C- Induced whole cell lysate.
B. Purification of wild type PLA_2 by size exclusion chromatography using superdex 75 prep column.
C. Mass of the protein determined by ESI Ion-Trap mass spectrometry.

2.3.2 Using full length PLA_2 as a tag for extracellular export

The prokaryotic PLA_2 exhibited an unique property to be secreted into the extracellular medium, instead of its retention in the periplasmic space. Therefore our first aim was to use the full length molecule for the expression of other target proteins extracellularly.

2.3.2.1 Construct design to express PLA_2-ProteinX extracellularly

Since the prokaryotic PLA_2 was exported to the extracellular media when expressed with pelB periplasmic signal, to use it as a tag to express other proteins in the culture media, the foremost thing was to design a general construct outline (Figure 2.2) where gene sequence corresponding to any protein of interest could be inserted. As shown in the figure, the segment containing the pelB signal, prokaryotic PLA_2 and gene of interest ending with a stop codon would be then ligated in between Nde1 and Xho1 in pET 22b vector.

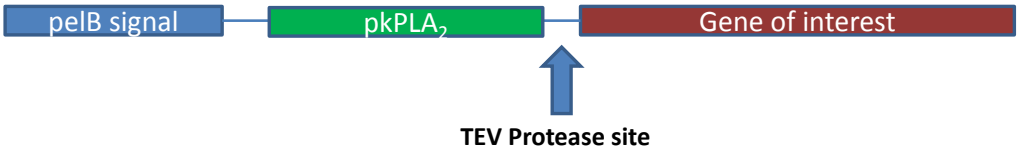

Figure 2.2 Design of construct to use the full length PLA_2 to express other proteins of interest

General design of sequence of genes in the construct for extracellular expression. Gene sequences of pelB signal and prokaryotic pla_2 are joined to the gene of interest with a linker containing the TEV protease site by overhang extension PCR. The entire gene construct is cloned between Nde1 and Xho1 in pET 22b vector.

2.3.2.2 Design and cloning of PLA_2-ΔHelix KNP fusion gene in pET 22b vector

In order to test our system for extracellular expression, the first test protein we selected was a natriuretic peptide, first identified from the cDNA library of the venom gland of Krait (*Bungarus flaviceps)*. This molecule is small in size with

a molecular weight 3855.4 Da and relatively simple with only one disulphide bond (Figure 2.3).

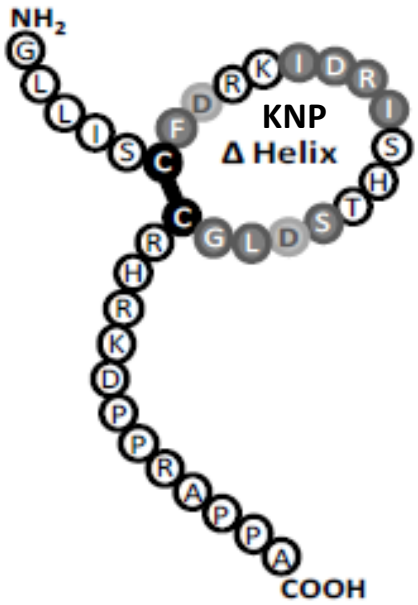

Adapted from thesis, S. Sridharan 2014.

Figure 2.3 Structure of ΔHelix KNP

Representation of structure of ΔHelix KNP, a molecule with a relatively simpler structure with one disulphide bond and molecular weight of 3855.4 Da.

The ΔHelix KNP used in our study is a deletion mutant (residues 1-34) which lacks its short C-terminal helix, hence referred to as ΔHelix KNP. Although the molecule is relatively simple with respect to its structure, it was a difficult protein to express in *E. coli*. This molecule was unable to express in *E. coli* with 6x His tag and MBP tag, but could only be expressed with thioredoxin

tag as insoluble inclusion body protein as reported by earlier studies (Figure 2.4)

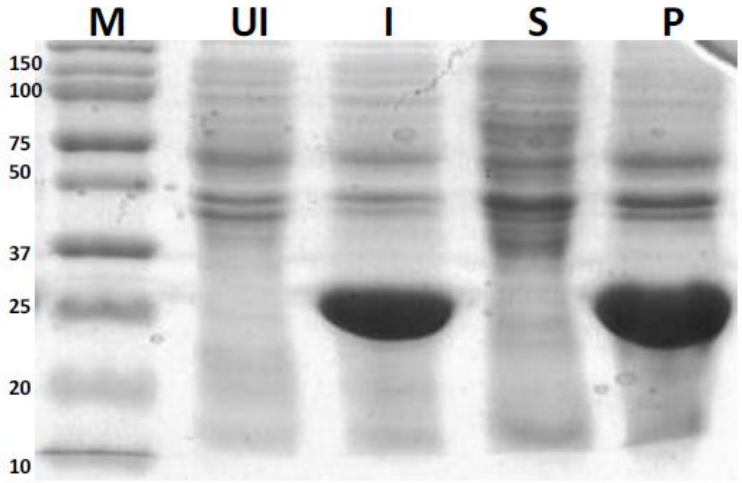

Adapted from thesis, S. Sridharan 2014.

Figure 2.4 Expression of ΔHelix KNP-thioredoxin fusion protein

SDS PAGE analysis showing the expression of ΔHelix KNP-thioredoxin fusion protein in the insoluble fraction in the form of inclusion body protein. M- marker, UI- uninduced, I- induced, S- soluble fraction of whole cell lysate, P- insoluble fraction of whole cell lysate.

Therefore, as shown is the figure, despite being a relatively small and simple molecule, it was equally difficult to express it in soluble form using bacterial expression system. Moreover purification and recovery of the protein from the inclusion body involved multiple steps and the final refolded purified protein yield was as low as 0.2 mg from 50 mg of fusion protein. Therefore we considered to use this protein as the first target to validate the feasibility of the proposed expression system.

The gene construct was designed as explained earlier, by joining the pelB-PLA_2 gene with the gene sequence of ΔHelix KNP with the inclusion of a protease cleavage site. Tobacco Etch Virus (TEV) protease was selected as the protease of our choice due to its ease of expression in bacterial system in our lab. The construct design and the protein sequence of pleB-PLA_2-ΔHelix KNP with protease site is elaborated in Figure 2.5 a and b.

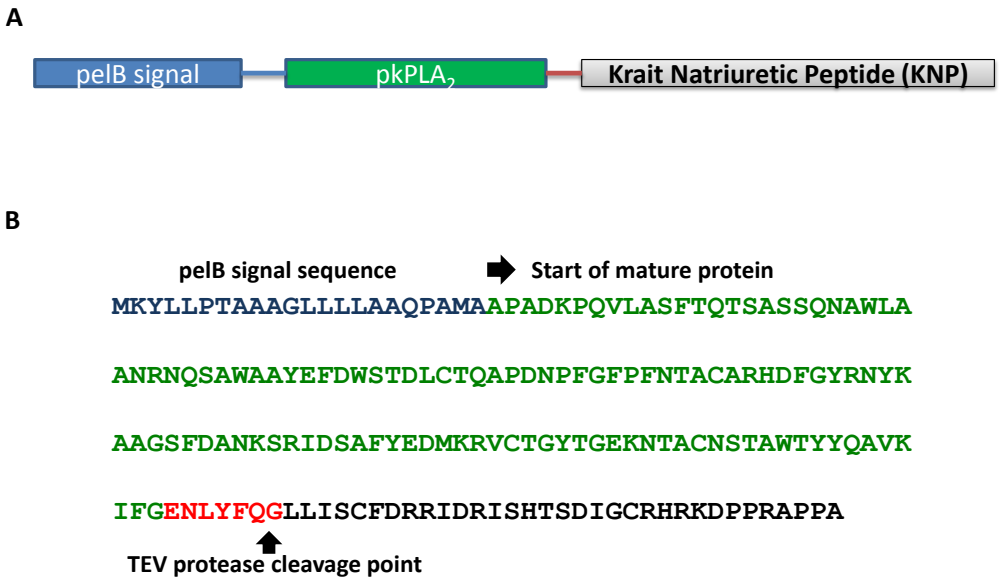

Figure 2.5 Design of PLA_2-ΔHelix KNP gene for extracellular expression

A. Schematic representation of a construct to express krait natriuretic peptide as a fusion partner of PLA_2 (tag) with TEV protease cleavage site as a linker between the tag and the target protein.
B. PLA_2 - ANP fusion sequence with pelB signal and TEV protease site.
Mature protein molecular weight is 18,187.1 Da.

This fusion gene was constructed and amplified by overhang extension PCR followed by cloning into pET 22b vector between Nde1 and Xho1 site. Finally the sequences were confirmed by DNA sequencing analysis prior to expression.

2.3.2.3 Expression and purification of PLA_2-ΔHelix KNP fusion protein

The PLA_2-ΔHelix KNP fusion protein was expressed by the optimized protocol followed for the full length PLA_2. After 18 h incubation at 27°C post induction, the culture was centrifuged and the supernatant was analyzed on SDS PAGE to confirm the extracellular expression of the fusion protein (Figure 2.6 a). The expressed protein in the culture supernatant was salted out by ammonium sulphate precipitation to 50% saturation. The salt precipitated protein was purified by size exclusion chromatography by loading on to GE Superdex 75 prep column (Figure 2.6 b). The fusion protein peak is shown by an arrow. The purified fusion protein was then run on ESI LCMS to analyze the molecular weight of the expressed protein (Figure 2.6 c). As shown in the figure, the molecular weight indicated the completely oxidized mass, giving us an idea that the fusion protein has formed all the 3 disulphide bonds, two from the tag (PLA_2) and one from the target protein ΔHelix KNP. The total yield of the purified fusion protein was estimated by Bradford protein assay using BSA as the standard. The yield per liter of culture supernatant was estimated to be 13.3±1.5 mg.

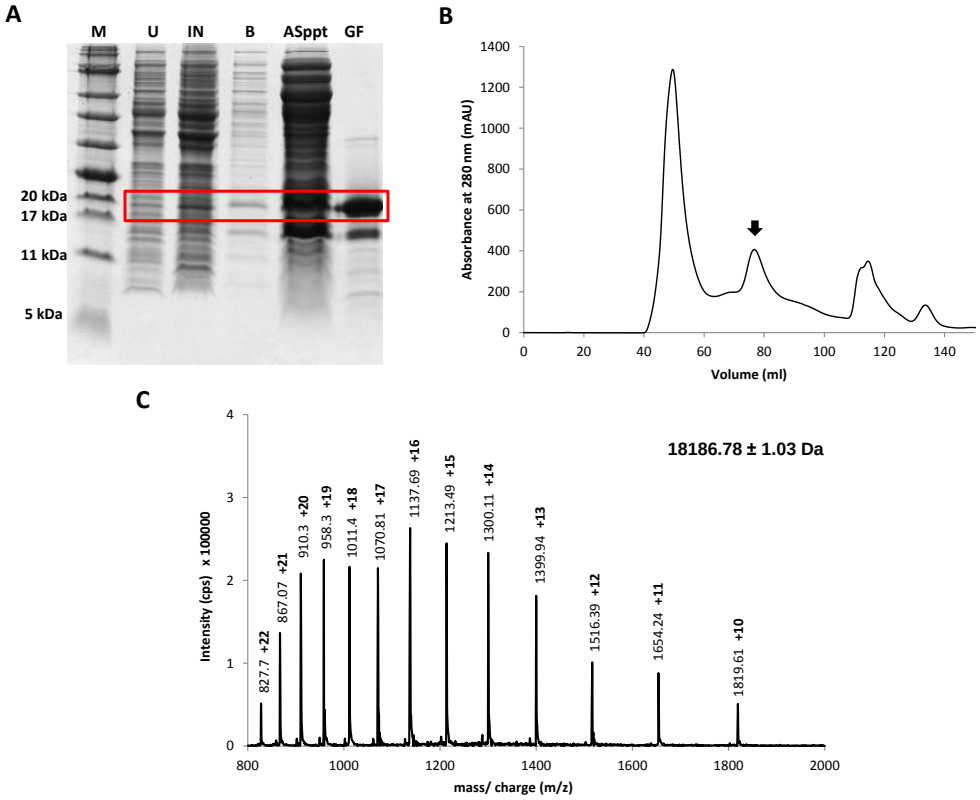

Figure 2.6 Expression and purification of PLA_2-ΔHelix KNP fusion protein

A. SDS PAGE analysis showing extracellular expression of PLA_2-ΔHelix KNP.
M- Marker, U- Uninduced whole cell lysate, IN- Induced whole cell lysate B- Culture supernatant, Asppt-Ammonium sulphate precipitate, GF-Protein peak from gel filtration chromatography.
B. Purification of PLA_2-ΔHelix KNP by size exclusion chromatography using Superdex 75 prep column, black arrow showing the peak corresponding to the fusion protein.
C. Mass of the protein determined by ESI Ion-Trap mass spectrometry .

2.3.2.4 TEV protease cleavage of fusion and purification of ΔHelix KNP

The fusion protein was subjected to TEV protease cleavage with a protein : protease ratio of 40:1 in the same buffer with 0.5 mM EDTA at 4°C for 16 h. The extent of cleavage is checked from SDS PAGE analysis (Figure 2.7 a)

performed by taking an aliquot after the above mentioned incubation time. As seen from the SDS PAGE analysis, the fusion band had reduced considerably with the increase in the PLA_2 tag band density, which gave us an approximate estimation of 80-90% cleavage efficiency. The cleavage reaction mix was next loaded on to a GE Hi trap SP HP cation exchange column, equilibrated with buffer A (50 mM Tris-HCl pH 8.0) and eluted with a linear gradient of 0-100 % buffer B (500 mM NaCl in 50 mM Tris-HCl). Figure 2.7 b depicts the purification profile by cation exchange chromatography, the ΔHelix KNP elution peak is indicated by an arrow. This peak was re-chromatographed by reversed phase chromatography by loading the sample onto a Jupiter C-18 analytical column (Figure 2.7 c). The purified ΔHelix KNP peak, shown by an arrow, eluted at around 30% B (buffer A: 0.1% TFA, buffer B: 0.1% TFA, 100% acetonitrile). The purified ΔHelix KNP was analyzed by ESI MS, which showed the expected oxidized mass (Figure 2.7 d). The peak was pooled and freeze dried. Later the freeze dried protein was reconstituted in 1x PBS for protein estimation and assay for biological activity. The total recovered ΔHelix KNP estimated by Bradford method was 0.5 ± 0.1 mg.

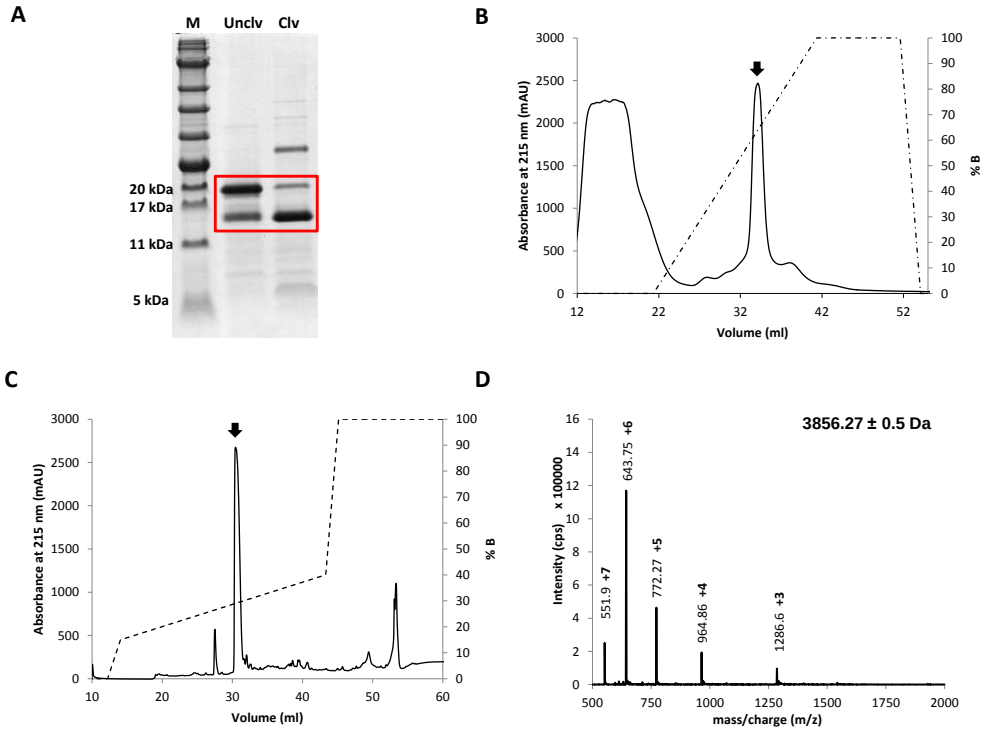

Figure 2.7 TEV protease cleavage of PLA_2-ΔHelix KNP fusion protein

A. SDS PAGE analysis showing TEV protease cleavage of PLA_2-ΔHelix KNP fusion protein.
M- Marker, Unclv- Uncleaved fusion protein, Clv- Cleavage products after 16 h incubation at 4°C.
B. Purification of the cleavage products by cation exchange chromatography using Hi-trap SP HP column, black arrow showing the peak corresponding to ΔHelix KNP.
C. Reversed phase chromatograpy of the peak from cation exchange purification, using Jupiter C18 column.
D. Mass of the protein determined by ESI Ion-Trap mass spectrometry.

2.3.2.5 Co-expression of truncated PLA_2-ΔHelix KNP fusion protein

Along with the fusion protein, we observed the expression of a second band of protein of mol. wt. between 10-15 kDa (based on the SDS PAGE marker), circled in Figure 2.8 a. We wanted to identify the protein as it consistently co-expressed in all batches of culture. Therefore we analyzed the protein by ESI

LCMS and deduced the mass of the protein (Figure 2.8 b). From the estimated molecular weight and the sequence of the fusion protein, the extra band of co-expressed protein was confirmed to be a truncated fusion protein, which stops just after the TEV protease cleavage site (Figure 2.8 c). The exact reason for the truncated protein expression though unclear to us, similar phenomenon is observed in the case of heterologous expression of complex proteins with well-known solubilization tags such as MBP and GST. Therefore most likely, ΔHelix KNP being a difficult to express target protein, exhibits similar phenomenon when expressed with PLA_2 as the tag.

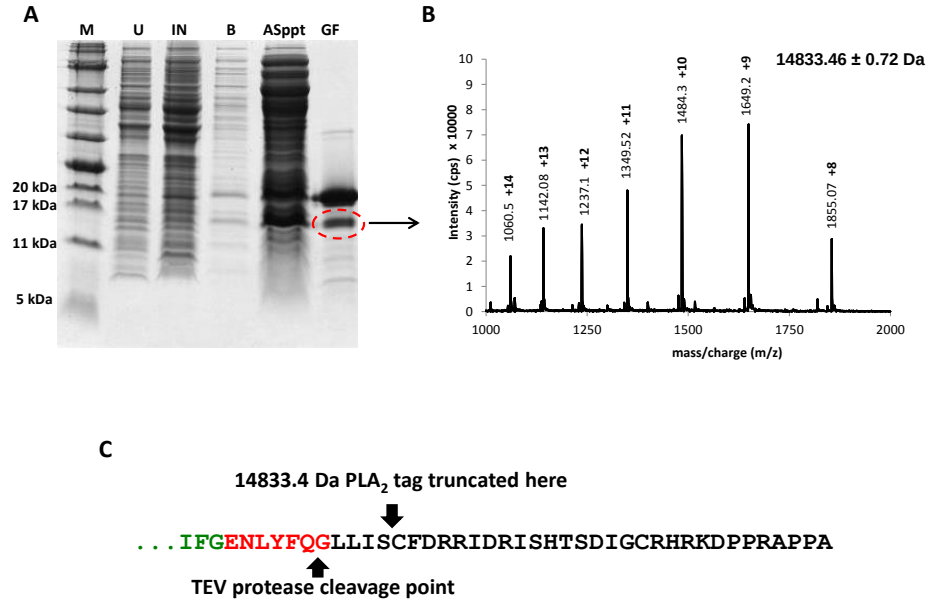

Figure 2.8 Co-expression of truncated PLA_2-ΔHelix KNP fusion protein

A. SDS PAGE analysis showing the truncated protein band (circled) of the fusion containing only the PLA_2 tag without ΔHelix KNP.
M- Marker, U- Uninduced whole cell lysate, IN- Induced whole cell lysate B- Culture supernatant, Asppt-Ammonium sulphate precipitate, GF-Protein peak from gel filtration chromatography.
B. Mass of the protein determined by ESI Ion-Trap mass spectrometry.
C. C-terminal end of PLA_2-ΔHelix KNP fusion protein, showing the point of truncation.

2.3.2.6 Assay for biological activity of ΔHelix KNP

After purifying the expressed and cleaved ΔHelix KNP to homogeneity, we further wanted to evaluate if the protein expressed using this system retains the same function as reported earlier. Therefore we went ahead to check its function by performing a cell-based assay. CHO K1 cells were transfected with plasmid containing NPR-A receptor gene, leading to the expression of NPR-A receptors on the CHO K1 cells. These cells were then treated with ΔHelix KNP in a dose dependent manner. The interaction of ΔHelix KNP with

NPR-A receptors led to cGMP response, which was measured. From the assay, the cGMP response elicited by ΔHelix KNP was 300 pmol/ml less than standard ANP, which is comparable to the earlier reported values (Figure 2.9). Therefore the ΔHelix KNP expressed by this method had a yield 2.5 times higher than the earlier reported values and retains the same biological activity.

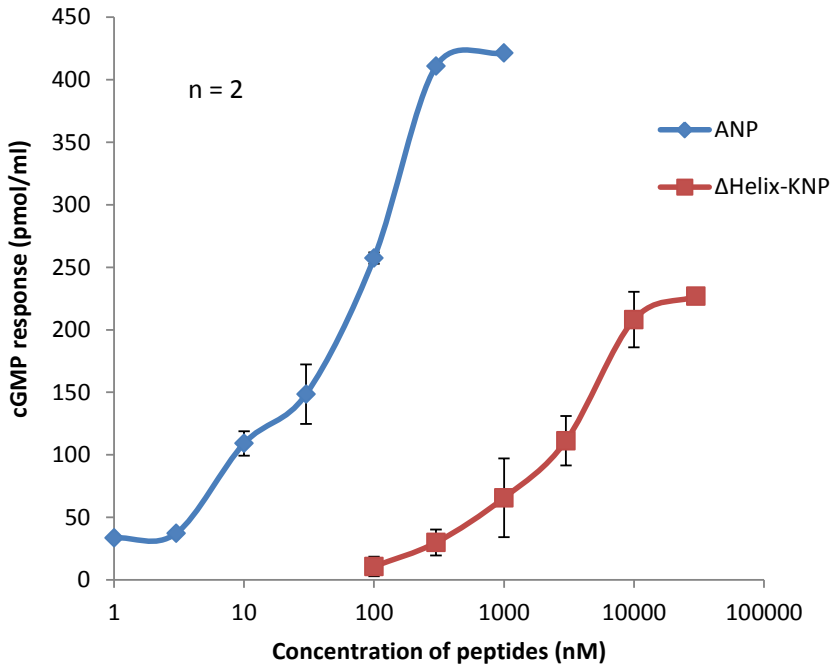

Figure 2.9 Functional assay for ΔHelix KNP

cGMP response of ΔHelix KNP compared with the standard ANP. cGMP response evoked by ΔHelix KNP was shown to be comparable to the reported values, which is 300 pmol/ml less than the standard ANP, taken as a positive control.

2.3.2.7 Design and cloning of PLA_2-Denmotoxin fusion gene in pET 22b vector

After our success with the extracellular expression of ΔHelix KNP using PLA_2 as a tag, we wanted to extrapolate this technique to test other target proteins with increased complexity. To test our system of extracellular expression using PLA_2 as a tag our next selected target protein was a three-finger toxin, denmotoxin. Denmotoxin is a three-finger neurotoxin from *Boiga dendrophila*. This molecule is relatively more complex than ΔHelix KNP, with five disulphide bonds and a molecular weight of 8524.87 Da (Figure 2.10).

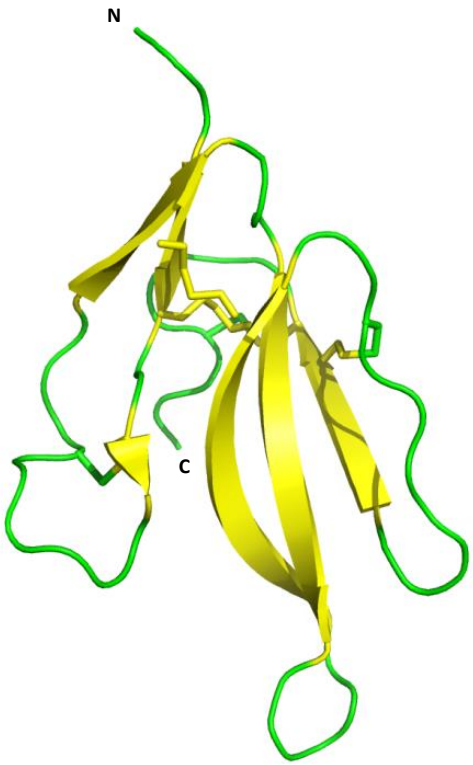

Figure 2.10 Crystal structure of denmotoxin (2H5F)

Representation of crystal structure of denmotoxin, a molecule with a relatively complex structure with five disulphide bonds and a molecular weight of 8524.87 Da.

Design of the gene construct and cloning into pET 22b vector was the same as followed in case of ΔHelix KNP, with the exception of addition of three extra glycines at the C-terminus of PLA_2 tag, which give a little more space for the access of the cleavage site by TEV protease. The construct design and the protein sequence of the fusion protein is depicted in Figure 2.11.

A

B

pelB signal sequence ➡ Start of mature protein

MKYLLPTAAAGLLLLAAQPAMAAPADKPQVLASFTQTSASSQNAWLA

ANRNQSAWAAYEFDWSTDLCTQAPDNPFGFPFNTACARHDFGYRNYK

AAGSFDANKSRIDSAFYEDMKRVCTGYTGEKNTACNSTAWTYYQAVK

IFGGGGENLYFQGAQAVGLPHGFCIQCNRKTWSNCSIGHRCLPYHMT

TEV protease cleavage point

CYTLYKPDENGEMKWAVKGCARMCPTAKSGERVKCCTGASCNSD

Figure 2.11 Design of PLA_2-DTX gene for extracellular expression

A. Schematic representation of a construct to express denmotoxin as a fusion partner of PLA_2 (tag) with TEV protease cleavage site as a linker between the tag and the target protein.
B. PLA_2 - DTX fusion sequence with pelB signal and TEV protease site.
Mature fusion protein molecular weight is 23153.8 Da.

2.3.2.8 Expression and purification of PLA_2-DTX fusion protein

PLA_2-DTX fusion protein was expressed using the same protocol followed in case of PLA_2-ΔHelix KNP. The SDS PAGE analysis of the culture supernatant (Figure 2.12 a) showed a band between 20-25 kDa. The culture supernatant was salted out to 50% saturation with ammonium sulphate. The precipitate was loaded on to GE superdex 200 prep column. The fusion protein peak is marked with an arrow in the chromatogram shown in Figure 2.12 b. The gel filtration peak was analyzed by ESI-LCMS and the molecular weight estimated was 23153.8 Da (Figure 2.12 c). The mass corresponds to the exact

expected oxidised mass of the fusion protein, taking into consideration the two disulphides in the tag and five disulphides in the target protein. This gave us an initial idea that the protein might be folded correctly, although cleavage of the tag and assessment of biological activity would confirm it. Moreover, the truncated PLA_2 tag was not found in case of this fusion protein expression. For estimating the yeild of the fusion protein, Bradford method was not followed due to the presence of contaminating proteins from the previous peak in the gel filtration elution, which would overestimate the total fusion protein. So we went ahead to calculate the yield from the total PLA_2 activity in the culture supernatent as the specific activity of PLA_2 was known.

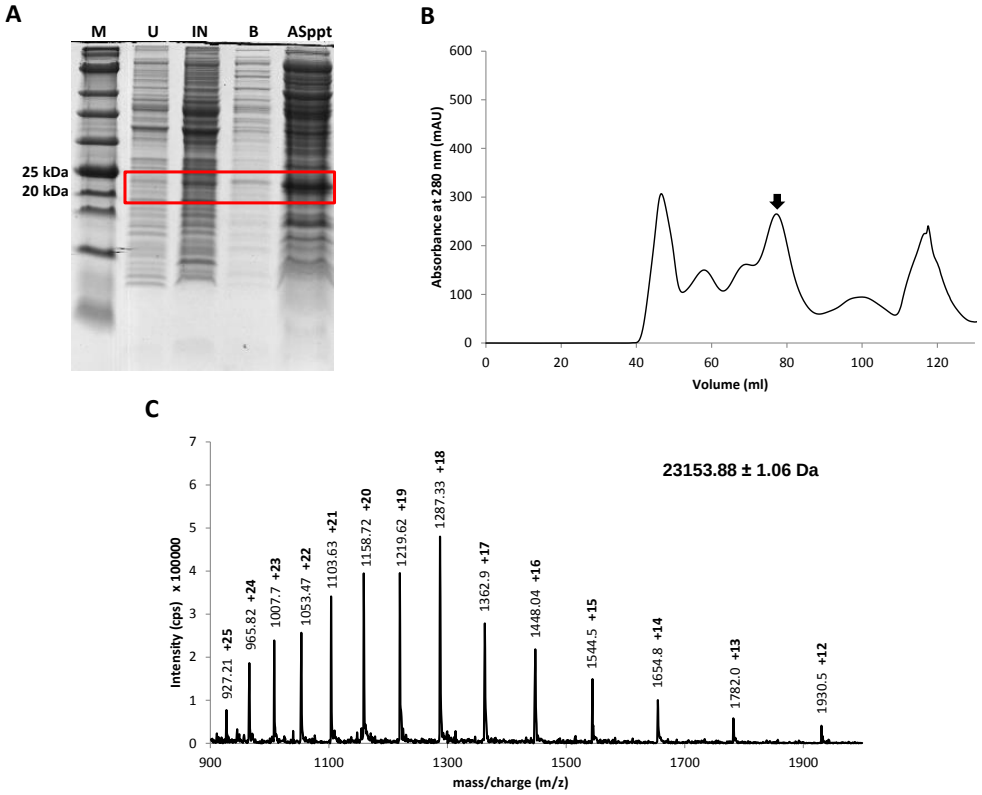

Figure 2.12 Expression and purification of PLA_2-DTX fusion protein

A. SDS PAGE analysis showing extracellular expression of PLA2-DTX.
M- Marker, U- Uninduced whole cell lysate, IN- Induced whole cell lysate B-Culture supernatant, Asppt-Ammonium sulphate precipitate.
B. Purification of PLA2-DTX by size exclusion chromatography using superdex 200 prep column, black arrow showing the peak corresponding to the fusion protein.
C. Mass of the protein determined by ESI Ion-Trap mass spectrometry.

2.3.2.9 TEV protease cleavage of PLA_2-DTX fusion protein

The fusion protein was set for cleavage reaction with TEV protease, using the same ratio of protein : protease as described earlier. But unfortunately, the fusion protein was resistant to TEV protease even after increasing the protease concentration in the cleavage reaction (Figure 2.13 a). We observed the precipitation of TEV protease in the cleavage solution (Figure 2.13 a, lane 5),

hence the ineffectiveness of TEV protease was thought to be due its lesser availability in the cleavage reaction due to precipitation.

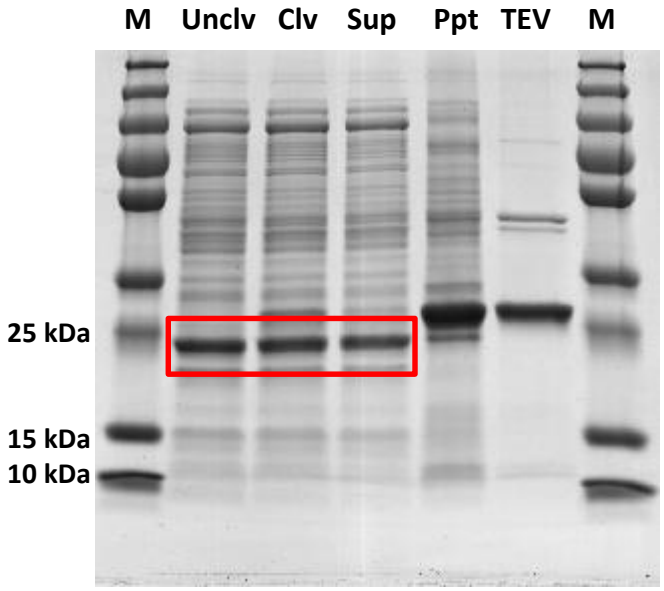

Figure 2.13 TEV protease cleavage of PLA_2-DTX fusion protein

SDS PAGE analysis of TEV protease cleavage reaction of PLA_2-DTX fusion protein.
M- Marker, Unclv- Uncleaved fusion protein, Clv- Cleavage products after 16 h incubation at 4°C, Sup-supernatant after centrifuging the cleavage reaction, Ppt-precipitate, TEV-TEV protease used in cleavage reaction, for reference.
As seen from the SDS PAGE analysis, no cleavage occurred after incubation with TEV protease. Moderate precipitation was observed, which was due to precipitation of TEV protease.

Therefore our first troubleshooting step was to change the TEV site in the construct with a protease which has a better solubility when compared to TEV. In this case we considered the HRV 3C protease.

2.3.2.10 Swap of cleavage site and HRV 3C protease cleavage of PLA_2-DTX fusion protein

The cleavage site was swapped with HRV 3C protease site as shown in Figure 2.14 a. After cloning the gene with the new protease site, followed by its expression and purification as described earlier for the same fusion with TEV site, the cleavage of the fusion was performed. But unfortunately, the fusion protein showed resistance to cleavage with HRV 3C protease site, even at a very high protease concentration (1:1 w/w) as shown in Figure 2.14 b and c.

A

PLA$_2$.....AVKIFGGGGENLYFQ/GAQAVGLPH.....DTX

PLA$_2$.....AVKIFGGGGLEVLFQ/GPQAVGLPH.....DTX

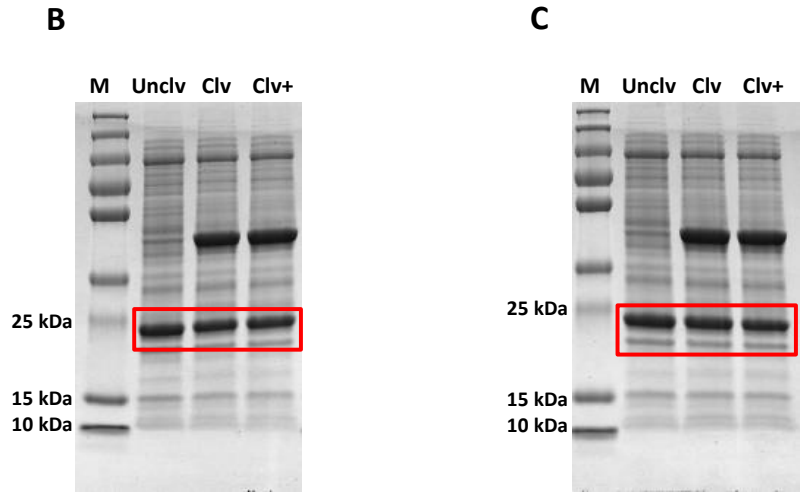

Figure 2.14 HRV 3C protease cleavage of PLA$_2$-DTX fusion protein with HRV 3C protease site

SDS PAGE analysis of HRV 3C protease (marketed as prescission protease by GE) cleavage reaction of PLA2-DTX fusion protein.
M- Marker, Unclv- Uncleaved fusion protein, Clv- Cleavage products after 16 h incubation, Clv+- Cleavage performed in presence of 1 mM DTT

A. Sequence of TEV protease site (top) and HRV 3C protease site (bottom) compared.
B. Cleavage reaction performed at 4°C
C. Cleavage reaction performed at 25°C

As seen from the both the SDS PAGE analysis, no cleavage occurred after incubation with HRV 3C protease.

Therefore the problem might be related to the linker, being of insufficient length for the access of the protease at the cleavage site due to stearic hindrance. Our current experiments are focused on increasing the linker length between the PLA$_2$ tag and target protein.

With this we move into the next aim of the chapter, to identify minimum region of the PLA_2 which retains the property of extracellular export.

2.3.3 Study of minimal region of PLA_2 required for export

Since the whole molecule was able to express target proteins extracellularly in reasonable amounts, we wanted to recognize minimum region of the molecule which could hold on to the property of extracellular secretion. This would not only make the tag smaller, reducing the burden of cellular resources used by the bacteria to synthesize the tag itself, but also give us insights about the region of the molecule responsible for the export. Moreover, if minimal PLA_2 domains could be expressed extracellularly, it could be readily assessed for function, which is the scope of our later part of the study regarding designing of minimized PLA_2 scaffolds, elaborated in the 3rd chapter of the thesis.

2.3.3.1 Design of truncated mutants to identify minimal region responsible for the export

To identify minimal region for export, truncated mutants were generated (Figure 2.15). As shown in this figure, the wild type enzyme is compared with the various truncated mutants generated. The first mutant is Helix 1 & 2 with only the first two helices (Figure 2.15 B, b). The second mutant is Δ Helix 1 &

2 in which the first two helices are removed (Figure 2.15 C, c). The third mutant was designed with deletions in between the helices 4th and 5th. This was done to make the helices shorter by one turn each, with a total reduction of 8 residues, as a strategy for minimizing the enzyme (Figure 2.15 D, d). Cloning was done in pET 22b in the same fashion as described for the full length enzyme.

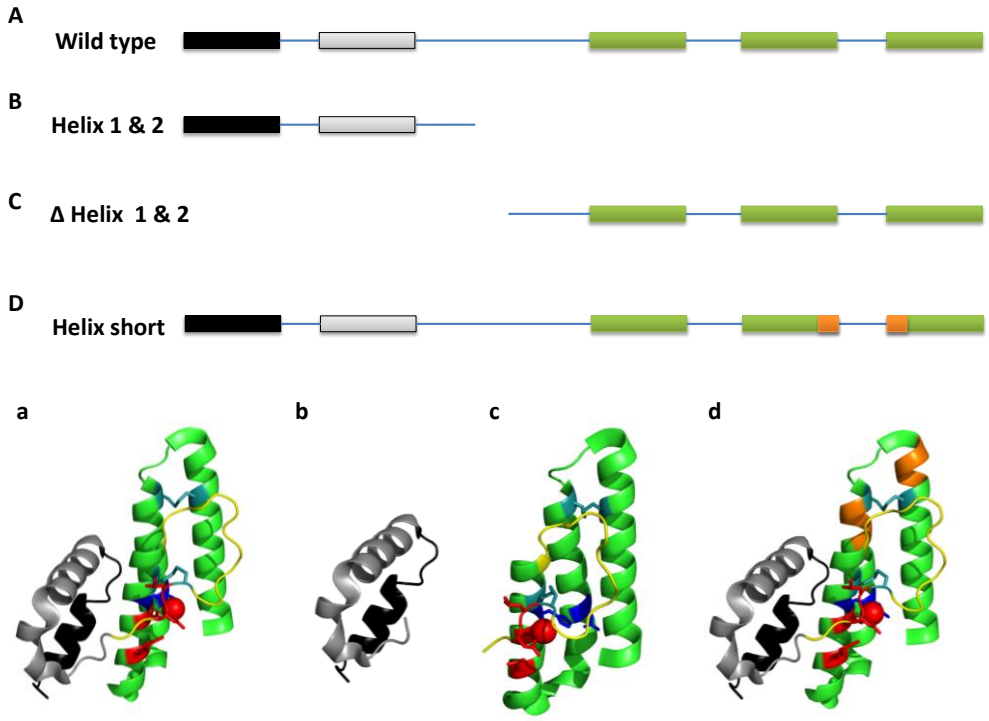

Figure 2.15 Design of truncated mutants to identify minimal region for export

A and a. Wild type enzyme
B and b. Helix 1 & 2
C and c. Δ Helix 1 & 2
D and d. Helix short

Figure 2.16 Construct designed with proposed minimal segment to use as extracellular expression system

A schematic representation of a construct designed to use as extracellular expression system. The proposed segment is the domain we wanted to identify, which was anticipated to responsible for exporting the molecule form the periplasmic space to the extracellular medium.

2.3.3.2 Expression of Helix 1 & 2 in pET22b with pelB signal sequence

Expression of Helix 1 & 2 was done in the same way as described for the wild type. As shown in the SDS PAGE analysis (Figure 2.17) there was no difference between the uninduced and induced whole cell lysate, indicating no expression of the mutant.

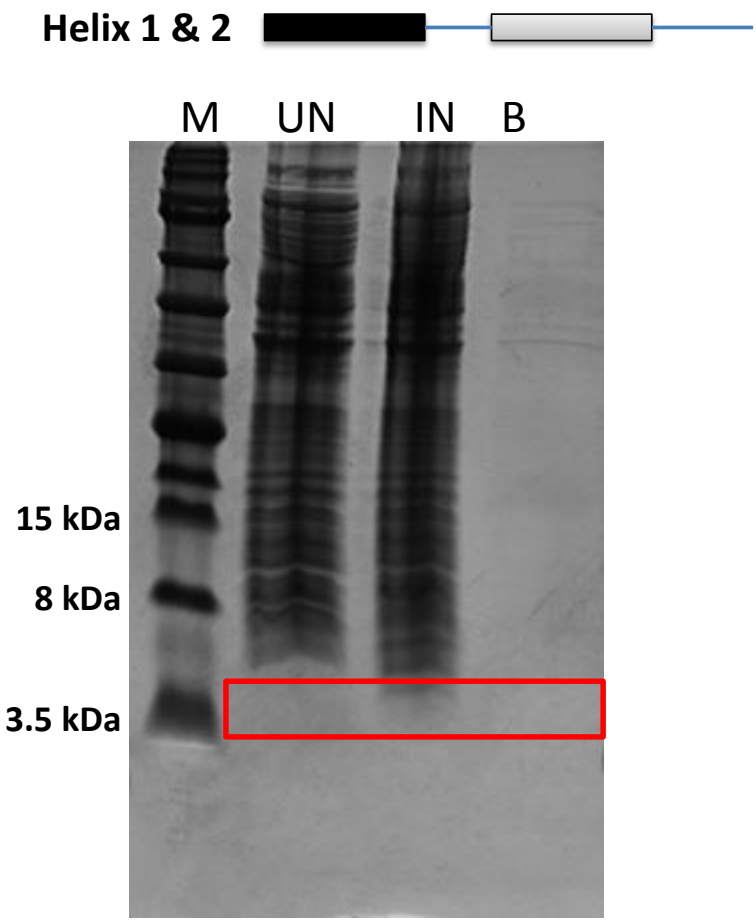

Figure 2.17 Expression of Helix 1 & 2 in pET22b with pelB signal sequence

SDS PAGE analysis showing the expression profile of helix 1 & 2. M-marker, UN-uninduced, IN-induded, B-culture supernatant. Induced lane shows no difference from the uninduced lane, confirming no expression of the construct with helix 1 & 2

2.3.3.3 Expression of Δ Helix 1 & 2 in pET22b with pelB signal sequence

Expression of Δ Helix 1 & 2 was done in the same way as described for the wild type. As shown in the SDS PAGE analysis (Figure 2.18) the mutant was expressed but was found in the insoluble fraction of the whole cell lysate, indicating the formation of inclusion body protein. Expressed protein was not

found in periplasmic space. Therefore the lack of the two N-terminal helices led to misfolding of the mutant resulting in the formation of inclusion body.

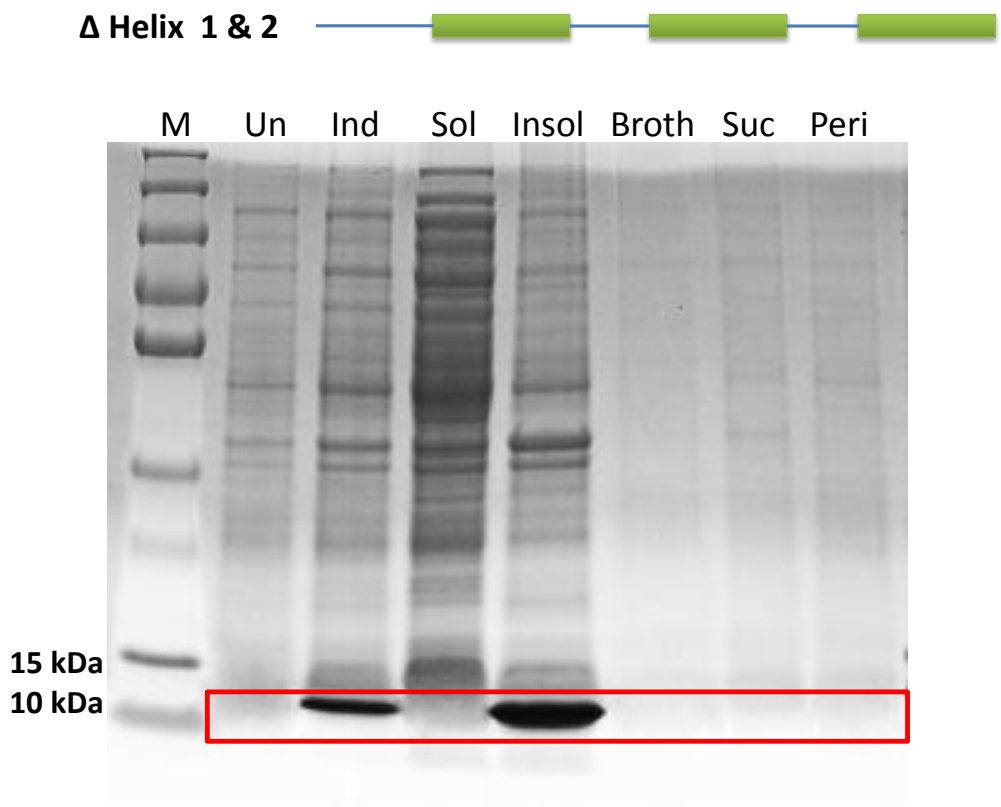

Figure 2.18 Expression of Δ Helix 1 & 2 in pET22b with pelB signal sequence

SDS PAGE analysis showing the expression profile of Δ helix 1 & 2.
M-marker, Un-uninduced, Ind-induced, Sol- soluble fraction of whole cell lysate, Insol- Insoluble fraction, containg inclusion body proteins,
Broth-culture supernatant, Suc-sucrose, Peri-periplasmic fraction.
Δ helix 1 & 2 expresses with the pET22b-pebB construct, but is found in the insoluble fraction.
No expression is seen in the culture supernatant and periplasmic fraction.
Formation of inclusion body protein is due to lack of proper folding of the Δ helix 1 & 2 in absence of the N-terminal helices.

2.3.3.4 Expression of Helix-short PLA_2 in pET22b with pelB signal sequence

Expression of Helix-short PLA_2 was done in the same way as described for the wild type. As shown in the SDS PAGE analysis (Figure 2.19 a and b) the mutant was expressed and found in the soluble fraction of the whole cell lysate. Periplasmic protein preparation showed the presence of expressed protein in periplasmic space. No protein expression was observed in the culture supernatant. Therefore with the shortened helices, the mutant was able to enter the periplasmic space but unable to cross the outer membrane to get secreted to the extracellular medium. Therefore the N-terminal helices seems to help improve the solubility of the protein allowing it to enter the periplasm, but probably lacks the structural features which is needed to secrete the protein to the extracellular space.

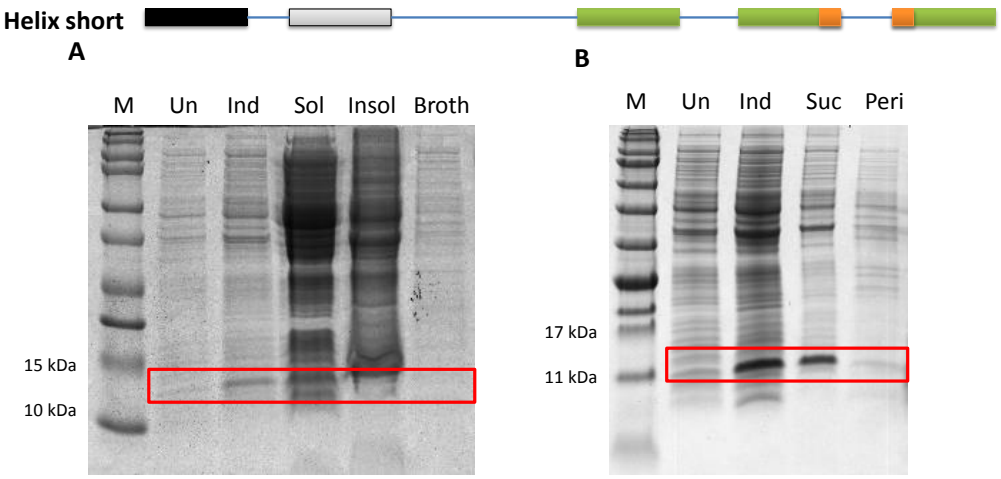

Figure 2.19 Expression of Helix-short PLA2 in pET22b with pelB signal sequence

SDS PAGE analysis showing the expression profile of Helix-short PLA2 .
A. SDS PAGE depicting expressed protein present in soluble fraction.
B. SDS PAGE of periplasmic protein preparation showing soluble protein is retained in the periplasmic space.
M-marker, Un-uninduced, Ind-induced, Sol- soluble fraction of whole cell lysate, Insol- Insoluble fraction, containg inclusion body proteins,
Broth-culture supernatant, Suc-sucrose, Peri-periplasmic fraction.
Helix-short PLA_2 expressed with the pET22b-pebB construct, and was found in the soluble fraction. No expression was seen in the culture supernatant but the periplasmic fraction contained the Helix-short PLA_2. The N-terminal helices are thus required for the solubility and folding , hence the Helix-short PLA_2 was retained in periplasm. But the changes in the tertiary structure due to shortening of the helix, impaired its ability to export to the extracellular media.

Therefore from the above experiments although we were unable to identify the minimal segment responsible for the export, we were able to get clear information about the role of N-terminal helices in improving the solubility of the expressed mutants. Next we wanted to check the expression level of the tag with point mutants in different culture conditions, elaborated in the following section.

2.3.4 Effect of point mutations and temperature on expression of the tag (PLA_2)

To design an expression system, the properties of the tag and its behavior in different culture conditions is very important. The tag should be studied thoroughly and its expression itself optimized carefully. In this section we studied the properties of the tag with respect to point mutations and culture temperature.

2.3.4.1 Point mutations in pET22b-PLA_2 plasmid

The basis of incorporation of point mutations in the PLA_2 comes from the aim of the 3rd chapter of the thesis, i.e., to design a minimal PLA_2 scaffold. Point mutations were introduced to aid chemical cleavage of the mutant full length molecule, which could be expressed in large amounts with pelB in extracellular medium. Following the purification of full length mutant molecule, it could be subsequently cleaved by specific chemicals leading to the generation of small scaffolds. The first strategy was to introduce a cyanogen bromide cleavage point after the first two N-terminal helices which would retain the three-helix catalytic core and the calcium binding loop. The mutations incorporated were A35M, M92L, first mutation being the CNBr cleavage point at 35th position and the second mutation at 92nd position to remove the cleavage point present in the wild type molecule (Figure 2.20 a, b, c).

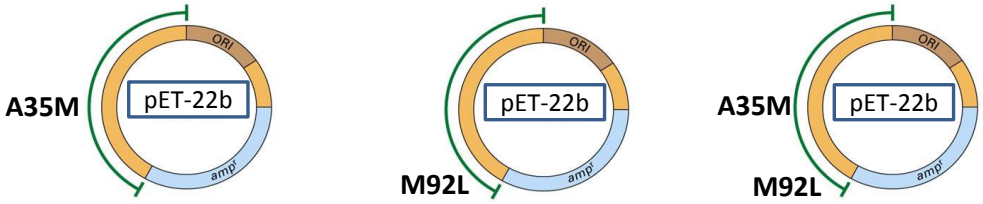

Figure 2.20 Point mutations in pET22b-PLA_2 plasmid

Point mutations designed for chemical cleavage of full length PLA_2, to make a small scaffold.
Expression of these mutants gave us information about optimal culture conditions for expression of the molecule as an extracellular expression tag.

Expression of the double mutant at culture conditions reported by earlier studies at 37°C, led to the decrease in yield by 80% compared to the wild type enzyme expressed in the same conditions (Figure 2.21 a). Two mutations leading to decrease in yield by 80% was intriguing, hence we wanted to pin point the mutation which led to the drastic decrease in the export. This was done by expressing the individual single mutants at the same culture condition. But from the yield information it was evident that the effect of double mutation was additive when compared to the single mutation.

Next we wanted to understand if the mutations in the enzyme led to its decrease in expression or decrease in export due to its possible retention in the cell. SDS PAGE analysis performed with the whole cell lysate (Figure 2.22) showed that the mutations caused the misfolding of the protein leading to formation of inclusion body, hence retained in the cytoplasm. This is evident from the insoluble fraction in the SDS PAGE analysis which shows the retention of the expressed protein in the cytoplasm in the form of inclusion

body. Therefore the mutations caused the misfolding leading to decreased extracellular secretion and did not reduce the expression of the enzyme.

A

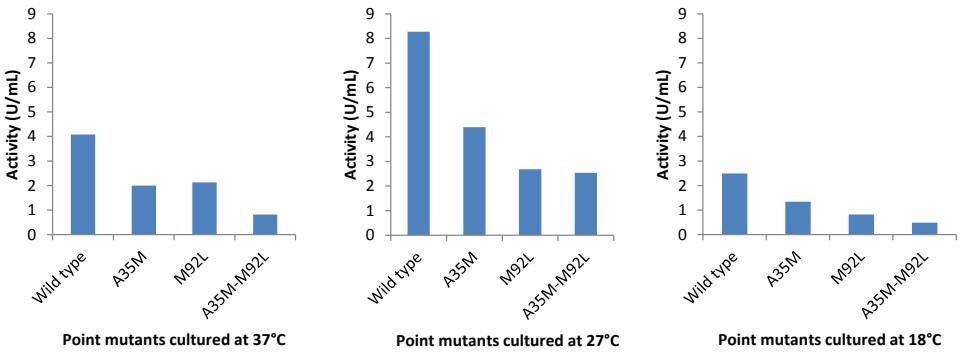

B

	Activity (U/mL)		
	37°C	27°C	16°C
Wild type	4.08	8.27	2.49
A35M	2	4.39	1.35
M92L	2.13	2.68	0.82
A35M-M92L	0.82	2.54	0.49

Figure 2.21 Expression of wild type PLA_2 and mutants at different incubation temperature

A. Bar graph showing the expression of PLA_2 mutants compared to the wild type at different incubation temperature**.**
B. Table representing the PLA_2 activity in the supernatant of culture grown at different temperatures.

2.3.4.2 Expression of wild type PLA_2 and mutants at different incubation temperature

Hence after understanding the effect of point mutations in the formation of insoluble enzymes, the wild type and the mutants were optimized for yield at 27°C and 18°C for 16-18 h. Culturing at 18°C further reduced the yield

whereas culturing at 27°C doubled the yield of wild type and the double mutant Figure 2.21 a and b). Therefore from these series of experiments we were able to standardize the optimal expression condition for the wild type and mutants, which is an important information when considering the expression of the tag with the target protein to enhance the final yield.

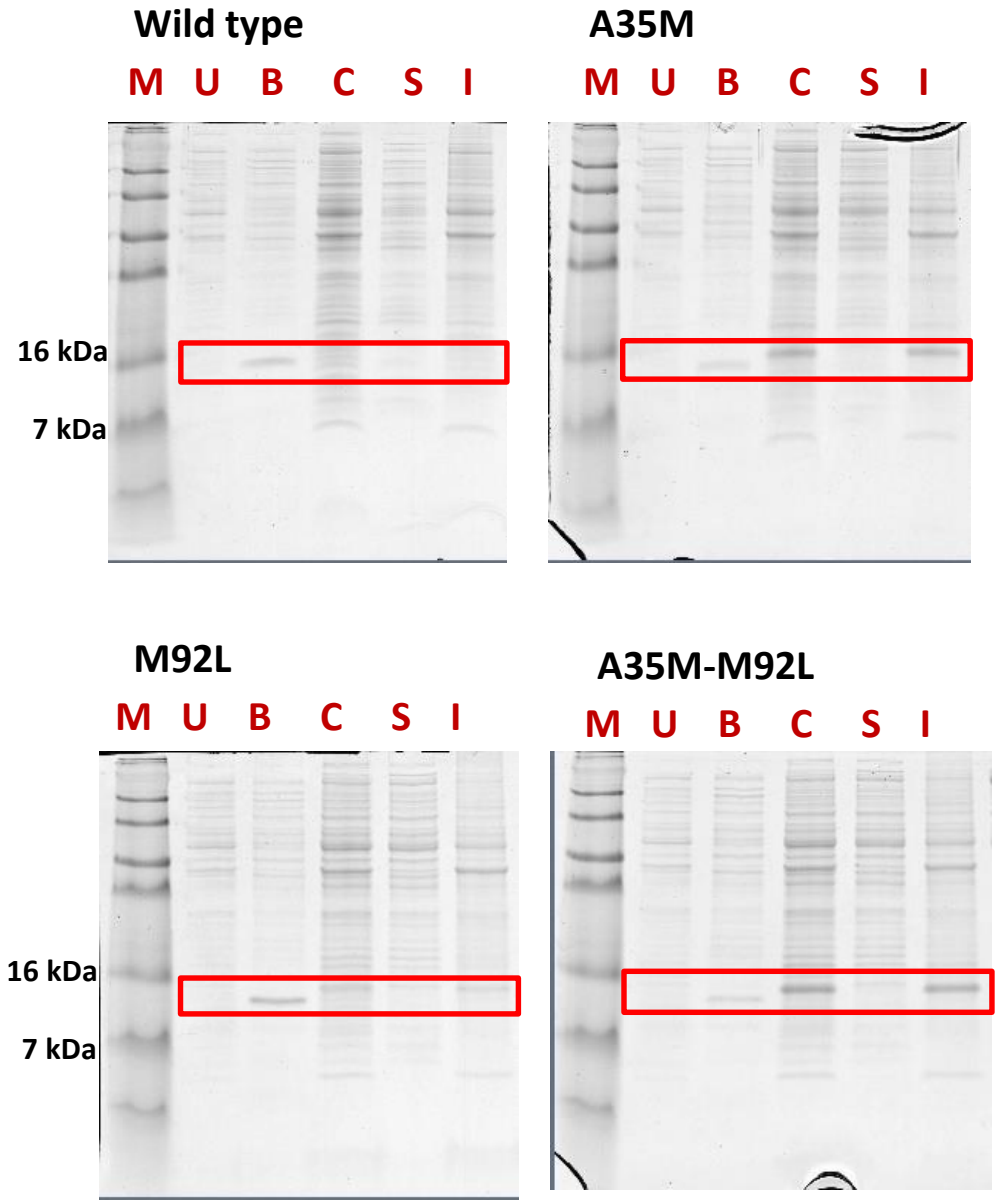

Figure 2.22 SDS PAGE analysis of wild type and mutant PLA_2 expression

SDS PAGE analysis showing the expression of wild type and mutant PLA_2. Point mutations in the molecule led to misfolding of the mutant PLA_2, leading to the formation of inclusion body, as seen in the insoluble fraction of the whole cell lysate. M-marker, U-uninduced, B-broth, C-cell lys, S-soluble, I-inclusion body

2.4 Discussion

In this chapter, we could demonstrate the use of prokaryotic PLA_2 as an extracellular expression tag. The first target protein we tested with this system was ΔHelix KNP. After cleavage of PLA_2-ΔHelix KNP fusion, the purified ΔHelix KNP was found to be biologically active. The yield of the final refolded target protein (ΔHelix KNP) was shown to be 2.5 times higher compared to the yield obtained by recovering the protein from the inclusion body, as reported earlier (Thesis, S. Sreedharan, 2014). Moreover fewer purification steps to obtain the pure protein compared to the conventional methods are an added advantage. Although from ~14 mg of fusion protein we could obtain ~0.5 mg purified ΔHelix KNP, two points worth mentioning for the final protein yield. First, around 50% of the total fusion protein is a truncated tag moiety co-expressed, hence the starting intact (full length) fusion can be considered to be roughly about 7 mg. Second, the ΔHelix KNP moiety is around 3 kDa compared to the fusion, which is around 18 kDa, therefore the expected mount of cleaved product (ΔHelix KNP) obtained theoretically would be around 1.2 mg. Finally after two purification steps following cleavage, the final yield of 0.5 mg is reasonable although single step reversed phase purification might allow better recovery.

During the expression of PLA_2-ΔHelix KNP as explained above, we observed the expression of a truncated fusion protein (section 2.3.1.5), which was later identified to be a part of the fusion protein with the C-terminus segment after the TEV protease site absent. Truncated proteins are usually produced due to

the use of rare codons in genes not well optimized for expression in E. coli (Kane, 1995). Although the gene sequence used for ΔHelix KNP expression was optimized for expression in E. coli, the truncated fusion was produced. Nevertheless these kinds of truncations are also seen occasionally with heterologous protein expression in E.coli, using other soluiblization tags such as GST or MBP, where only the tag moiety is seen to express along with the fusion protein. The reason behind this phenomenon being unclear, it is often speculated to be an issue when the bacteria fail to translate the complete fusion containing a heterologous protein which is complex/difficult for the bacteria to express. Therefore after translating the tag which is usually an endogenous, highly soluble bacterial protein, the process stops leading to the formation of truncated proteins.

Since the tag is an active PLA_2 enzyme, this kind of truncated fusion protein production containing only the tag, would not allow the extracellular expression system to be used to readily estimate the protein yield from the total activity in the culture broth. In other words, expression of the tag along with the fusion would overestimate the yield if total activity is considered for estimating total fusion protein yield. Nevertheless for target proteins where no truncated fusion is produced (for example, PLA_2-Denmotoxin) estimating total activity and correlating with the expression yield could provide additional way to assess the extent of expression and provide a tool for expression optimization by studying the time course of expression. Commercially

available PLA_2 assay kits might be used for simple and quick assessment of expression.

The failure of the cleavage of PLA_2-Denmotoxin fusion with both TEV and HRV 3C protease (figure 2.12, 2.13) necessitates the need for increasing the linker between the tag and the target protein. The problem was seen in the denmotoxin fusion protein as the earlier expressed ΔHelix KNP had relatively simpler structure which probably provided ample space for the protease to act on the site. More work is needed in this area to figure out the optimal linker length for efficient cleavage of fusion protein.

Our next part of the study involved the identification of minimal segment which could retain the property of extracellular export. Although the mutants designed to identify the minimal segment were not secreted into the extracellular medium, we could understand other properties of the molecule and the importance of the N-terminus two-helix bundle in the solubility of the molecule. The Δ Helix 1 & 2 misfolded as inclusion body whereas the Helix short PLA_2 was able to express as soluble protein and enter the periplasmic space, but not secreted into the extracellular medium. This could give us information regarding the necessity of the N-terminal two helixes in enhancing solubility of the protein and in the same time the subtle changes in the structure of the Helix short mutant, which could forbid it from secreting into the extracellular medium. Studying this mutant further may give us information regarding the region or fold of the molecule which might interact

with some unknown partners of the bacterial secretion systems to aid its secretion into the extracellular medium.

The point mutations on PLA_2, although incorporated for structural minimization (the focus of chapter 3) by chemical cleavage, provided us a model to test effect of mutations on PLA_2 secretion. Initial observations of highly reduced yield of mutant (A35M-M92L) due to the presence of only two point mutations made us question whether the mutations causes the reduced expression or reduced export to the extracellular medium. Though the mutations in the molecule did not affect the expression, it led to misfolding at 37°C causing the decrease in the amount of enzyme secreted. On the other hand, lowering the temperature to 27°C increased the yield of the mutants by 2 folds. Further reduction of the incubation temperature to 18°C led to much decrease in the protein yield. These experiments also concluded that the maximum protein yield could be obtained by reducing the culture temperature to 27°C and extending the incubation time to 18 h.

Overall, we could develop an extracellular expression system exploiting the unusual property of secretion of prokaryotic PLA_2 into the culture medium. This system seems to be helpful in expression of disulphide rich proteins in soluble and correctly folded form. The secretion property would reduce the downstream purification steps and provide the added benefit of assessment of expression yield from total activity in broth.

CHAPTER THREE

Design of a mini PLA_2 scaffold

3 CHAPTER THREE: Design of a mini PLA_2 scaffold

3.1 Introduction

Mini proteins or protein domains are considered to be the smallest functional unit of a protein. Protein minimization, a type of protein engineering endeavor, help us understand the first principles of protein folding, structure-function relationship and design of stable scaffolds.

Mini proteins serve as stable scaffolds which can be used as a starting template for the design of other useful molecules. Desired function can be imparted into small scaffolds by grafting of active sites (Stricher et al., 2006). Small stable scaffolds with a desired biological activity can be used for the design of other modular biologics or biotechnological tools.

The prokaryotic PLA_2 is structurally very unique. It is the first PLA_2 described with least structural complexity (Matoba et al., 2002). Unlike other secretory PLA_2s which has five to seven disulphides, the prokaryotic enzyme has only two disulphides. Moreover this enzyme retains the same topologically conserved three-helix catalytic core seen in secretory PLA_2 enzymes. The three dimensional structure of the prokaryotic enzyme shows the presence of a N-terminal two-helix bundle protruding away from the three helix catalytic core. With these structural features, the prokaryotic enzyme provided us a model to attempt the design of a mini scaffold with just the three-helix catalytic core and at the same time, trying to retain its enzymatic activity.

The prokaryotic PLA_2 is one of the smallest PLA_2 enzymes with a molecular weight of 13.5 kDa. Being a small enzyme and possessing structural regions which seemed to be unnecessary for its enzymatic activity, we minimized the enzyme from the N-terminus, by removing the two-helix bundle to make a scaffold with a molecular weight of 9.1 kDa. Although the smallest mutant (Δ Helix 1 & 2) was 32% smaller in size compared to the wild type, it completely lost its enzymatic activity. In order to regain its activity, we re-designed the same mutant by altering the hydrophobic surface with polar residues. Although we failed to regain or improve the function of this 2^{nd} generation mutant, we are trying to crystallize the smallest mutant, which may give us valuable information regarding design of next generation of mutants.

3.2 Materials and Methods

3.2.1 Materials

Many materials used in the experiments described in this chapter are already mentioned in the previous chapter. Apart from those, pET-21a vector (Novagen, Merck biosciences), DTT and reduced/oxidised glutathione (Nacalai Tesque, Kyoto, Japan), Trypsin Gold, Mass Spectrometry Grade (Promega corporation, Madison, Wisconsin, USA), crystallization screens, crystallization trays, coverslips and grease were purchased from Hampton Research (Aliso Viejo, CA, USA). Other reagents and chemicals used in the experiments were of analytical grade.

3.2.2 Cloning of prokaryotic $PLA_{2,}$ wild type and minimized mutants

The optimised gene sequence was obtained as described before. Cloning of the wild type and minimized mutants were done in pET-21a vector between Nde1 and Xho1 restriction sites. Other cloning and mutagenic methods followed are same as described before.

3.2.3 Expression of prokaryotic $PLA_{2,}$ wild type and minimized mutants

Most of the bacterial expression protocol is same as described earlier. The expression conditions were altered for aiding the formation of inclusion body proteins. At OD_{600} = 0.6, the culture was induced to 500 mM IPTG and incubated at 37°C for 5-6 hours.

3.2.4 Inclusion body preparation

Since the protein was expressed as inclusion body, which forms a major part of the insoluble fraction of the cell lysate, the inclusion body protein was first partially purified from the other cellular debris by giving several washes with a buffer containing detergent (50 mM Tris pH 8, 1 mM EDTA, 2% sodium deoxycholate). For each of the washes, the insoluble fraction was dissolved by sonicating for 2 min with the detergent buffer, followed by centrifugation of the dissolved insoluble fraction containing the inclusion body. This cycle was repeated for a total of three times, which led to the reduction of other contaminating proteins in the preparation.

3.2.5 Refolding wild type and minimized mutants

The inclusion body proteins obtained from 1 l culture were first dissolved in 10 ml of denaturing buffer containing reducing agent (100 mM Tris pH 8, 6 M guanidine hydrochloride, 100 mM DTT). The solubilized inclusion body solution was incubated for 3-4 h on a rocker at room temperature to ensure complete denaturation and reduction of the disulphide bonds in the proteins. Next the pH of the solution was reduced by addition of 0.1 ml of concentrated HCl, to inhibit disulphide shuffling. This solution was dialyzed against 2 l buffer (20 mM acetic acid, 4 M guanidine hydrochloride) for 16 h to remove the reducing agent DTT before proceeding for refolding. The dialysed protein was quantified by Bradford protein assay and used for refolding at a concentration of 50 µg/ml. To confirm the complete reduction of the disulphide bonds in the proteins, an aliquot was taken for molecular mass

determination by ESI- LCMS (LCQ Fleet Ion trap, Thermo Scientific, Massachusettes, USA). Optimal refolding condition was screened with the refolding buffer containing additives like arginine and glycerol, the final condition used for refolding the wild type and the mutants was 0.5 M Tris pH 8, 10 mM $CaCl_2$, 1 mM EDTA, 1 mM oxidised glutathione and 5 mM reduced glutathione. Refolding was performed by the dilution technique, where the reduced and denatured protein was diluted to the final refolding concentration by adding the protein slowly into the pre-chilled refolding buffer. The refolding solution was then incubated at 4°C for 48 h.

3.2.6 Purification of refolded wild type and mutants

Purification of the refolded proteins were performed by reversed phase chromatography using Akta system (GE Healthcare Life Sciences, Little Chatfont, UK). Refolding solution was directly loaded onto reversed phase column (Jupiter C18, 5 µm, 300 Å, 250 mm X 10 mm) with buffer A- 0.01 % TFA and buffer B- 0.01% TFA with 100% Acetonitrile on a linear gradient of 24-45% B. The elution profile was monitored at 280 nm. The purified protein was analysed by ESI- LCMS (LCQ Fleet Ion trap, Thermo Scientific, Massachusettes, USA) for assessing complete refolding which is indicated by the reduction in the molecular weight due to loss of hydrogen as a result of disulphide bond formation.

3.2.7 CD spectroscopy

CD spectra (Far-UV, 260-190 nm) were recorded using a spectropolarimeter (Jasco J-810, Jasco Corporation, Tokyo, Japan). The wild type and the mutant protein at a concentration of 0.25 mg/ml was dissolved in 5 mM phosphate buffer pH 7.5 and placed in a quartz cuvette with 0.1 cm path length. The instrument optics and cuvette chamber were purged continuously with nitrogen gas during the entire span of the experiment to provide an oxygen-free environment. The spectra were recorded with data pitch of 0.1 nm, a bandwidth of 1 nm and at a scanning speed of 50 nm/min. To increase the signal to noise ratio, an average of three scans was taken and finally the baseline was subtracted with a blank reading.

3.2.8 Disulphide bond determination

The disulphide bonding pattern in the refolded mutants were determined by cleavage of the protein by trypsin (Trypsin Gold, Mass Spectrometry Grade (Promega corporation, Madison, Wisconsin, USA) followed by analysing the mass of peptide containing the disulphide bonds. The mutant proteins were dissolved in 50 mM phosphate buffer pH 7 at a concentration of 0.2 mg/ml. The cleavage reaction was set in a 200 µl reaction tube with the protein: protease ratio of 50:1. The cleavage solution was incubated at 37°C for 16 h. After the completion of incubation, the cleavage solution was analysed by ESI-LCMS (LCQ Fleet Ion trap, Thermo Scientific, Massachusettes, USA), using a Aeris (C18, 5 µm, 300 Å, 250 mm X 2.1 mm) reverse phase column with buffer A- 0.01 % FA and buffer B- 0.01% FA with 100% Acetonitrile on

a linear gradient of 5-40% B over 60 min at a flow rate of 0.4 ml/min. The peptide masses obtained were analysed and compared against the theoretical expected mass of the peptides containing the disulphide bonds. Presence of the disulphide bonds were confirmed by the reduction in the molecular weight by 2 Daltons in the peptide mass.

3.2.9 Crystallization

Crystallization conditions for ΔHelix 1 & 2 were screened with different crystallization screens (Crystal Screen 1, Crystal Screen 2, Index, Wizard 1, Wizard 2, Wizard 3, Wizard 4, JCSG 1, JCSG 2) using a sitting-drop vapour-diffusion method. The lyophilized protein was dissolved in deionised water due to its poor solubility in any buffered solution after reversed phase purification. The protein concentrations used for setting the drops were 5 mg/ml and 20 mg/ml. The drops were set by Mosquito crystallization robot, by mixing equal volume (0.4 µl each) of protein and crystallization solutions. Each well was filled with 80 µl of respective reservoir solution (crystallization solution). The plates were set at 25ºC. The plates were periodically observed once in a week for 3 months.

3.2.10 sPLA$_2$ Assay

PLA$_2$ enzymatic activity was assayed by commercially available secretory PLA$_2$ kit from Cayman Chemicals (Ann Arbor, MI, USA). Wild type and the mutant enzymes were diluted in assay buffer (25 mM Tris-HCl, pH 7.5

containing 10 mM $CaCl_2$, 100 mM KCl and 0.3 mM Triton X-100) prior to assaying. 10 µl of sample is added in a 96 well clear bottom plate (Corning, NY, USA) followed by 10 µl 10 mM DTNB. The reaction is initiated by addition of 200 µl substrate solution (1.66 mM Diheptanoyl thio-PC). Absorbance is read at 405 nm using a Tecan Sunrise plate reader (Tecan, Maennedorf, Switzerland) at an interval of 30 sec for 15 min. Activity is calculated from the mean slope (OD/min).

3.3 Results

3.3.1 Rational design of 1st generation mutants

In the prokaryotic PLA_2, since the first two N-terminal helices are situated away from the C-terminal three-helix catalytic core, it was predicted to not take part in the catalysis. So our first set of mutants designed to generate smaller scaffold was to remove the helices from the N-terminus of the molecule. Based on the available x-ray crystal structure, our first generation of mutants comprised of Δ Helix 1; first helix removed, and Δ Helix 1 & 2; first and second helix removed (Figure 3.1).

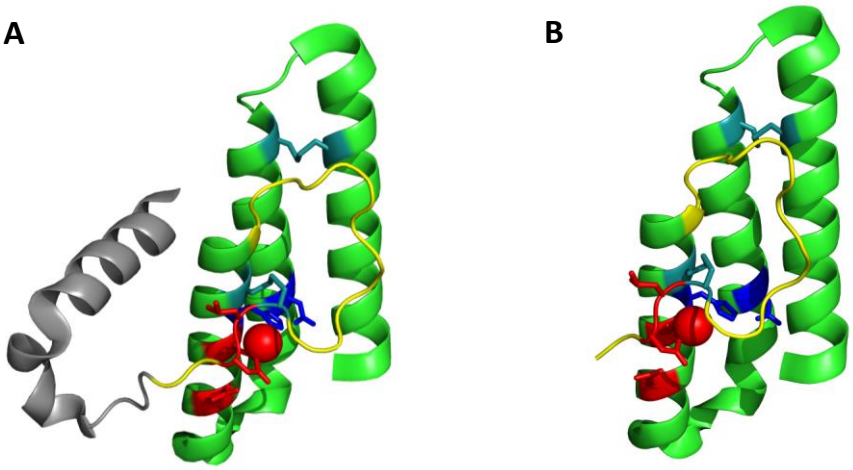

Figure 3.1 Rational design of 1st generation mutants

A. Δ Helix 1; first helix removed. B. Δ Helix 1 & 2; first and second helix removed.

3.3.2 PLA_2 minimization by chemical cleavage

As discussed in section 2.3.3.1, regarding the basis of point mutations and optimization of point mutant expression, our first strategy for generation of smaller scaffold was to express and purify the full length molecule with incorporated point mutations (to assist chemical cleavage), followed by its cleavage by specific chemicals. To generate Δ Helix 1, chemical cleavage point was introduced after the first helix with the mutation A22G. This led to the introduction of cleavage point by hydroxylamine (N-G). In the similar way to generate Δ Helix 1 & 2, cyanogen bromide cleavage point was introduced by two round of mutagenesis A35M and M92L. The sequences of the two mutants aligned with the wild type sequence are shown in the Figure 3.2.

```
Wild Type:     APADKPQVLASFTQTSASSQNAWLAANRNQSAWAAYEFDW
Δ Helix 1:     APADKPQVLASFTQTSASSQNGWLAANRNQSAWAAYEFDW
Δ Helix 1 & 2: APADKPQVLASFTQTSASSQNAWLAANRNQSAWAMYEFDW

Wild Type:     STDLCTQAPDNPFGFPFNTACARHDFGYRNYKAAGSFDANKR
Δ Helix 1:     STDLCTQAPDNPFGFPFNTACARHDFGYRNYKAAGSFDANKR
Δ Helix 1 & 2: STDLCTQAPDNPFGFPFNTACARHDFGYRNYKAAGSFDANKR

Wild Type:     SIDSAFYEDMKRVCTGYTGEKNTACNSTAWTYYQAVKIFG
Δ Helix 1:     SIDSAFYEDMKRVCTGYTGEKNTACNSTAWTYYQAVKIFG
Δ Helix 1 & 2: SIDSAFYEDLKRVCTGYTGEKNTACNSTAWTYYQAVKIFG
```

Figure 3.2 Mutations introduced to assist chemical cleavage

Top row; wild type sequence. Middle row; Δ Helix 1 sequence, point mutation A22G inserted to facilitate cleavage by hydroxylamine. Bottom row; Δ Helix 1 & 2 sequence, point mutations A35M and M92L inserted to facilitate cleavage by cyanogen bromide at 35^{th} position and prevent the same at 92^{nd} position, respectively.

3.3.2.1 Expression and purification of wild type PLA_2

The wild type PLA_2 was expressed and purified as a control. The enzyme was expressed by the optimized protocol described earlier. After expression, the culture media was analyzed by SDS PAGE to access for expression of the protein in the culture supernatant (Figure 3.3 a). After confirmation of expression, the culture supernatant was salted out to 50% saturation by ammonium sulphate. The precipitate was purified by size exclusion chromatography by loading onto GE Superdex 75 prep column. The protein peak indicated by an arrow (Figure 3.3 b) was analyzed by ESI LCMS to confirm the fully oxidized mass (Figure 3.3 c). After confirmation of the mass, the peak was pooled and lyophilized.

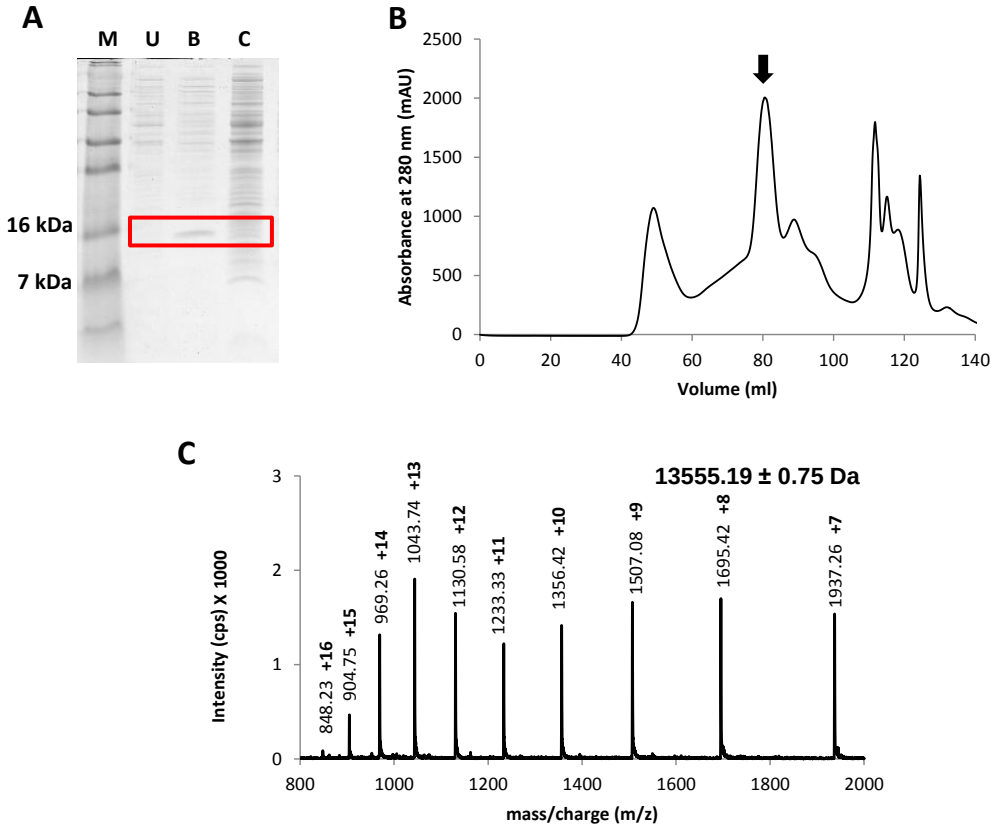

Figure 3.3 Expression and purification of wild type PLA_2

A. SDS PAGE analysis showing extracellular expression of wild type PLA_2.
M- Marker, U- Uninduced whole cell lysate, B- Culture broth, C- Induced whole cell lysate.
B. Purification of wild type PLA_2 by size exclusion chromatography using superdex 75 prep column.
C. Mass of the protein determined by ESI Ion-Trap mass spectrometry.

3.3.2.2 Expression and purification of mutant A22G

Expression and purification protocol followed for the mutant A22G was exactly the same as that of the wild type. The SDS PAGE analysis, gel filtration chromatogram and the mass spectrum of the purified protein is shown in Figure 3.4.

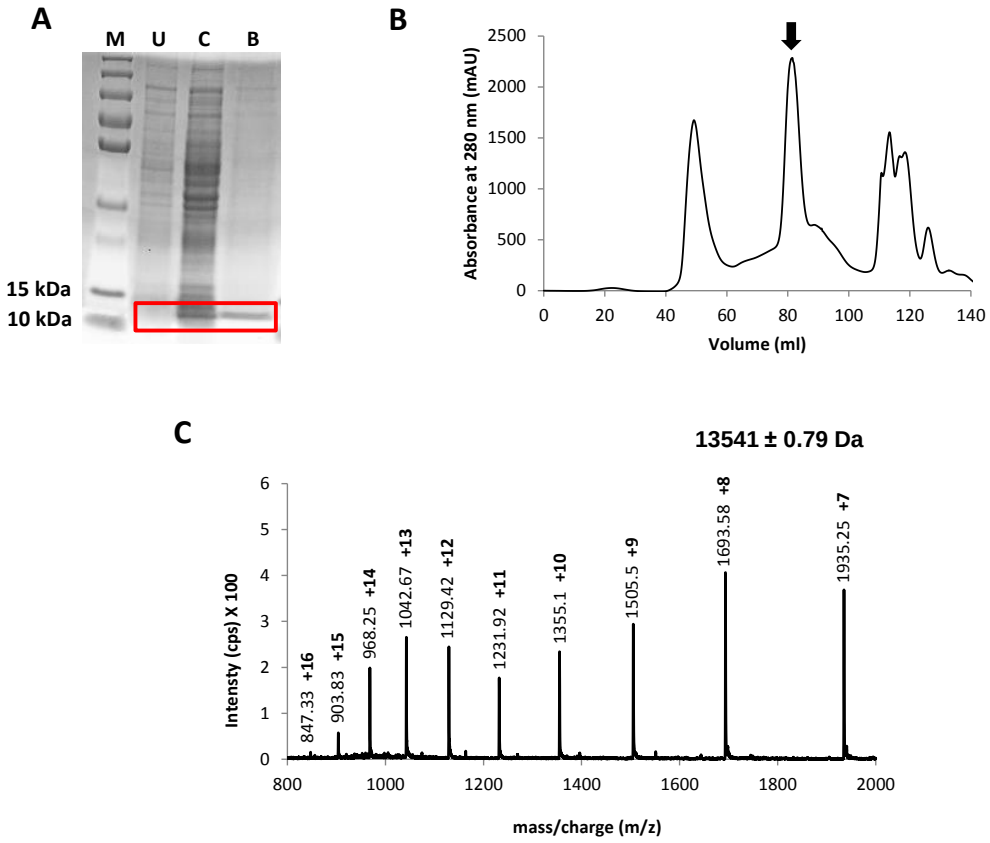

Figure 3.4 Expression and purification of mutant A22G

A. SDS PAGE analysis showing extracellular expression of mutant A22G. M- Marker, U- Uninduced whole cell lysate, B- Culture broth, C- Induced whole cell lysate.
B. Purification of wild type PLA_2 by size exclusion chromatography using superdex 75 prep column.
C. Mass of the protein determined by ESI Ion-Trap mass spectrometry.

3.3.2.3 Expression and purification of mutant A35M-M92L

Expression and purification protocol followed for the mutant A35M-M92L was exactly the same as that of the wild type. The SDS PAGE analysis, gel filtration chromatogram and the mass spectrum of the purified protein is shown in Figure 3.5.

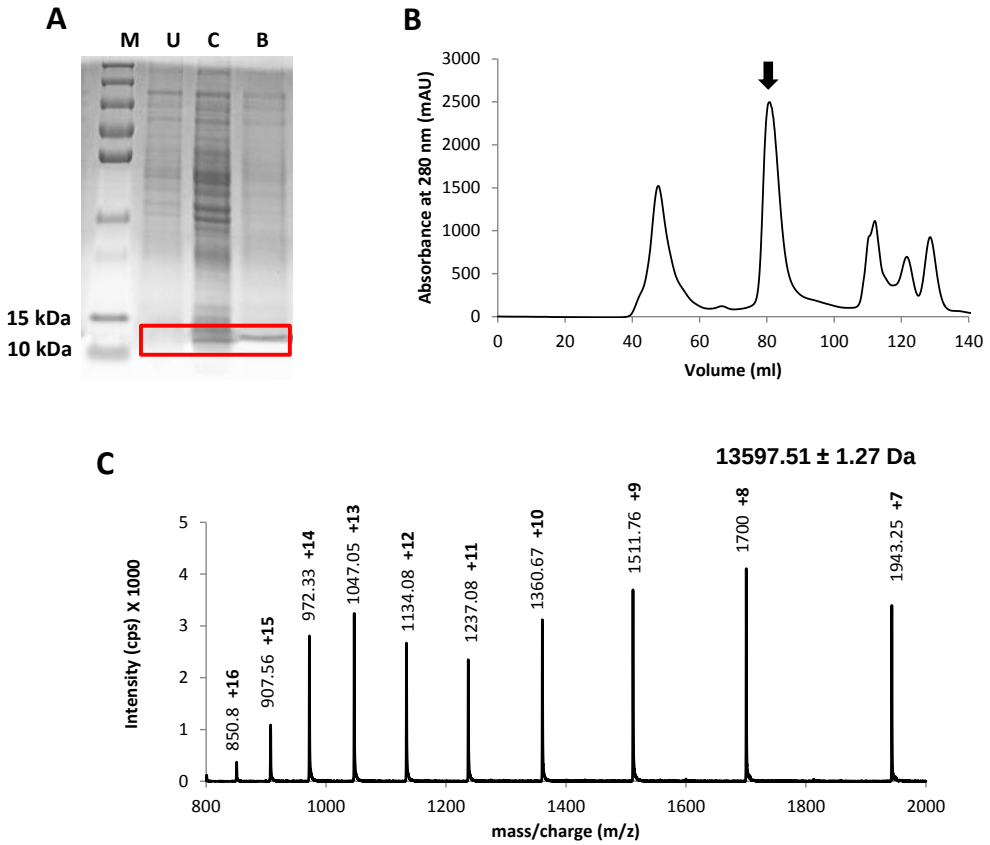

Figure 3.5 Expression and purification of mutant A35M-M92L

A. SDS PAGE analysis showing extracellular expression of mutant A35M-M92L.
M- Marker, U- Uninduced whole cell lysate, B- Culture broth, C- Induced whole cell lysate.
B. Purification of wild type PLA_2 by size exclusion chromatography using superdex 75 prep column.
C. Mass of the protein determined by ESI Ion-Trap mass spectrometry.

3.3.2.4 Cleavage of mutant A22G with hydroxylamine

To generate the mutant Δ Helix 1, hydroxylamine cleavage was performed on the mutant A22G. The lyophilized protein was dissolved in hydroxylamine cleavage buffer (2 M hydroxylamine, 2 M urea, 0.5 mM EDTA, 200 mM tris-HCl pH 9) at a concentration of 0.2 mg/ml. The cleavage reaction was

incubated at 45°C and monitored until 20 h by withdrawing aliquots at 0, 4, 8, 20 h. The extent of cleavage was assessed from the SDS PAGE analysis (Figure 3.6 a). The SDS PAGE analysis shows that the maximum amount of cleavage product formed at 4 h after which the cleaved protein band disintegrated probably due to degradation at higher temperature for longer incubation time. Therefore the cleavage reaction was stopped at 4 h followed by separation by reversed phase chromatography (Figure 3.6 b). As depicted from the chromatogram, the peak was not able to resolve completely even with a very shallow gradient. The mass spectrum shows the exact molecular weight of the cleaved Δ Helix 1, with contaminating full length uncleaved enzyme (Figure 3.6 c). Since the uncleaved full length protein was not removed completely, the function of the mutant was not assayed as it would give false positive results.

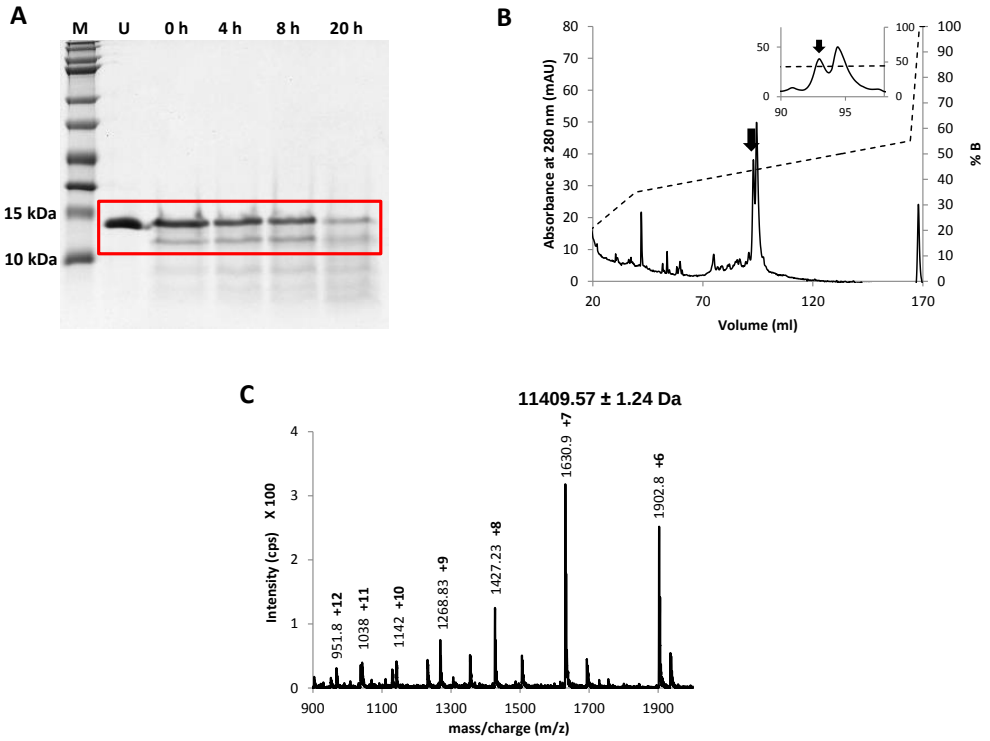

Figure 3.6 Cleavage of mutant A22G with hydroxylamine

A. SDS PAGE analysis showing time course of hydroxylamine cleavage reaction. The extent of cleavage
with respect to incubation time (0 h, 4 h, 8 h, 20 h run on lanes 3 through 6) compared with uncleaved sample (lane2).
B. Purification of cleaved products by reversed phase chromatography using Jupiter C-18 analytical column.
The cleaved product was not resolved completely from the uncleaved, full length molecule.
C. Mass of the truncated protein determined by ESI Ion-Trap mass spectrometry.

3.3.2.5 Cleavage of mutant A35M-M92L with cyanogen bromide

To generate the mutant Δ Helix 1 & 2, cyanogen bromide cleavage was performed on the mutant A35M-M92L. Lyopholized protein was dissolved in CNBr cleavage solution (300 times molar excess of CNBr over met residues, 70% TFA) to a final concentration of 1 mg/ml protein. The reaction was incubated in dark at RT for 16-18 h. After the completion of incubation, the

cleavage mixture was lyophilized followed by purification by reversed phase chromatography. Although the CNBr cleavage reaction is >90% efficient, the sticky nature of the uncleaved full length mutant made it to elute over a broad range at the same %B on the gradient where the cleaved mutant eluted. The peak of the mutant Δ Helix 1 & 2 had carryover of the uncleaved full length protein which interfered with the assay giving us false positive results. The reversed phase chromatogram and the mass spectrum of the cleaved mutant Δ Helix 1 & 2 is shown in Figure 3.7 a and b.

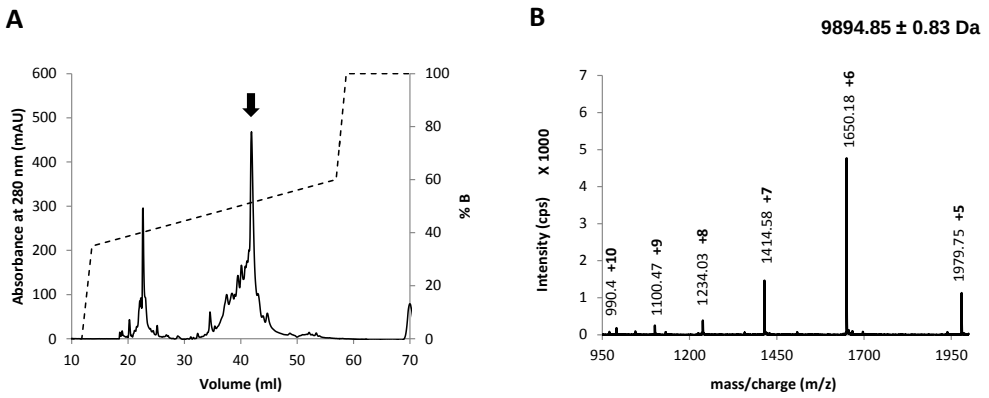

Figure 3.7 Cleavage of mutant A35M-M92L with cyanogen bromide

A. Purification of cleaved products by reversed phase chromatography using Jupiter C-18 analytical column.
B. Mass of the truncated protein determined by ESI Ion-Trap mass spectrometry.

The problems faced using the strategy of chemical cleavage, was partly due to the sticky behavior of the prokaryotic PLA_2 to reversed phase matrix and partly due to the nature of chemical cleavage, which led to side reactions leading to chemical modification of the protein to some extent. Therefore, the

next strategy was to clone and express the first generation mutants with solubilization tags.

3.3.3 Expression of minimized mutants Δ Helix 1 and Δ Helix 1 & 2 with solubilization tags

The mutants were cloned and expressed with commonly used solubilization tags such as the thioredoxin, GST and MBP as fusion which would be later cleaved to generate the mutants.

3.3.3.1 Expression of wild type PLA_2, Δ Helix 1 and Δ Helix 1 & 2 with thioredoxin (Trx) tag in pET 32a

The first generation mutants along with the wild type enzyme was cloned in pET 32a and expressed. The wild type expressed as soluble protein but the mutants were formed as inclusion body protein (Figure 3.8 a and b). Therefore we moved on to check the expression of the mutants with a larger tag, i.e, GST.

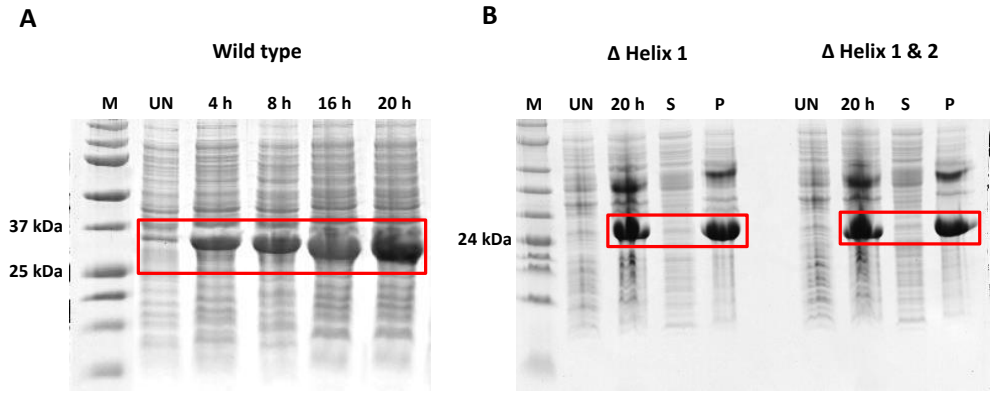

Figure 3.8 Expression of wild type PLA2, Δ Helix 1 and Δ Helix 1 & 2 with thioredoxin (trx) tag in pET 32a

SDS PAGE analysis showing expression of wild type and mutant PLA_2 with trx tag.
M- Marker, U- Uninduced whole cell lysate, h- hours after induction, S- soluble fraction of whole cell lysate, P- pellet containing insoluble fraction of whole cell lysate .
A. Wild type with trx tag expressed as soluble protein.
B. Δ Helix 1 and Δ Helix 1 & 2 with trx tag expressed as insoluble protein.

3.3.3.2 Expression of wild type PLA_2, Δ Helix 1 and Δ Helix 1 & 2 with glutathione S-transferase (GST) tag

After the failure of expression of mutants in soluble form with Trx tag, the first generation mutants along with the wild type enzyme was cloned as a GST fusion and expressed. The wild type expressed as soluble fusion protein, bound and cleaved on column to yield active enzyme but, Δ Helix 1 was expressed as insoluble fusion protein and Δ Helix 1 & 2 although expressed as soluble fusion, was unable to bind to the glutathione sepharose matrix (Figure 3.9 a, b and c). Therefore we further moved on to check the expression of the mutants with a much larger tag, i.e, MBP.

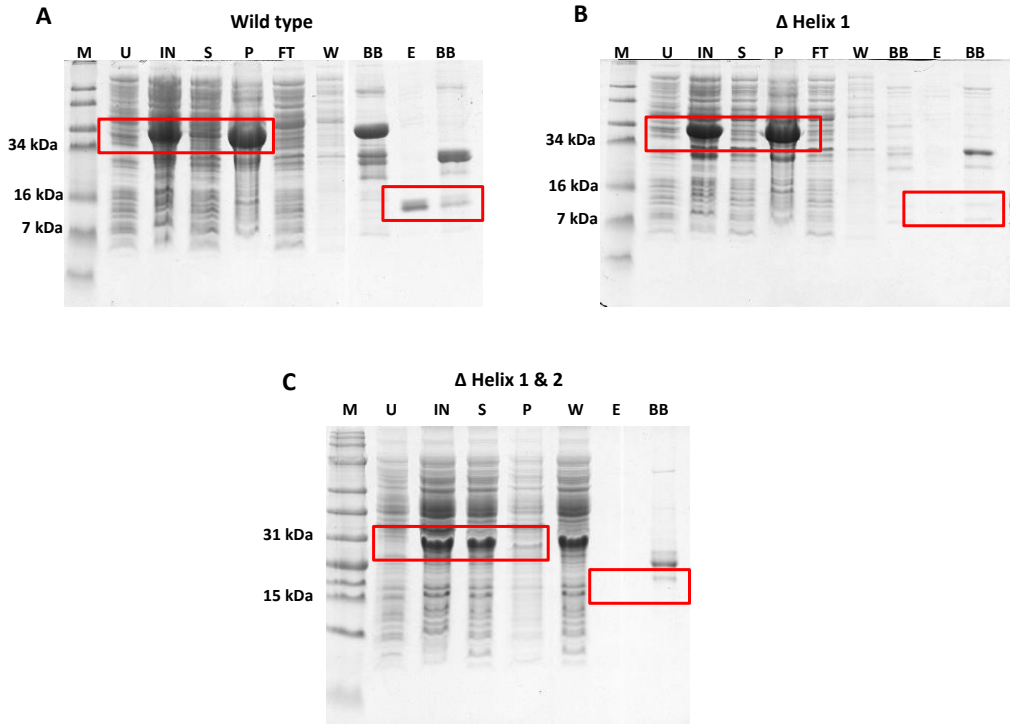

Figure 3.9 Expression of wild type PLA2, Δ Helix 1 and Δ Helix 1 & 2 with glutathione S-transferase (GST) tag

SDS PAGE analysis showing expression of wild type and mutant PLA_2 with GST tag for increasing solubility, 6x His tag (in pLIC-GST) used in A and B for affinity purification.
M- Marker, U- Uninduced whole cell lysate, S- soluble fraction of whole cell lysate, P- pellet containing insoluble fraction of whole cell lysate, FT- flow thorugh, W- wash, E-eluate, BB- bound beads.
A. Wild type with GST tag (pLIC-GST) expressed as soluble protein in very low amount, followed by Ni-NTA chromatography and on-column TEV cleavage.
B. Δ Helix 1 with GST tag (pLIC-GST) expressed as insoluble protein (major part), followed by Ni-NTA chromatography and on-column TEV cleavage.
C. Δ Helix 1 & 2 with GST tag (pGEX-4T1) expressed as soluble protein (although a part was insoluble), followed by Glutathione Sepharose chromatography and on-column thrombin cleavage.

3.3.3.3 Expression of wild type PLA_2, Δ Helix 1 and Δ Helix 1 & 2 with maltose binding protein (MBP) tag

After encountering problems with expression of mutants in soluble form with Trx and GST tag, we gave a final try on a much larger MPB tag. The first generation mutants along with the wild type enzyme was cloned as a MBP fusion and expressed. The wild type expressed as soluble fusion protein, bound and cleaved on column to yield active enzyme. On the other hand, Δ Helix 1 and Δ Helix 1 & 2 although expressed as soluble fusion, bound to amylose matrix, but after cleavage of the tag was not eluted out of the column and found to be precipitated on to the matrix (Figure 3.10 a, b and c).

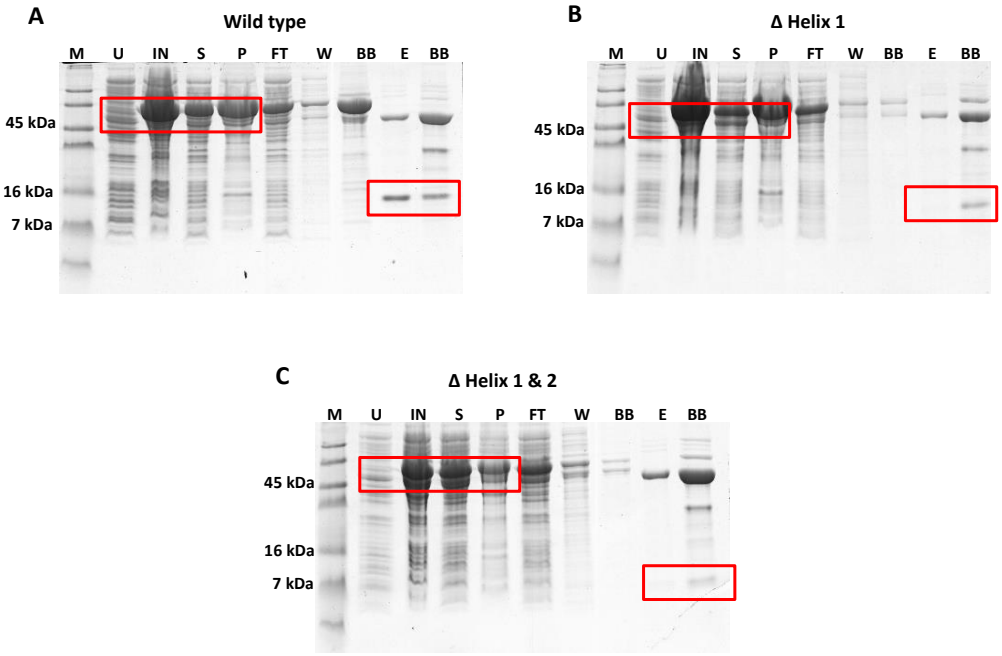

Figure 3.10 Expression of wild type PLA_2, Δ Helix 1 and Δ Helix 1 & 2 with maltose binding protein (MBP) tag

SDS PAGE analysis showing expression of wild type and mutant PLA_2 with MBP tag for increasing solubility and 6x His tag for affinity purification.
M- Marker, U- Uninduced whole cell lysate, S- soluble fraction of whole cell lysate, P- pellet containing insoluble fraction of whole cell lysate, FT- flow thorugh, W- wash, E-eluate, BB- bound beads.
A. Wild type with MBP tag (pLIC-MBP) expressed as soluble protein, followed by Ni-NTA chromatography and on-column TEV cleavage.
B. Δ Helix 1 with MBP tag (pLIC-MBP) expressed as soluble protein (although a part was insoluble), followed by Ni-NTA chromatography and on-column TEV cleavage.
C. Δ Helix 1 & 2 with MBP tag (pLIC-MBP) expressed as soluble protein (major part), followed by Ni-NTA chromatography and on-column TEV cleavage

Expression with different solubilization tags were able to produce the wild type enzyme in the soluble form but the first generation mutants were mostly expressed as inclusion body protein. Therefore we went forward to refold the wild type and the mutants from the inclusion body.

3.3.4 Expression of wild type, Δ Helix 1 and Δ Helix 1 & 2 for refolding from inclusion body

Although refolding of proteins to their active forms from inclusion body is a relatively complex process, there are advantages in refolding proteins from inclusion body. A large amount of protein is produced as inclusion body which can be purified by established protocols. Inclusion body proteins due to their misfolded nature, are not susceptible to protease cleavage during the course of purification and if refolding process is optimized well, we can get a good final refolded yield.

Since the wild type and the mutants are relatively simple in their structure with two disulphide bonds, we first wanted to refold them on column by binding the His tagged protein to the Ni-NTA resin, without reducing their disulphide bonds.

3.3.4.1 Expression and on-column refolding of wild type PLA_2 and Δ Helix 1 & 2 with 6x His tag

Wild type PLA_2 and Δ Helix 1 & 2 was cloned in to pET M (modified pET vector) for expression with 6x His tag. These His tagged proteins were expressed as inclusion body (Figure 3.11 a and b), denatured in buffer containing 8 M urea. Following denaturation, the protein solution was bound to Ni-NTA resin and gradually re-natured by washing the resin with buffers containing decreasing amounts of urea. Finally after wash with buffer containing 2 M urea, the proteins were eluted with native condition buffer

containing 250 mM imidazole. The wild type protein was able to refold and elute from the column and was fully functional (Figure 3.11 a) but the mutant was not eluted and found to be precipitated on the resin (Figure 3.11 b).

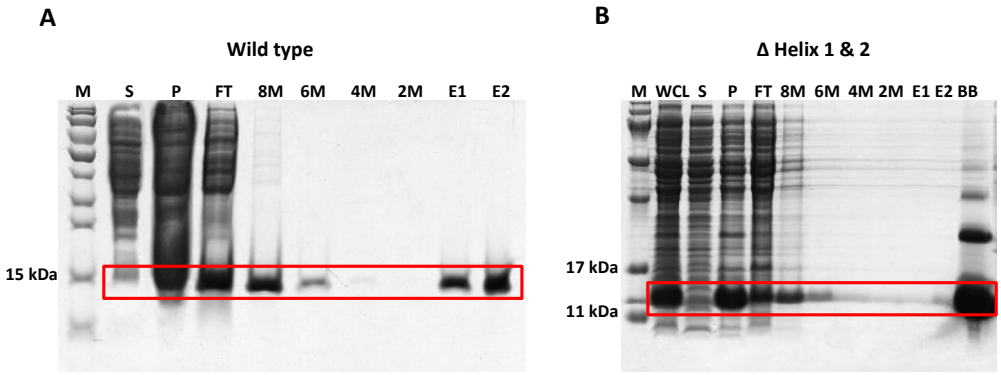

Figure 3.11 Expression and on-column refolding of wild type PLA_2 and Δ Helix 1 & 2 with 6x His tag

SDS PAGE analysis showing expression and on-column refolding of wild type and Δ Helix 1 & 2 with 6x His tag .
M- Marker, WCL-induced whole cell lysate, S- soluble fraction of whole cell lysate, P- pellet containing insoluble fraction of whole cell lysate, FT- flow thorugh, W- wash, E-eluate, BB- bound beads, 8-2M-Urea molar concentration in wash buffer.
A. Wild type with 6x his tag denatured in 8 M urea buffer followed by Ni-NTA chromatography and on-column refolding
by gradual reduction in the urea concentration in wash buffer. The wild type enzyme was successfully refolded on-column
and eluted with native condition buffer containing imidazole. The eluted enzyme showed activity comparable to reported value.
B. Δ Helix 1 & 2 with 6x his tag denatured and refolded as explained above, but no protein was eluted in the native condition buffer
and most of the protein was found bound to the beads, suggesting protein precipitation during the course of decrease in the
urea concentration in the wash buffer. Hence the Δ Helix 1 & 2 was unable to refold on-column as seen for the wild type.

Since the mutant was not able to re-fold to soluble form using this technique of on-column refolding, we finally resorted to refolding the wild type and the

mutants by denaturation, reduction followed by refolding using a redox couple.

3.3.4.2 Expression, refolding and purification of wild type PLA_2

For refolding using a redox couple, first the expressed inclusion body (Figure 3.12 a) was washed several times with lysis buffer containing a detergent to get rid of other contaminating membrane fractions and cellular debris. This semi-purified inclusion body (Figure 3.12 b) is completely denatured and reduced. The complete reduction of the protein is assessed by analyzing the reduced protein by ESI LCMS (Figure 3.12 d). The reducing agent is removed by extensive dialysis followed by refolding in a redox buffer. The refolding is performed by dilution technique as explained earlier. The refolding solution is purified by reversed phase chromatography (Figure 3.12 c) and finally the purified refolded protein is analyzed by ESI MS to confirm the complete oxidation of cysteines (Figure 3.12 e).

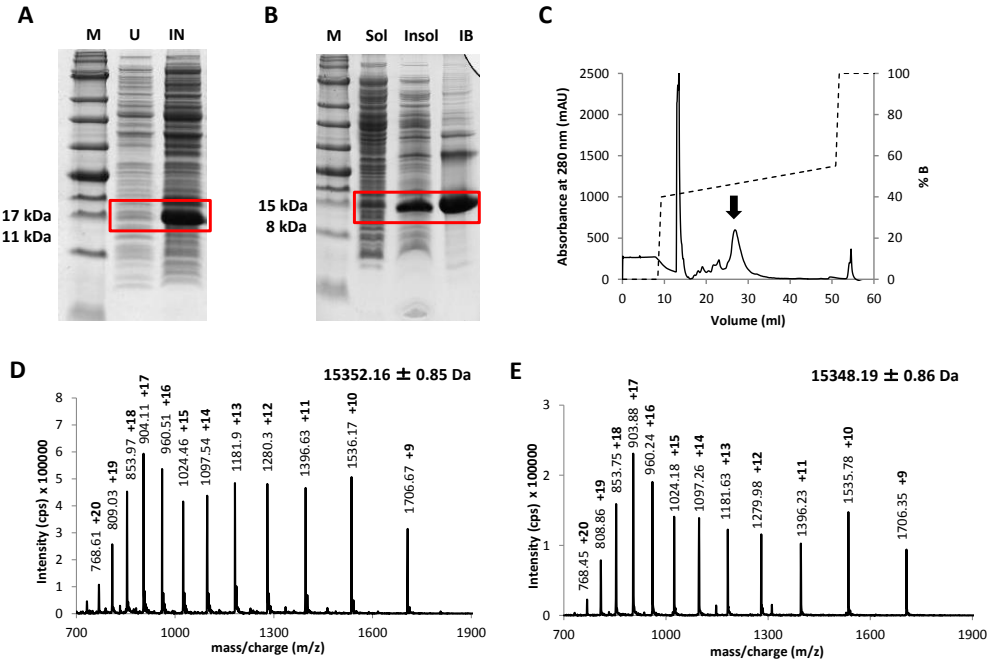

Figure 3.12 Expression, refolding and purification of wild type PLA_2

A and B. SDS PAGE analysis showing expression and inclusion body preparation, respectively.
M- Marker, U- Uninduced whole cell lysate, IN- Induced whole cell lysate, Sol- Fraction containing soluble proteins, Insol- Fraction containing insoluble proteins, IB- Inclusion body after washing with 2% sodium deoxycholate.
C. Purification of refolded wild type PLA_2 by reversed phase chromatography using Jupiter C-18 column.
D and E. Mass of the reduced and refolded proteins, respectively, determined by ESI Ion-Trap mass spectrometry, showing the reduction of four Daltons as a result of two disulphide bond formation.

3.3.4.3 Expression, refolding and purification of Δ Helix 1

The expression, refolding and purification method followed was the same as for the wild type. The expression, inclusion body preparation, purification chromatogram and mass spectrum of reduced and refolded protein is shown in Figure 3.13.

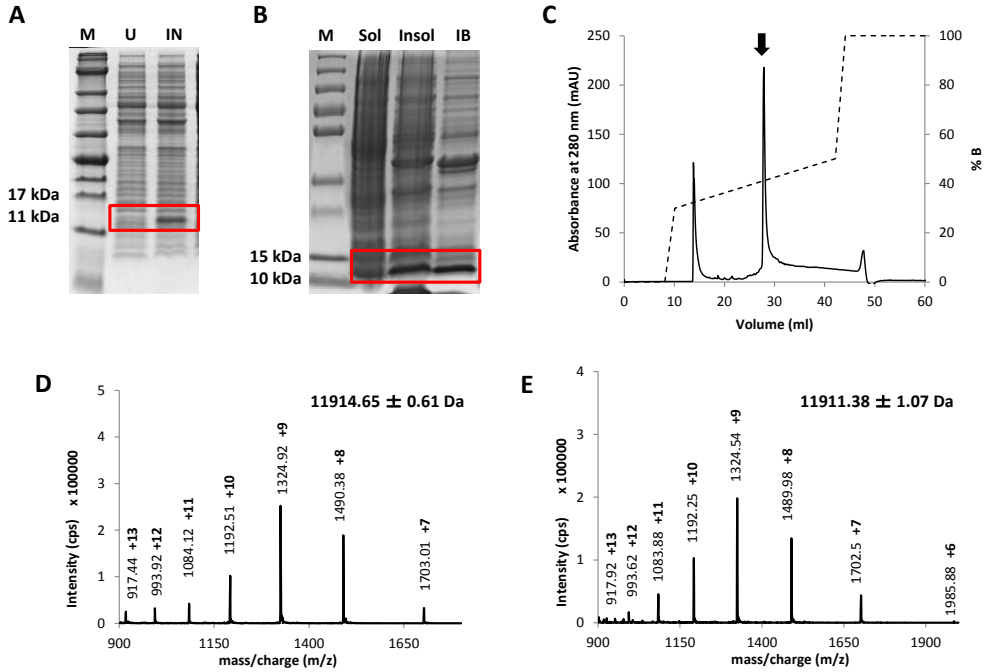

Figure 3.13 Expression, refolding and purification of Δ Helix 1

A and B. SDS PAGE analysis showing expression and inclusion body preparation, respectively.
M- Marker, U- Uninduced whole cell lysate, IN- Induced whole cell lysate, Sol- Fraction containing soluble proteins, Insol- Fraction containing insoluble proteins, IB- Inclusion body after washing with 2% sodium deoxycholate.
C. Purification of refolded wild type PLA_2 by reversed phase chromatography using Jupiter C-18 column.
D and E. Mass of the reduced and refolded proteins, respectively, determined by ESI Ion-Trap mass spectrometry, showing the reduction of four Daltons as a result of two disulphide bond formation.

3.3.4.4 Expression, refolding and purification of Δ Helix 1 & 2

The expression, refolding and purification method followed was the same as for the wild type. The expression, inclusion body preparation, purification chromatogram and mass spectrum of reduced and refolded protein is shown in Figure 3.14.

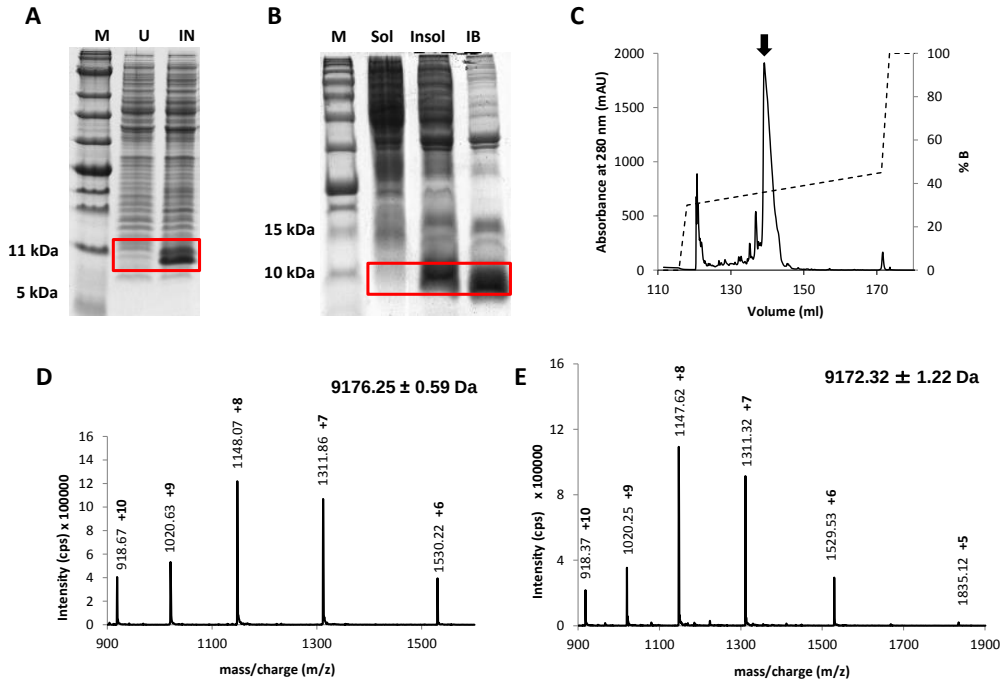

Figure 3.14 Expression, refolding and purification of Δ Helix 1 & 2

A and B. SDS PAGE analysis showing expression and inclusion body preparation, respectively.
M- Marker, U- Uninduced whole cell lysate, IN- Induced whole cell lysate, Sol- Fraction containing soluble proteins, Insol- Fraction containing insoluble proteins, IB- Inclusion body after washing with 2% sodium deoxycholate.
C. Purification of refolded wild type PLA_2 by reversed phase chromatography using Jupiter C-18 column.
D and E. Mass of the reduced and refolded proteins, respectively, determined by ESI Ion-Trap mass spectrometry, showing the reduction of four Daltons as a result of two disulphide bond formation.

3.3.5 Circular dichroism spectroscopy of refolded wild type and mutants

After refolding the wild type and the mutants and assessing their complete oxidation of the cysteines, the next step was to check their secondary structure by CD spectroscopy. The refolded protein solutions were made and CD spectra (Far-UV, 260-190 nm) were recorded using a spectropolarimeter in

triplicates and finally the base line was substracted from the average. From the spectra generated for the wild type and the mutants, the minima at 208 and 222 nm confirms the presence of alpha helical content (Figure 3.15).

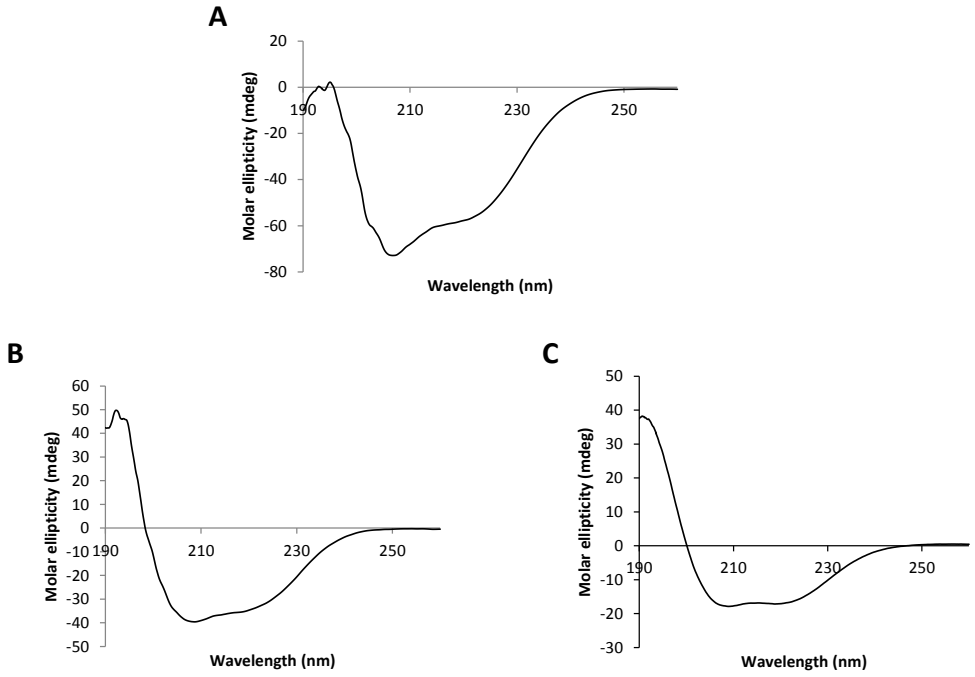

Figure 3.15 Circular dichroism spectroscopy of refolded wild type and mutants

A. Wild type B. Δ Helix 1 C. Δ Helix 1 & 2. Minima at 208nm and 222nm show the presence of alpha helical content in the proteins.

3.3.6 Disulphide linkage determination of first generation mutants

Refolding proteins using a redox couple after complete reduction of the disulphides would form new disulphide bonds in thermodynamically most preferred combination where the free energy is the minimum. Therefore after knowing the presence of alpha helical content in the mutants we wanted to check the pattern of disulphide linkage in the mutants.

Disulphide linkage was determined by trypsin digest of the mutants followed by ESI LCMS. The fragments detected form the total ion chromatogram was matched with the theoretical fragments. By tallying the exact mass of the fragment from the mass spectrum and the expected theoretical mass, the disulphide linkage pattern for the mutants were deduced.

3.3.6.1 Disulphide linkage determination of Δ Helix 1

From the total ion chromatogram, the peaks corresponding to the theoretical mass of the peptides containing the disulphide were identified (Figure 3.16 a, b and c). These fragments were matched with the theoretical fragments containing the disulfide bonds shown in Table 3.1. With these information the final disulphide linkage was determined to be in 1-2 3-4 pattern, which is the same found in the wild type enzyme (Figure 3.17 a and b).

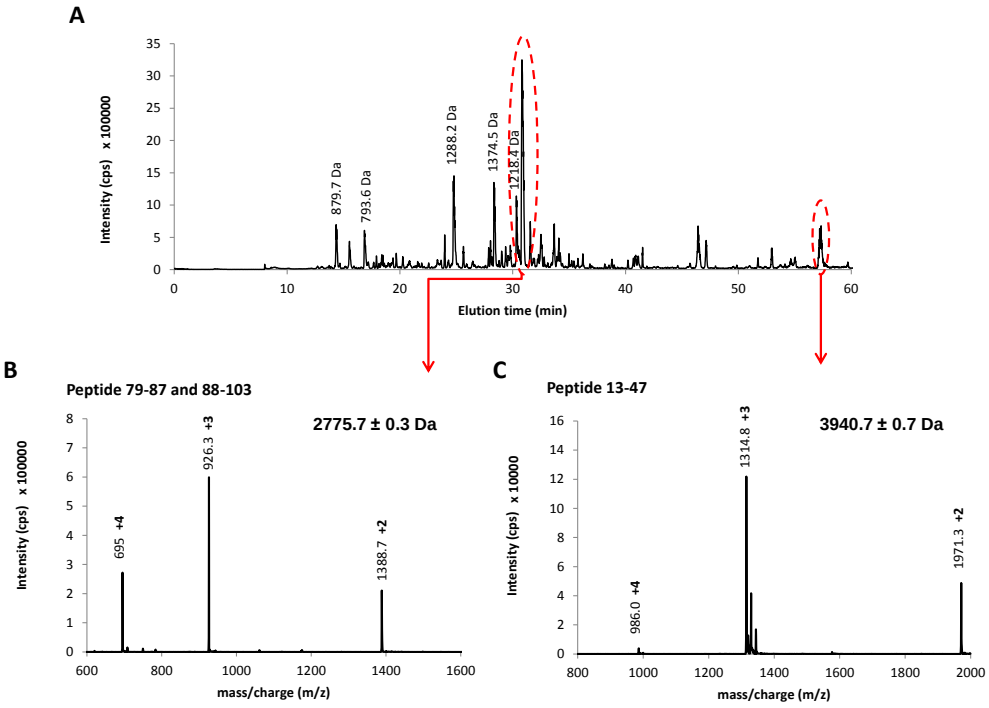

Figure 3.16 Disulphide bond determination of Δ Helix 1

A. Total ion chromatogram of LC-MS run of tryptic digest of Δ Helix 1
B. Mass of peptide 79-87 and 88-103, linked by the second disulphide bond.
C. Mass of peptide 13-47 containing the first disulphide bond.

Table 3.1 Theoretical and experimental masses of tryptic fragments of Δ Helix 1.

Position	Peptide Sequence	Theoretical Mass (Av)	Theoretical Mass (cysteines oxidised)	Experimental Mass
1-12	ASSQNAWLAANR	1288.3853		1288.2
13-47	**NQSAWAAYEFDWSTDLCTQA PDNPFGFPFNTACAR**	**3943.2492**	**3941.25**	**3940.9**
48-53	HDFGYR	793.8370		793.6
54-56	NYK	423.4692		
57-65	AAGSFDANK	879.9249		879.7
66-67	SR	261.2810		
68-77	IDSAFYEDMK	1218.3437		1374.5/1218.4
78-78	R	174.2028		
79-87	**VCTGYTGEK**	**957.0663**	**2776.05**	**2775.7**
88-103	**NTACNSTAWTYYQAVK**	**1820.9942**		
104-106	IFG	335.4032		

Figure 3.17 Disulphide linkage assignment of Δ Helix 1

A. Disulphide bonding pattern of Δ Helix 1, as deduced from the above peptide masses, showing wild type-like cysteine pairing.
B. The peptides with disulphide bonds.

3.3.6.2 Disulphide linkage determination of Δ Helix 1 & 2

From the total ion chromatogram, the peaks corresponding to the theoretical mass of the peptides containing the disulphide were identified (Figure 3.18 a, b and c). These fragments were matched with the theoretical fragments containing the disulfide bonds shown in Table 3.2. With these information the final disulphide linkage was determined to be in 1-2 3-4 pattern, which is the same found in the wild type enzyme (Figure 3.19 a and b).

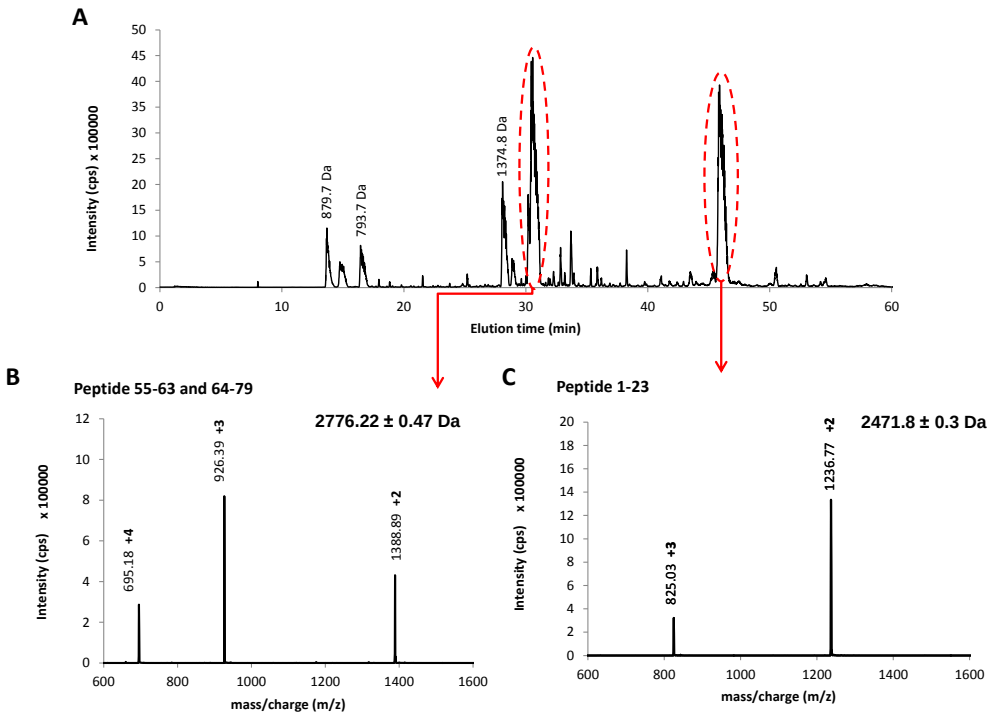

Figure 3.18 Disulphide bond determination of Δ Helix 1 & 2

A. Total ion chromatogram of LC-MS run of tryptic digest of Δ Helix 1 &2
B. Mass of peptide 55-63 and 64-79, linked by the second disulphide bond.
C. Mass of peptide 1-23 containing the first disulphide bond.

Table 3.2 Theoretical and experimental masses of tryptic fragments of Δ Helix 1 & 2

Position	Peptide Sequence	Theoretical Mass (Av)	Theoretical Mass (cysteines oxidised)	Experimental Mass
1-23	STDLCTQAPDNPFGFPFNTACAR	2473.7170	2471.71	2471.7
24-29	HDFGYR	793.8370		793.7
30-32	NYK	423.4692		
33-41	AAGSFDANK	879.9249		879.7
42-43	SR	261.2810		
44-53	IDSAFYEDMK	1218.3437		1374.8/1218.4
54-54	R	174.2028		
55-63	VCTGYTGEK	957.0663	2776.05	2776.2
64-79	NTACNSTAWTYYQAVK	1820.9942		
80-82	IFG	335.4032		

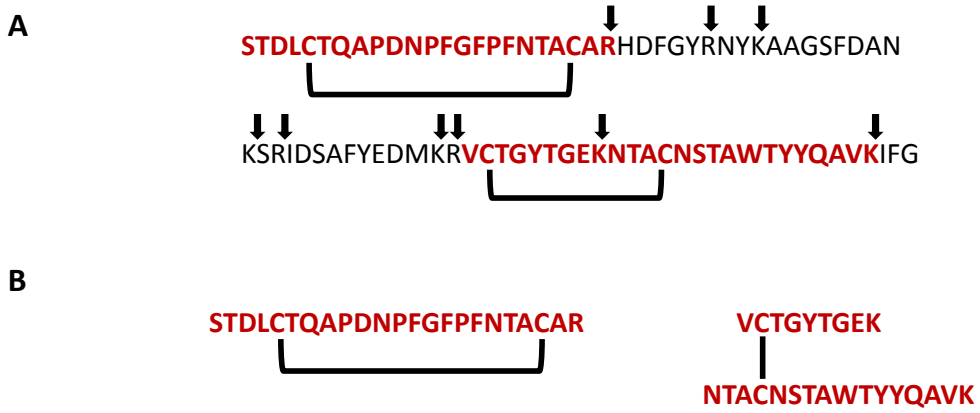

Figure 3.19 Disulphide linkage assignment of Δ Helix 1 & 2

A. Disulphide bonding pattern of Δ Helix 1 & 2, as deduced from the above peptide masses, showing wild type-like cysteine pairing.
B. The peptides with disulphide bonds.

3.3.7 Assay for PLA_2 activity for refolded wild type, Δ Helix 1 and Δ Helix 1 & 2

Assay for enzymatic activity of the wild type and the first generation mutants were performed using commercially available assay kit from Cayman

chemicals. The assay methodology is described earlier. From the assay, although the wild type enzyme showed enzymatic activity as reported before, the first generation mutants failed to show any detectable activity up to a molar concentration of 400 folds higher than the wild type enzyme (Figure 3.20).

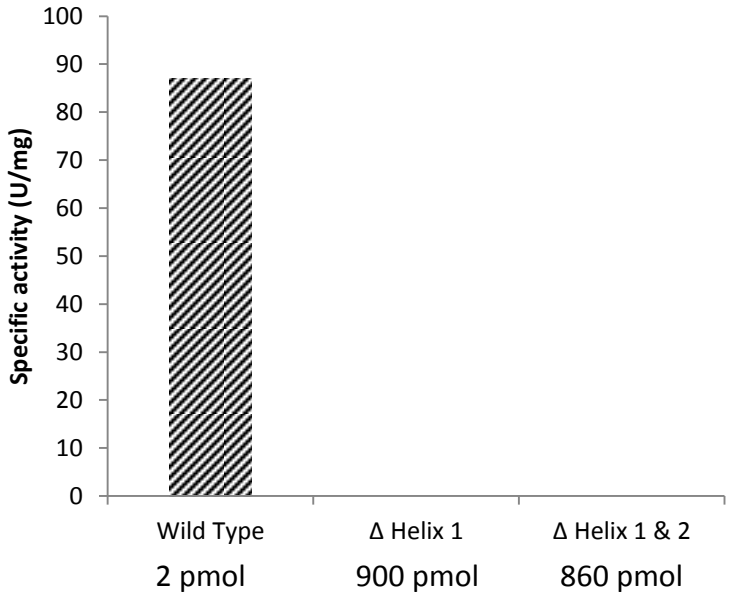

Figure 3.20 Assay for PLA2 activity for refolded wild type, Δ Helix 1 and Δ Helix 1 & 2

Although the wild type refolded enzyme was active with specific activity comparable with reported values, the mutants failed to show detectable enzymatic activity.

3.3.8 Rational design of 2nd generation mutants

After the 1st generation of mutants failed to show any enzymatic activity, despite with correct disulphide linkage and alpha helical content in the secondary structure, we wanted to design a 2nd generation of mutant. We

analyzed the structure and looked into the interface between the C-terminal three-helix catalytic core and the N-terminal 2-helix domain. After the removal of the N-terminal 2-helix domain, the interface would be exposed to the polar solvent. Hydrophobic nature of the exposed surface might cause distortion to the molecule (Figure 3.21 a), possibly leading to the loss of activity due to subtle changes in the geometry of the active site residues. Therefore, our first step towards re-engineering the mutant was to neutralize the hydrophobic surface of the mutant Δ Helix 1 & 2 (Figure 3.21 b). The exposed surface had two hydrophobic residues, phenylalanine at 66^{th} position and tyrosine at 71^{st} position. Therefore we replaced these hydrophobic residues to polar residue glutamine. The new generation of mutant was Δ Helix 1 & 2 F66Q-Y71Q.

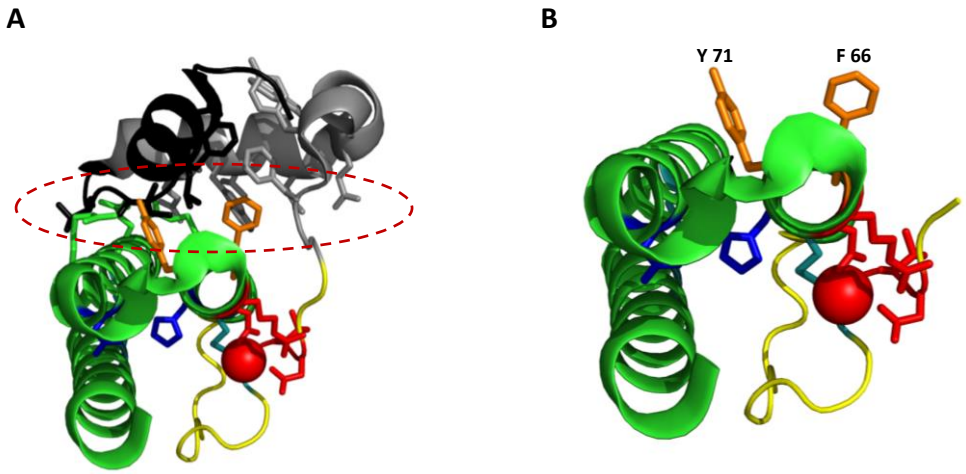

Figure 3.21 Rational design of 2st generation mutants

A. Residues at interface, hydrophobic residues of mutant Δ Helix 1 & 2 highlighted in orange.
B. Protruding hydrophobic residues at the interface, which are exposed to the solvent in mutant Δ Helix 1 & 2.

3.3.8.1 Expression, refolding and purification of Δ Helix 1 & 2- F66Q-Y71Q

The expression, refolding and purification method followed was the same as for the wild type. The expression, inclusion body preparation, purification chromatogram and mass spectrum of reduced and refolded protein is shown in Figure 3.22.

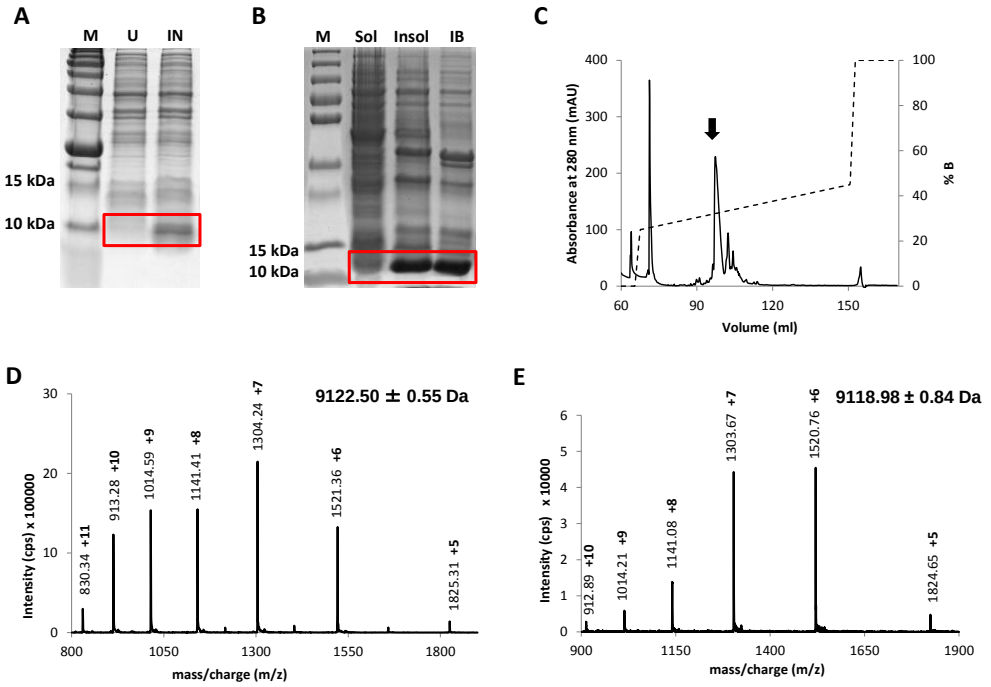

Figure 3.22 Expression, refolding and purification of 2nd generation mutant, Δ Helix 1 & 2- F66Q-Y71Q

A and B. SDS PAGE analysis showing expression and inclusion body preparation, respectively.
M- Marker, U- Uninduced whole cell lysate, IN- Induced whole cell lysate, Sol- Fraction containing soluble proteins, Insol- Fraction containing insoluble proteins, IB- Inclusion body after washing with 2% sodium deoxycholate.
C. Purification of refolded wild type PLA_2 by reversed phase chromatography using Jupiter C-18 column.
D and E. Mass of the reduced and refolded proteins, respectively, determined by ESI Ion-Trap mass spectrometry, showing the reduction of four Daltons as a result of two disulphide bond formation.

.

3.3.8.2 Circular dichroism spectroscopy of refolded wild type and mutants

After refolding the 2nd generation mutant and assessing the complete oxidation of the cysteines, the next step was to check its secondary structure by CD spectroscopy. CD spectra (Far-UV, 260-190 nm) were recorded using a

spectropolarimeter in triplicates and finally the base line was substracted from the average. From the spectra generated for the 2nd generation mutant, the minima at 208 and 222 nm confirms the presence of alpha helical content (Figure 3.23).

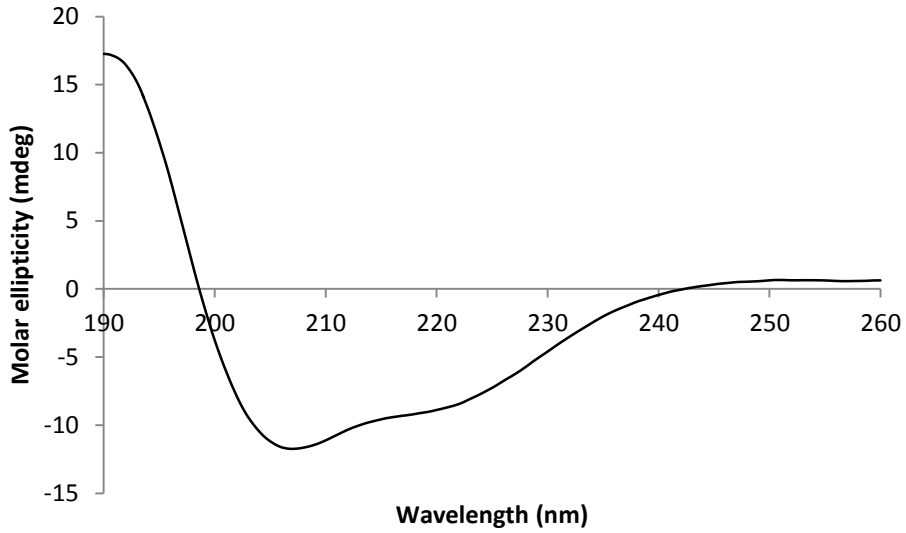

Figure 3.23 Circular dichroism spectroscopy for Δ Helix 1 & 2- F66Q-Y71Q

Minima at 208nm and 222nm show the presence of alpha helical content in the mutant Δ Helix 1 & 2- F66Q-Y71Q.

3.3.8.3 Disulphide linkage determination of Δ Helix 1 & 2- F66Q-Y71Q

From the total ion chromatogram, the peaks corresponding to the theoretical mass of the peptides containing the disulphide were identified (Figure 3.24 a, b and c). These fragments were matched with the theoretical fragments containing the disulfide bonds shown in Table 3.3. With these information the final disulphide linkage was determined to be in 1-2 3-4 pattern, which is the same found in the wild type enzyme (Figure 3.25 a and b).

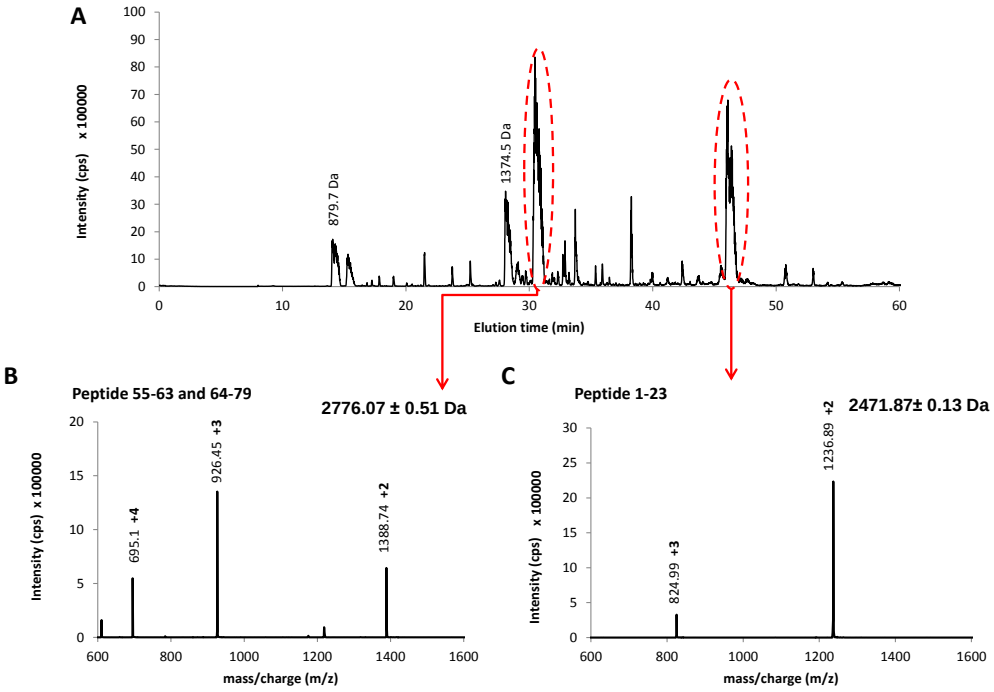

Figure 3.24 Disulphide bond determination for Δ Helix 1 & 2- F66Q-Y71Q

A. Total ion chromatogram of LC-MS run of tryptic digest of Δ Helix 1 & 2- F66Q-Y71Q
B. Mass of peptide 55-63 and 64-79, linked by the second disulphide bond.
C. Mass of peptide 1-23 containing the first disulphide bond.

Table 3.3 Theoretical and experimental masses of tryptic fragments of Δ Helix 1 & 2- F66Q-Y71Q

Position	Peptide Sequence	Theoretical Mass (Av)	Theoretical Mass (cysteines oxidised)	Experimental Mass
1-23	STDLCTQAPDNPFGFPFNTACAR	2473.7170	2471.71	2471.9
24-29	HDQGYR	774.7911		
30-32	NQK	388.4239		
33-41	AAGSFDANK	879.9249		879.7
42-43	SR	261.2810		
44-53	IDSAFYEDMK	1218.3437	1374.54	1374.5
54-54	R	174.2028		
55-63	VCTGYTGEK	957.0663	2776.05	2776.0
64-79	NTACNSTAWTYYQAVK	1820.9942		
80-82	IFG	335.4032		

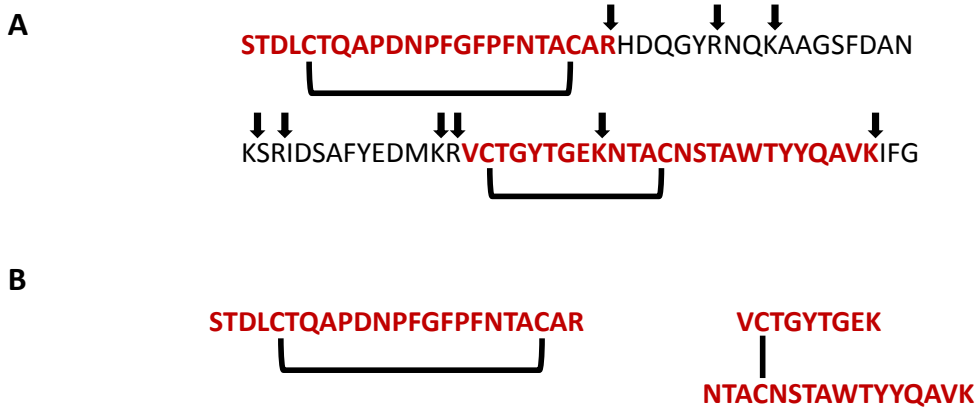

Figure 3.25 Disulphide linkage assignment of Δ Helix 1 & 2- F66Q-Y71Q

A. Disulphide bonding pattern of Δ Helix 1 & 2- F66Q-Y71Q, as deduced from the above peptide masses, showing wild type-like cysteine pairing.
B. The peptides with disulphide bonds.

3.3.8.4 Assay for PLA_2 activity for refolded Δ Helix 1 & 2- F66Q-Y71Q

Assay for enzymatic activity of the 2nd generation mutant was performed using commercially available assay kit from Cayman chemicals. The assay

methodology is described earlier. From the assay, although the wild type enzyme showed enzymatic activity as reported before, the 2nd generation mutant failed to show any detectable activity up to a molar concentration of 400 folds higher than the wild type enzyme (Figure 3.26).

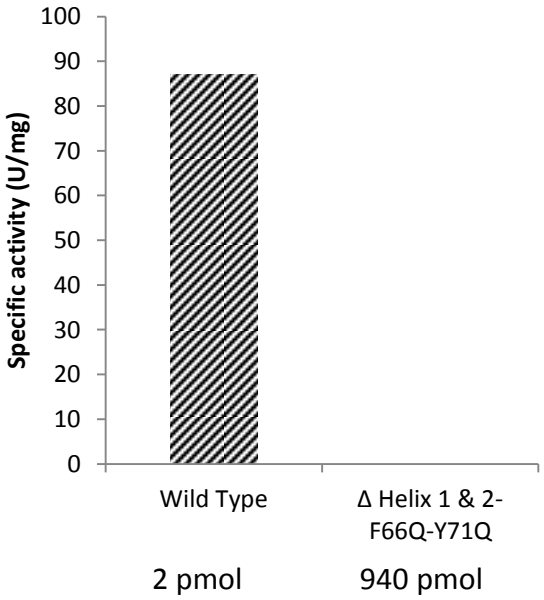

Figure 3.26 Assay for PLA_2 activity for refolded Δ Helix 1 & 2- F66Q-Y71Q

Although the wild type refolded enzyme was active with specific activity comparable with reported values, the 2nd generation mutant failed to show detectable enzymatic activity.

3.3.9 Crystallization of refolded Δ Helix 1 & 2

Crystallization conditions for ΔHelix 1 & 2 were screened with different crystallization screens (Crystal Screen 1, Crystal Screen 2, Index, Wizard 1, Wizard 2, Wizard 3, Wizard 4, JCSG 1, JCSG 2) using a sitting-drop vapour-diffusion method. The lyophilized protein was dissolved in deionised water

due to its poor solubility in any buffered solution after reversed phase purification. The drops were set at a concentration of 10 and 20 mg/ml by Mosquito crystallization robot. The plates were set at 25ºC. After 24 hours of setting the drops, heavy precipitation was seen in more than 80% of the conditions. The remaining clear drops were monitored every week upto 3 months. No hits were seen in any of the conditions.

3.4 Discussion

In this chapter we were able to design and test the function of two generations of mini prokaryotic PLA_2 mutants. Although the design of the mini mutants, were based on conserved topology of catalytic core and active site geometry in secretory PLA_2s (Hariprasad et al., 2013; Nevalainen and Cardoso, 2012), rational design was chosen as our preferred method as the three dimensional structure of the prokaryotic PLA_2 was available. The rational approach lets us design mutants based on the existing information of the structure or fold of the protein. On the other hand computational methods, although used in some studies to engineer proteins, have met with limited success (Bolon and Mayo, 2001; Korkegian et al., 2005; Stevens et al., 2006). Moreover the huge number of possible mutants generated by computational algorithms would make it a mammoth task to produce and test them.

The prokaryotic PLA_2 being one of the smallest and structurally simplest among secretory PLA_2 enzymes, with just two disulphides and N-terminal protruding 2-Helix bundle, provides a model which seems to be more amenable to minimization, deletion mutations and more importantly disulphide bond formation and its easy assessment. The conserved nature of the PLA_2 catalytic core and active site geometry evoked initial questions that, can the conserved catalytic core can be designed as a functional mini PLA_2 scaffold? A small active PLA_2 scaffold would not only test our understanding of protein folding and function, but also provide a starting point for the further design of other biologics in a modular fashion.

To minimize the prokaryotic PLA_2, a few approaches have been taken. The first approach considered was chemical cleavage of the full length protein incorporating specific mutations to aid the cleavage. Although the efficiency of chemical cleavage depends on the nature of the cleavage (chemicals used for cleavage; hydroxylamine ~30% efficiency, CNBr ~90% efficiency) (Crimmins et al., 2005) and the strategic optimization with the protein, the prokaryotic PLA_2 harboring the mutations seemed to cleave with cleavage efficiency reported earlier (Andreev et al., 2010; Milner et al., 1996). However the approach was not reliable in our case due to the sticky nature of the protein on the reversed phase matrix, leading to co-elution and contamination of the protein fragment peak of interest with the full length enzyme. If complete separation of the fragment of interest could not be achieved, it would give false positive results in the downstream functional assessment.

Therefore our next strategy was to express the minimized mutants with solubilization tags, which would eliminate any possibility of contamination with the full length, wild type enzyme. The wild type and the first generation mutants (Δ Helix 1, Δ Helix 1 & 2) were expressed with commonly used solubilization tags such as thioredoxin, GST and MBP. Although in all the cases the wild-type fusion protein was produced in soluble form, the mutants either expressed as inclusion body proteins or precipitated after removing the tag (observed in case of MBP fusion (section 3.3.3.3). Therefore finally we resorted to refolding the mutants from the inclusion body. Initial refolding experiments were performed by denaturing followed by re-naturing the protein

on column, without reducing the disulphides. But we had success only with the wild type as the mutant was precipitated on column. These sets of experiments on expression of the mutants lacking either the first or the first 2-helices indicated that these two helices were important for the folding of the molecule hence aiding its production in soluble form. This was consistent with the observation of the expression of Helix short mutant with pelB signal (section 2.3.2.4), where it having the N-terminal two helices intact was able to express in soluble form and get transported into the periplasm.

The final and the fool-proof way of producing the mutants were to denature, reduce and refold using a redox couple followed by assessment of the disulphide linkages. Refolding using a redox couple shuffles the disulphide bonds till the molecule reaches a thermodynamically stable energy state (Vallejo and Rinas, 2004). This leads to the formation of majority of the refolded proteins with identical disulphide linkage pattern. After the purification of the refolded protein, it was evaluated for correct folding by analysis of its refolded mass and determination of its disulphide linkage pattern. Reduction in the same number of Daltons as the number of cysteines confirmed its complete oxidation and the tryptic fragments of the mutants corresponding to its theoretical mass confirmed its correct dilulphide pairing compared to the wild type enzyme.

As the first generations of the mutants were non-functional despite its correct disulphide pairing and alpha helical secondary structure, the second generation of the mutant was designed by neutralizing the hydrophobic surface of Δ Helix

1 & 2. Two hydrophobic residues protruding to the solvent was replaced with polar residue glutamine. The designed second generation mutant, Δ Helix 1 & 2- F66Q-Y71Q, following refolding and assessment of its disulphides linkages was also found to be inactive. To probe into the exact structural changes which led to the functional inactivation of the mutants, the three dimension structural information was needed. Therefore the smallest mutant Δ Helix 1 & 2 was set for crystallization. But due to the solubility issues, >80% of the drops precipitated. The reduction in solubility of the protein was observed after purification by reversed phase chromatography, therefore alternate ways of purifying in milder condition (using only aqueous buffers) need to be devised followed by screening for crystallization.

The functional inactivation of the mutants may be attributed to two reasons. First, changes in the geometry of active site residues may lead to loss of activity. Second, distortion of the calcium binding loop may render calcium coordination faulty, leading to loss of activity. Although the x-ray crystal structure can provide us valuable information regarding both the issues, the property of the mutants to bind calcium can be assessed to get clues regarding orientation of the calcium binding loop. Therefore further work is needed to understand the structure of the current generation mutants to design the next generation mutants in order to make the minimized scaffolds functional.

CHAPTER THREE

Conclusions and

future perspectives

4 CHAPTER FOUR: Conclusions and future perspectives

4.1 Design of an extracellular expression system

Exploiting one of the most interesting properties of the prokaryotic PLA_2 to get secreted into the culture medium, we have demonstrated its usefulness as a tag in the extracellular production of other target proteins. To test the system, the first target protein selected was krait natriuretic peptide (residues 1-34, ΔHelix KNP), a molecule with relatively small and simpler structure. PLA_2-ΔHelix KNP fusion protein was successfully recovered and purified from the culture supernatant. Following the tag cleavage and purification, the target protein ΔHelix KNP was found to be biologically active. Moreover, the final yield of ΔHelix KNP produced using this system was 2.5 folds higher than the yield obtained by conventional way of recovering from inclusion body. As demonstrated from the above test protein, using this system for producing complex disulphide rich proteins would not only help production of soluble and correctly folded protein, but also decrease the downstream purification steps. Therefore the next protein selected to test the system was denmotoxin, a three finger toxin with five disulphides, much larger and complex than ΔHelix KNP. Although the denmotoxin-PLA_2 fusion was able to express in the extracellular medium with the correct oxidized mass, it resisted cleavage by both TEV and HRV 3C protease. Further work need to be done in the future to troubleshoot the cleavage problem. The resistance to protease may be due to

the stearic hindrance caused by the tag and demnotoxin resulting in burying of the protease site in the fusion protein. The linker length near the protease cleavage site needs to be optimized for the access of the protease and efficient tag cleavage. Next we also wanted to identify the minimal segment of the PLA_2 which could retain the property of extracellular secretion. Although none of the truncated mutants were able to secrete into the extracellular medium, Δ Helix 1 & 2 misfolded as inclusion body and Helix short was able to enter the periplasmic space. This experiment illustrated the importance of the N-terminal helices in enhancing the solubility of the molecule. Also the Helix short mutant which was small by just eight residues, failed to secrete to the extracellular medium and retained in the periplasmic space. From this information, the region of the molecule aiding in the interaction with any unknown partners of the bacterial secretion systems leading to its secretion can be probed. Next the study of the PLA_2 point mutants showed the reduction in the yield was due to the lack of secretion rather than expression. The point mutations led to the misfolding of the molecule, leading to reduced secretion. Optimization at lower temperature was able to increase the yield to considerable amount.

Not only do the system needs to be optimized with different linker lengths for efficient tag cleavage, it also needs to be tested with proteins with different size and with different complexities, number of disulphide bonds. It also needs to be tested with proteins which can only be expressed with solubilization tags and proteins which have expression problems even with tags. It would also be

of interest to understand the mechanism underlying this export process in *E. coli.*

4.2 Design of a mini PLA_2 scaffold

Another interesting property of the prokaryotic PLA_2 is its tertiary structure and its preservation of the same topologically conserved three helix catalytic core and active site geometry. These unique structural properties provided us with a model to design a minimized PLA_2 scaffold. Although we were able to design and produce the minimized PLA_2 scaffold which was 30% smaller than the wild type, their biological activity was completely lost. The first generation involved the design and production of two mutants, Δ Helix 1 and Δ Helix 1 & 2. After the failure of initial trials of minimization with chemical cleavage and usage of solubilizaton tags to express the mutants, we refolded the mutants using a redox couple. The purified refolded protein was checked for its secondary structure and disulphide linkage. After confirming the structural details, the assay for activity was conducted, which showed a complete loss of activity. The second generation of mutant was designed by reducing the hydrophobic surface of the first generation mutant and the final mutant Δ Helix 1 & 2- F66Q-Y71Q was expressed, refolded and assessed for its disulphide linkages. This mutant also showed the complete loss of activity. To probe into the structural changes that was responsible for the loss of activity, the smallest of the first generation mutant Δ Helix 1 & 2 was set for

crystallization. Unfortunately, the crystallization was not successful due to heavy precipitation seen in majority of the drops. The reduction in the solubility of the protein was due to its purification by revered phase chromatography; hence further work is needed in the future to devise strategies to purify the mutant using mild purification condition.

Crystallization of this mutant is an important future work, as crystal structure can only give us detailed insights about the mutant and ideas for designing next generation of mutants. Since the mutant Δ Helix 1 & 2 is around 9 kDa, Nuclear Magnetic Resonance spectroscopy might be used to determine the solution structure. Structural information would give us idea about the changes in the active site geometry, which resulted in total activity loss of the mutants. Also we need to check if the mutants retain the calcium binding property. This could be achieved by Isothermal Titration Calorimetry. Negative binding results would give us an idea about distortion in calcium binding loop, which could have rendered the calcium coordination faulty.

Bibliography

Aloulou, A., Ali, Y.B., Bezzine, S., Gargouri, Y., and Gelb, M.H. (2012). Phospholipases: an overview. Methods in molecular biology (Clifton, NJ) *861*, 63-85.

Andreev, Y.A., Kozlov, S.A., Vassilevski, A.A., and Grishin, E.V. (2010). Cyanogen bromide cleavage of proteins in salt and buffer solutions. Analytical biochemistry *407*, 144-146.

Arnold, F.H., Technology, C.I.o., Moore, J.C., and Technology, C.I.o. (2015). Optimizing industrial enzymes by directed evolution. Advances in Biochemical Engineering, 1-14.

Assenberg, R., Wan, P.T., Geisse, S., and Mayr, L.M. (2013). Advances in recombinant protein expression for use in pharmaceutical research. Current opinion in structural biology *23*, 393-402.

Baker, M. (2011). Protein engineering: navigating between chance and reason. Nature methods *8*, 623-626.

Baneyx, F. (1999). Recombinant protein expression in Escherichia coli. Curr Opin Biotechnol *10*, 411-421.

Berry, S.M., and Lu, Y. (2011). Protein Structure Design and Engineering.
Bolon, D.N., and Mayo, S.L. (2001). Enzyme-like proteins by computational design. Proc Natl Acad Sci U S A *98*, 14274-14279.

Braisted, A.C., and Wells, J.A. (1996). Minimizing a binding domain from protein A. Proc Natl Acad Sci U S A *93*, 5688-5692.

Cabrita, L.D., and Bottomley, S.P. (2004). Protein expression and refolding--a practical guide to getting the most out of inclusion bodies. Biotechnology annual review *10*, 31-50.

Cereghino, J.L., and Cregg, J.M. (2000). Heterologous protein expression in the methylotrophic yeast Pichia pastoris. FEMS microbiology reviews *24*, 45-66.

Choe, W.S., Clemmitt, R.H., Chase, H.A., and Middelberg, A.P. (2002). Comparison of histidine-tag capture chemistries for purification following chemical extraction. Journal of chromatography A *953*, 111-121.

Corey, M.J., and Corey, E. (1996). On the failure of de novo-designed peptides as biocatalysts. Proc Natl Acad Sci U S A *93*, 11428-11434.

Crimmins, D.L., Mische, S.M., and Denslow, N.D. (2005). Chemical cleavage of proteins in solution. Current protocols in protein science / editorial board, John E Coligan [et al] *Chapter 11*, Unit 11.14.

de Vos, W.M., Kleerebezem, M., and Kuipers, O.P. (1997). Expression systems for industrial Gram-positive bacteria with low guanine and cytosine content. Curr Opin Biotechnol *8*, 547-553.

Dill, K.A., and MacCallum, J.L. (2012). The Protein-Folding Problem, 50 Years On. American Association for the Advancement of Science.

Eiben, C.B., Siegel, J.B., Bale, J.B., Cooper, S., Khatib, F., Shen, B.W., Players, F., Stoddard, B.L., Popovic, Z., and Baker, D. (2012). Increased Diels-Alderase activity through backbone remodeling guided by Foldit players. Nature biotechnology *30*, 190-192.

Gellissen, G. (2000). Heterologous protein production in methylotrophic yeasts. Applied microbiology and biotechnology *54*, 741-750.

Hariprasad, G., Srinivasan, A., and Singh, R. (2013). Structural and phylogenetic basis for the classification of group III phospholipase A2. Journal of molecular modeling *19*, 3779-3791.

Harper, S., and Speicher, D.W. (2011). Purification of proteins fused to glutathione S-tranferase. Methods in molecular biology (Clifton, NJ) *681*, 259-280.

Harwood, C.R. (1992). Bacillus subtilis and its relatives: molecular biological and industrial workhorses. Trends in biotechnology *10*, 247-256.

Holliger, P., and Hudson, P.J. (2005). Engineered antibody fragments and the rise of single domains. Nature biotechnology *23*, 1126-1136.

Huang, P.S., Ban, Y.E., Richter, F., Andre, I., Vernon, R., Schief, W.R., and Baker, D. (2011). RosettaRemodel: a generalized framework for flexible backbone protein design. PLoS One *6*, e24109.

Jain, M.K., and Berg, O.G. (1989). The kinetics of interfacial catalysis by phospholipase A2 and regulation of interfacial activation: hopping versus scooting. Biochimica et biophysica acta *1002*, 127-156.

Kane, J.F. (1995). Effects of rare codon clusters on high-level expression of heterologous proteins in Escherichia coli. Current Opinion in Biotechnology *6*, 494–500.

Katti, S.K., LeMaster, D.M., and Eklund, H. (1990). Crystal structure of thioredoxin from Escherichia coli at 1.68 A resolution. Journal of molecular biology *212*, 167-184.

Khatib, F., Cooper, S., Tyka, M.D., Xu, K., Makedon, I., Popovic, Z., Baker, D., and Players, F. (2011). Algorithm discovery by protein folding game players. Proc Natl Acad Sci U S A *108*, 18949-18953.

Kini, R.M. (2003). Excitement ahead: structure, function and mechanism of snake venom phospholipase A2 enzymes. Toxicon : official journal of the International Society on Toxinology *42*, 827-840.

Kjeldsen, T. (2000). Yeast secretory expression of insulin precursors. Applied microbiology and biotechnology *54*, 277-286.

Korkegian, A., Black, M.E., Baker, D., and Stoddard, B.L. (2005). Computational thermostabilization of an enzyme. Science (New York, NY) *308*, 857-860.

LaVallie, E.R., DiBlasio, E.A., Kovacic, S., Grant, K.L., Schendel, P.F., and McCoy, J.M. (1993). A thioredoxin gene fusion expression system that circumvents inclusion body formation in the E. coli cytoplasm. Bio/technology (Nature Publishing Company) *11*, 187-193.

Li, B., Tom, J.Y., Oare, D., Yen, R., Fairbrother, W.J., Wells, J.A., and Cunningham, B.C. (1995). Minimization of a polypeptide hormone. Science (New York, NY) *270*, 1657-1660.

Lunn, C.A., Kathju, S., Wallace, B.J., Kushner, S.R., and Pigiet, V. (1984). Amplification and purification of plasmid-encoded thioredoxin from Escherichia coli K12. The Journal of biological chemistry *259*, 10469-10474.
Lutz, S. (2010). Biochemistry. Reengineering enzymes. Science (New York, NY) *329*, 285-287.

Matoba, Y., Katsube, Y., and Sugiyama, M. (2002). The Crystal Structure of Prokaryotic Phospholipase A2.

Milner, S.J., Thomas, S.M., Ballard, F.J., and Francis, G.L. (1996). Optimization of the hydroxylamine cleavage of an expressed fusion protein to produce recombinant human insulin-like growth factor (IGF)-I. Biotechnology and bioengineering *50*, 265-272.

Nanda, V., and Koder, R.L. (2010). Designing Artificial Enzymes by Intuition and Computation. Nat Chem *2*, 15-24.

Narayan, A.R., and Sherman, D.H. (2013). Chemistry. Re-engineering nature's catalysts. Science (New York, NY) *339*, 283-284.

Nevalainen, T.J., and Cardoso, J.C. (2012). Conservation of group XII phospholipase A2 from bacteria to human. Comparative biochemistry and physiology Part D, Genomics & proteomics *7*, 340-350.

Ozturk, S.S. (1996). Engineering challenges in high density cell culture systems. Cytotechnology *22*, 3-16.

Prazeres, D.M., Ferreira, G.N., Monteiro, G.A., Cooney, C.L., and Cabral, J.M. (1999). Large-scale production of pharmaceutical-grade plasmid DNA for gene therapy: problems and bottlenecks. Trends in biotechnology *17*, 169-174.

Presta, L.G. (2005). Selection, design, and engineering of therapeutic antibodies. The Journal of allergy and clinical immunology *116*, 731-736; quiz 737.

Reiter, Y., Brinkmann, U., Lee, B., and Pastan, I. (1996). Engineering antibody Fv fragments for cancer detection and therapy: disulfide-stabilized Fv fragments. Nature biotechnology *14*, 1239-1245.

Ricciotti, E., and FitzGerald, G.A. (2011). Prostaglandins and Inflammation. Arterioscler Thromb Vasc Biol *31*, 986-1000.

Rothlisberger, D., Khersonsky, O., Wollacott, A.M., Jiang, L., DeChancie, J., Betker, J., Gallaher, J.L., Althoff, E.A., Zanghellini, A., Dym, O., *et al.* (2008). Kemp elimination catalysts by computational enzyme design. Nature *453*, 190-195.

Schaloske, R.H., and Dennis, E.A. (2006). The phospholipase A2 superfamily and its group numbering system. Biochimica et biophysica acta *1761*, 1246-1259.

Scott, D.L., and Sigler, P.B. (1994). Structure and Catalytic Mechanism of Secretory Phospholipases A2. *45*, 53-88.

Siegel, J.B., Zanghellini, A., Lovick, H.M., Kiss, G., Lambert, A.R., St Clair, J.L., Gallaher, J.L., Hilvert, D., Gelb, M.H., Stoddard, B.L., *et al.* (2010). Computational design of an enzyme catalyst for a stereoselective bimolecular Diels-Alder reaction. Science (New York, NY) *329*, 309-313.

Smith, D.B., and Johnson, K.S. (1988). Single-step purification of polypeptides expressed in Escherichia coli as fusions with glutathione S-transferase. Gene *67*, 31-40.

Stevens, B.W., Lilien, R.H., Georgiev, I., Donald, B.R., and Anderson, A.C. (2006). Redesigning the PheA domain of gramicidin synthetase leads to a new understanding of the enzyme's mechanism and selectivity. Biochemistry *45*, 15495-15504.

Stricher, F., Martin, L., and Vita, C. (2006). Design of miniproteins by the transfer of active sites onto small-size scaffolds, Vol 340, 2006/09/08 edn.

Sugiyama, M., Ohtani, K., Izuhara, M., Koike, T., Suzuki, K., Imamura, S., and Misaki, H. (2002). A Novel Prokaryotic Phospholipase A2.

Takemori, D., Yoshino, K., Eba, C., Nakano, H., and Iwasaki, Y. (2012). Extracellular production of phospholipase A2 from Streptomyces violaceoruber by recombinant Escherichia coli. Protein Expr Purif *81*, 145-150.

Terpe, K. (2006). Overview of bacterial expression systems for heterologous protein production: from molecular and biochemical fundamentals to commercial systems. Applied microbiology and biotechnology *72*, 211-222.

Tsigos, I., Mavromatis, K., Tzanodaskalaki, M., Pozidis, C., Kokkinidis, M., and Bouriotis, V. (2001). Engineering the properties of a cold active enzyme through rational redesign of the active site. Eur J Biochem *268*, 5074-5080.

Ulmer, K.M. (1983). Protein Engineering. Science (New York, NY) *Vol. 219*, 666-671.

Vallejo, L.F., and Rinas, U. (2004). Strategies for the recovery of active proteins through refolding of bacterial inclusion body proteins. Microbia
l cell factories *3*, 11.

Van den Burg, B., Vriend, G., Veltman, O.R., Venema, G., and Eijsink, V.G. (1998). Engineering an enzyme to resist boiling. Proc Natl Acad Sci U S A *95*, 2056-2060.

Verger, R., and De Haas, G.H. (1973). Enzyme reactions in a membrane model. 1. A new technique to study enzyme reactions in monolayers. Chemistry and physics of lipids *10*, 127-136.

Vita, C., Roumestand, C., Toma, F., and Menez, A. (1995). Scorpion toxins as natural scaffolds for protein engineering. Proc Natl Acad Sci U S A *92*, 6404-6408.

Vrancken, K., Van Mellaert, L., and Anne, J. (2010). Cloning and expression vectors for a Gram-positive host, Streptomyces lividans. Methods in molecular biology (Clifton, NJ) *668*, 97-107.

Yoon, S.H., Kim, S.K., and Kim, J.F. (2010). Secretory production of recombinant proteins in Escherichia coli. Recent patents on biotechnology *4*, 23-29.

Appendix

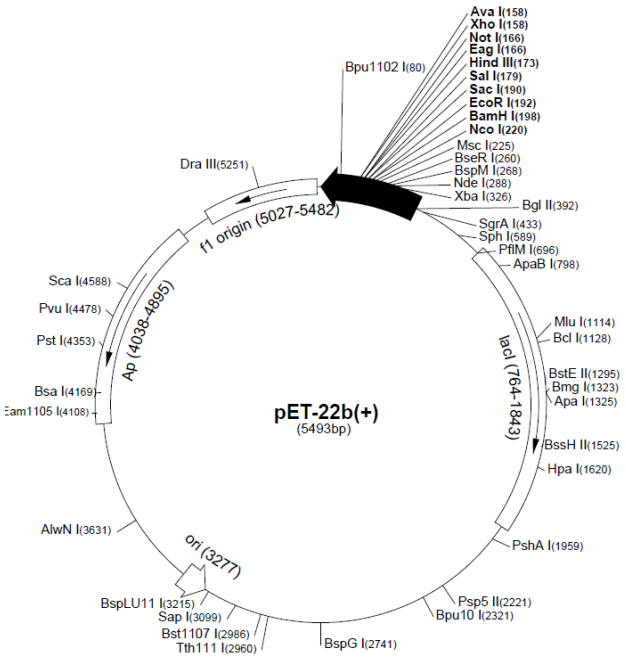

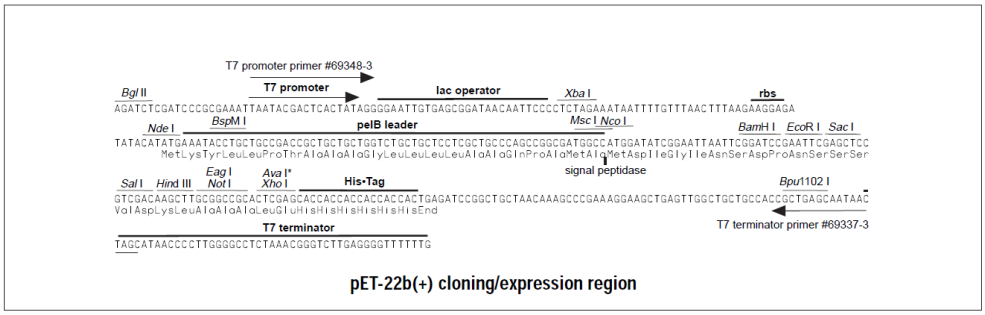

pET-22b(+) cloning/expression region

A 1 Vector Map of pET-22b

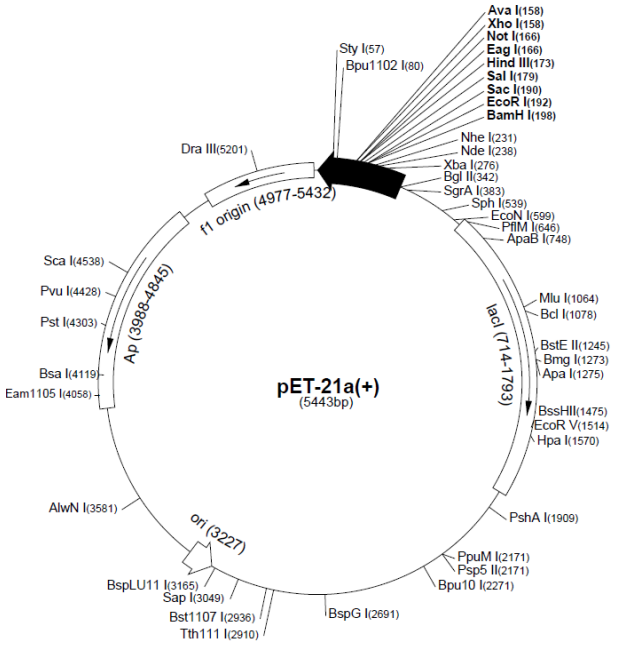

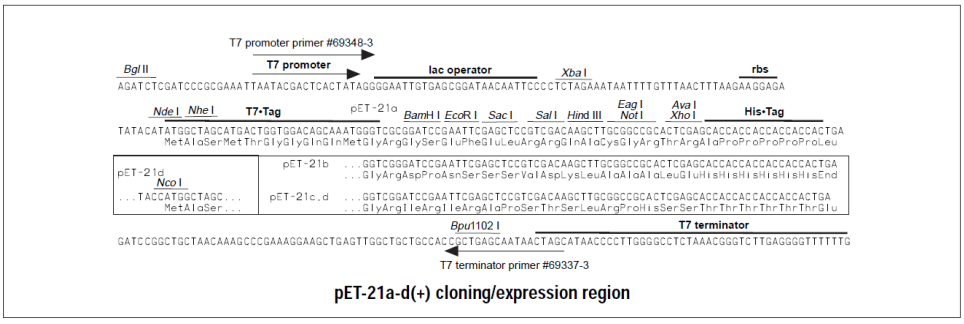

pET-21a-d(+) cloning/expression region

A 2 Vector Map of pET-21a-d